Analysis of the Unsteady Aerodynamics Experiment for National Full-Scale Aerodynamics Complex Testing

Volume 2 of 2: Stress Analysis Document

Presented to the

National Full-Scale Aerodynamics Complex

by

Jason R. Cotrell, M.S.

The National Wind Technology Center

07/09/99

TOC

1. Summary of results

Table 1.1 presents the results of this document for the critical components. Components not listed were determined not to be a significant hazard to personnel or facilities if they failed.

Table 1.1: Summary of results for critical components.

Assembly	Component	Stress type	Safety factor		Fatigue life	Comments
			Yield	Ultimate		
Hardlink	Entire assembly	Buckling	-	3.0	-	Monitored load
	Rod ends	Tension	8.8	Not available	Infinite life	Monitored load
	Force sensor	Tri-axial	1.7	2.0	Infinite life	Class 3 load
	Hardlink stud	Tension	-	5.4	Infinite life	Monitored load
	Hardlink turnbuckle	Thread pull-out	5.2	-	Infinite life	Monitored load
Plate structure	Hub weldment	Tri-axial	3.2	5.2	Infinite life	Monitored load
	Cheek plate	Tri-axial	1.5	2.4	Infinite life	Class 3 load
	Cheek plate welds	Tri-axial	1.9	2.5	Infinite life	Monitored load
	Hardlink sleeve	Tri-axial	3.4	3.8	Infinite life	Monitored load
	Hardlink pins		5.6	7.1	Infinite life	Monitored load
	Cheek plate stiffener	Compressive	2	2.3	Infinite life	Class 3 load
Dampers	Teeter damper pins	Shear	4.4	5.1	Infinite life	Monitored loads
	Teeter damper caps	Bending	3.8	4.8	Infinite life	Monitored loads
	Teeter damper plates	Tri-axial	3.3	4.1	Infinite life	Monitored loads
	Teeter damper plate dowel pins	Shear	-	18.3	Infinite life	Monitored loads
Hub shaft assembly	Hub shaft	Tri-axial	2.4	3.1	Infinite life	Class 2 load
	Teeterpin cap bolts	Shear and Tension	-	3.0	Infinite life	-
	Teeterpin	Tri-axial	4.8	6.2	Infinite life	Monitored load
	Adapter	Tri-axial	24	35	Infinite life	-
	Adapter bolts	Tension & shear	-	4.3	Infinite life	-
Tower	Yaw shaft	Tri-axial	2.0	3.0	-	Class 2 load
	Yaw bearing	Tri-axial	5	>5	Infinite life	-
	Yaw bearing fasteners	Tension and shear	N/A	131	Infinite life	-
	Tower-top	Tri-axial	3.6	5.0	Infinite life	-
	Tower body	Tri-axial	5.8	10	Infinite life	-

	Semi-span mount	Shear & bending	72	116	-	-
	Tower lifting eyes	Shear	-	17	-	-
	Turn table limits	Drag	-	28.1	-	-
	Turn table limits	Post force	-	8.6	-	-
Blade	Blade weight clamp	Bending	8.1	-	-	Pre-load
	Blade weight all-thread	Tension	29.6	-	-	-
	Root	Bending	2.8	5.5	-	Class 3 load
	Pitch shaft	Tri-axial	3.0	3.2	Infinite	Class 3 load
	Pitch shaft nut	Tension	-	36	-	-
	Studs	Tension & shear	3.7	4.3	-	-
Nacelle	LSS	Tri-axial	3.1	3.3	Infinite	Class 3 load
	LSS nut	Tension	-	67.5	-	-
	Shaft main bearings	L10 life 5000 hours	2.4	-	-	Against L-10 life
	Mainframe	Tri-axial	3.0	4.5	Infinite	Monitored load
Boom	PCM/PWR/PSC boxes	Tension	5.8	-	Infinite	-
	Rodends	Tension	5.5	-	-	-
	Boom mount	Tri-axial	3.1	4.4	115,000 hrs	-
	Boom bars	Tension	18.3	19.5	Infinite	-
	Boom mount adapter plate	Tri-axial	7.7	9.7	Infinite	-
	Gusset/flange weld	Tri-axial	-	47.2	Infinite	-
	Cleavis mount bolts	Tension	-	10.5	-	-
	Boom spacer bolts	Tension	-	109	-	-
	Tripod adapter	Shear	-	16	-	-

2. Purpose & scope

The purpose of this document is to demonstrate that the Unsteady Aerodynamics Experiment (UAE) two-bladed rotor will withstand testing in the National Full-Scale Aerodynamics Complex without structural failure.

The Unsteady Aerodynamics Experiment has been performed in six phases (I through VI). The previous draft of the stress analysis document analyzed the phase V configuration. Phase VI incorporated several structural changes to the turbine—such as the newly designed blades, hub shaft, boom, and tower. These changes are reflected in this document.

The calculation of the anticipated NFAC loads is presented in the accompanying loads document (Volume 1). The loads document uses measured field loads and a commercial dynamics simulation code (ADAMS) to predict the loads during NFAC testing [1].

For this document I used an FEA software package called Cosmosworks made by Structural Analysis and Research Corporation [2]. All the FEA results in this document were obtained using a high order (with mid-side nodes) tetrahedral element. I used strength-of-materials calculations to validate the FEA results.

The UAE components were designed for an infinite life. In this document I use an endurance limit approach to demonstrate that fatigue will not be problematic during NFAC testing.

3. Component analyses

I reviewed all structures and parts on the wind turbine to determine whether they meet the NFAC requirements for either a critical or non-critical structure. The NFAC test planning guide defines a critical structure as "…a part whose failure would lead to a significant hazard to personnel and/or facilities if they failed or if they contributed to an accident." [3] The following sections discuss the classifications of the components as critical or non-critical and present the stress and fatigue analysis results for the critical components.

3.1. Hub weldment

The hub weldment consists of welded plates which transfer the blade loads to the teeterpin. The two-bladed hub was designed to allow the two hub weldment to flap independently or teeter together. The hardlink fastens the two hub weldments together so that it will teeter. Figure 3.1 presents the names of the plates which form the hub weldment and the hardlink. This section discusses the stresses in the hub weldment. The hardlink is discussed in the following section.

The top plate and webs of the hub weldment are made from ¼" thick A36 plate steel (36 kpsi minimum yield strength and 58 kpsi minimum tensile strength). The bottom plate and tuning forks are made from 3/8" A36 plate steel. The plates have been TIG welded using an AWS E70XX electrode (70 kpsi tensile strength). The welds are continuous beads along every possible joint.

The hardlink transfers the loads to the cheek plates through the hardlink sleeves, hardlink pins, and cheekplate doublers. The doublers are made from A36 steel and welded around the circumference. The doublers are 3/8" thick with an outside diameter of 2 ¼". The doublers are welded around A36 steel tubes which have a ¼" wall with an outside diameter of 1 1/8". The tubes are bored to fit drill bushings for the 5/8" diameter hardlink pins.

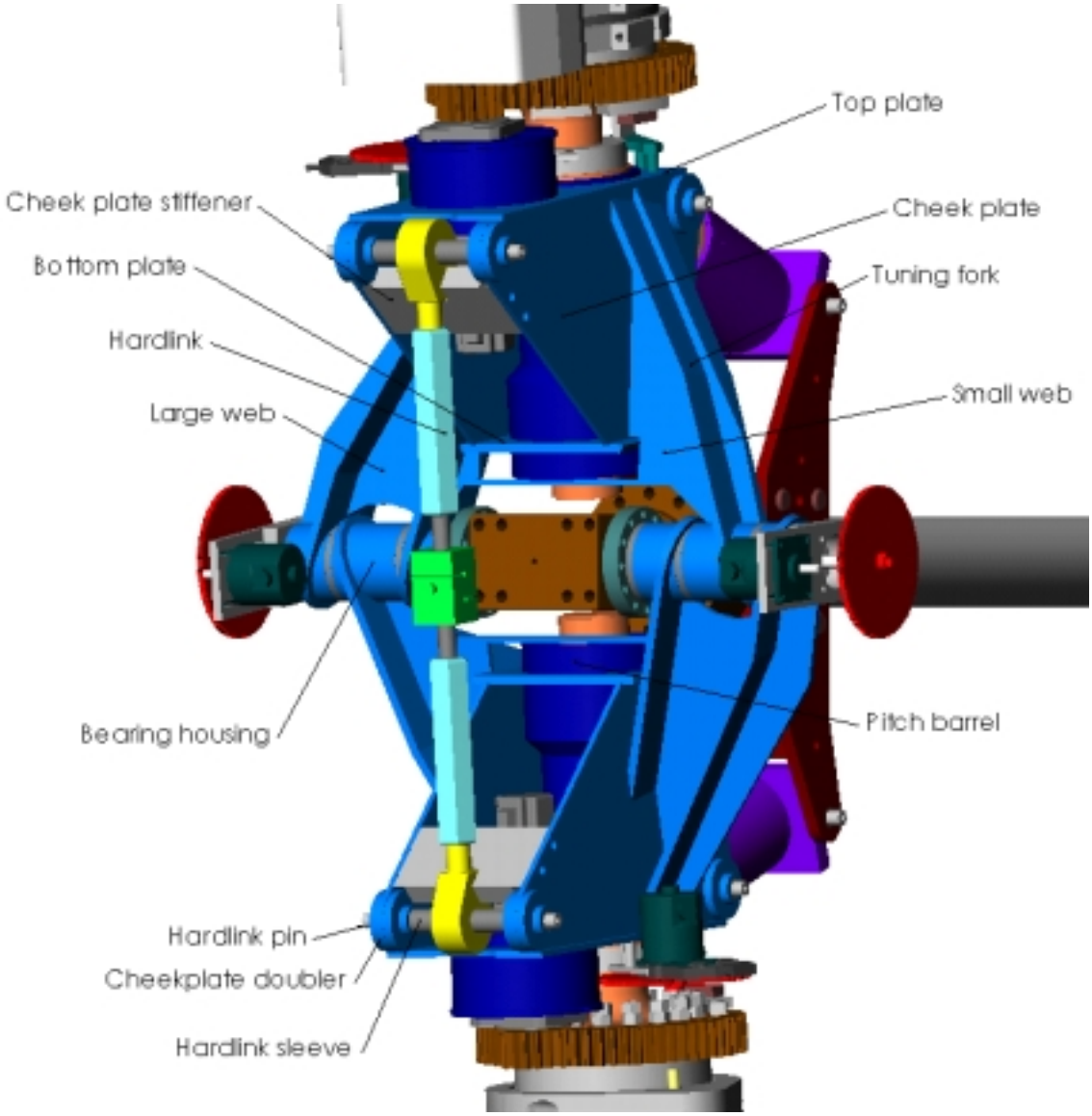

Figure 3.1: Hub weldment and hardlink components.

3.1.1. Hub weldment stress analysis.

I performed several hours of finite element analyses on the hub. I have come to the conclusion that it is extremely difficult to accurately constrain the hub in a finite element analysis. The difficulty stems from the ability of the weldment to rotate about the teeterpin. This degree of freedom can not be modeled using Cosmos/Works FEA software.

In place of this analysis, I am referring the reader to Chapters 3 and 4 of my thesis *The Mechanical Design, Analysis, and Testing of a Two-Bladed Wind Turbine Hub.*. In these chapters I perform an analytical analysis of the hub strength and I describe the static testing we have performed on a prototype hub.

The most significant loads are the hub flapwise and edgewise moments. My thesis performed the stress analysis using flapwise and edgewise moments of 17,957 ft-lb. In contrast the ADAMS simulations predict that the peak flapping and edgewise moments of only 9,758 ft-lb and 4,667 ft-lb.

The peak stress corresponding to the 17,957 ft-lb loads was 11,206 psi. The safety factors against exceeding the yield and ultimate strength are

$$F.S._{yield} = 36{,}000 / 11{,}206 = 3.2$$

$$F.S._{ultimate} = 58{,}000 / 11{,}206 = 5.2$$

To static test the hub, we applied 22,446 ft-lb of flapping moment and then edgewise blade moment. This corresponds to over twice the peak flapwise load predicted by ADAMS. We measured the displacement and deformation of the hub during testing. No noticeable deformations or weld cracking occurred.

3.2. Hardlink

The hardlink is used to link the two halves of the hub together and set the cone angle. The hardlink consists of a force sensor, two turnbuckles, and two spherical rod ends (see Figure 3.2). A sleeve is mounted through each rod end and a ∅5/8" pin is pressed through each sleeve and into the cheekplate bushings.

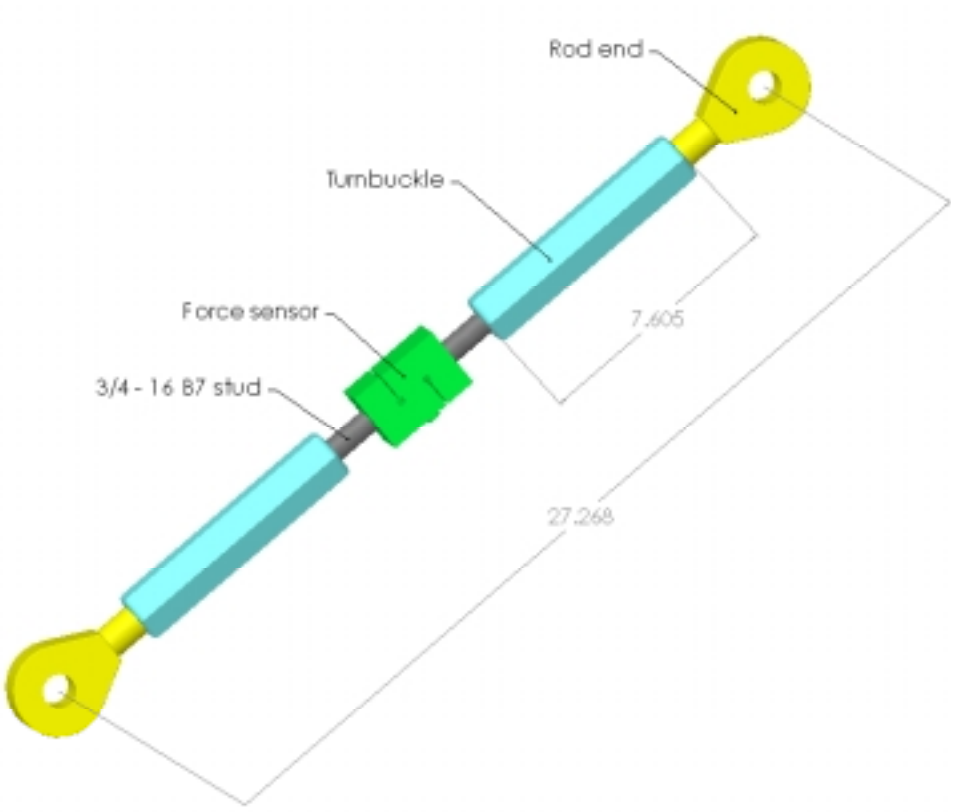

Figure 3.2: Hardlink components.

3.2.1. Hardlink force sensor

The hardlink force sensor is a hermetically sealed universal load cell (HSW series) made by Transducer Techniques. It is made from 17-4 precipitation hardened (HRC 36) stainless steel. Assuming it has been heat treated to the H1075 condition, S_{yt} = 125 kpsi and S_{ut} = 145 kpsi. The transducer is accurate to 10,000 lbs. According to the manufacturer, the transducer will yield at 150% of the rated load and will withstand 100 million cycles of 10,000 lb completely reversed load cycles [4].The hardlink force sensor is actively monitored. In order to meet NASA requirements for a monitored load, we will restrict the turbine operating range at 25 m/s to yaw angles which result in a hardlink force less than 8,700 lb. Thus, the safety factor against yielding is

$$F.S._{yield} = 15{,}000 / 8{,}700 = 1.7$$

The tensile strength of stainless steel aged to the H1075 condition is 16% greater than the yield strength. Assuming that the manufacturer rating for ultimate tensile load is also 16% greater than the rated yield load, the sensor will withstand 17,400 lbs before breaking. Thus, the safety factor against fracturing is

$$F.S._{ult} = 17{,}400 / 8{,}700 = 2.0$$

Although these safety factors do not meet the standard NFAC requirements ($F.S._{ultimate}$ is below 4.0) the LSS does meet the safety factor requirements to qualify for a class 3 NASA load case ($F.S._{yield}$ = 1.5 and $F.S._{ultimate}$=2.5 * FB). FB for 15-5 VAR stainless steel is at most 1 [5].

In order to qualify for a class 3 load, the hardlink must be proof tested up to 125% of the peak load. We will limit the load cases we run so that the hardlink loads remain under 8,700 lb. To static test the hardlink force sensor, we placed them in a jig used to calibrate them. We applied 11,000 lb of force in tension and then compression. We repeated the process and checked compared the calibration curves. There was no change in the calibration curve, thus the load cell did not yield.

We anticipate that the turbine will have been run no more than 50 hours before beginning the NFAC testing and at most another 150 hours in the NFAC for a total runtime of at most 200 hours. In a worst case scenario, with the hub rotating at 72 RPM, the force will be subjected to roughly 8.6×10^5 cycles of fluctuating reversed loads. Since the sensor is rated at 10,000 lb for 1.0×10^8 cycles, fatigue should not cause the sensor to fail.

3.2.2. Hardlink buckling analysis

I performed a finite element buckling analysis on the hardlink. The hardlink forces will be limited to 8700 lb. I had to model the hardlink as a link with fixed ends rather than pinned at both ends due to limitations in the FEA software. To compensate for these non-conservative end conditions, I reduced the resulting critical load by four. This reduction corresponds to the difference in the end condition constant when using the Euler equation to model long columns with pinned ends and long columns with fixed ends [6].

Figure 3.3 displays the first buckling mode for the hardlink. The buckling analysis was originally run using an applied load of 6800 lb. This load is still adequate because the derivation of a load factor is independent of the magnitude of the applied load. The load factor was determined to be 15.83. Compensating for the fixed end assumption, the load factor is 15.83 / 4 =3.96. Thus the critical buckling load is 3.96* 6800 lb = 26,920 lb and the safety factor against buckling is

$$F.S._{buckling} = 26{,}920\ lb / 8700 = 3.0$$

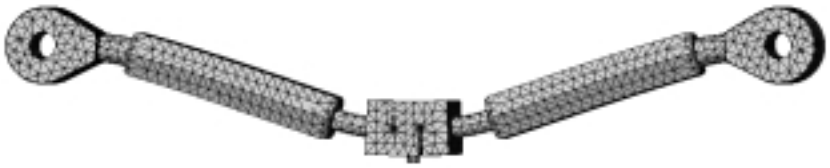

Figure 3.3: Hardlink bending (deflection x 40).

3.2.3. Hardlink turnbuckle

The hardlink turnbuckles were made from 4140 annealed and cold finished, 1½", steel hex stock (S_{yt} = 102 kpsi, S_{ut} = 90 kpsi). The hex stock was tapped on each end to make a turnbuckle. One end was tapped ¾-16 UNC for a B7 stud ($S_{y\ min}$ = 101 kpsi) the other end was tapped 1-14 for the rod end. The critical strength of the hardlink turnbuckle is the thread pull out strength.

3.2.3.1. Thread pullout

According to the NFAC Test Planning Guide

"Calculations for thread pull out strength(shear) shall assume that all of the load is resisted by the thread engagement equivalent to one bolt diameter and that 75% of the load is carried by the first three threads." [7]

The NFAC Test Planning guide gives the formula for the acting stress as

$$\sigma_{acting} = \frac{Load}{(Bolt\ circumference)(thread\ depth)(.5)} = \frac{8700lb}{\pi(.75in)(.75in)(.5)} = 9{,}835\,psi$$

According to the distortion energy theory, the allowable strength of material in shear is .57 times the yield strength of the material [8]. The turnbuckle is the weaker material, thus, the allowable stress for the turnbuckle is (.57)(90 kpsi) = 51.3 kpsi.

The safety factor on yield is then

$$\boxed{F.S._{yield} = 51.3 / 9.8 = 5.2}$$

The minimum value safety factor on yield specified in the NFAC manual is 3.0. Thus, the design is acceptable. The lock washers are used to preload the tapped turnbuckle threads in tension. Thus, fatigue should not cause a failure in the turnbuckle threads.

3.2.3.2. Stud tension

The hardlink studs are made from B7 all thread (S_y = 105 kpsi, S_{ut} = 125 kpsi). B7 studs are made from AISI 4140, 4142, or 4145 quenched and tempered at 1150 °F [9]. Thus they are comparable to a SAE grade 5 bolt. A ¾ - 16 bolt has a stress area of .3730 in^2. The tensile strength is

$$F_{ult} = .3730\ in^2 * 125{,}000\ psi = 46{,}625\ lb$$

Thus, the factor of safety against exceeding the tensile strength of the studs is

$$\boxed{F.S._{yield} = 46{,}625 / 8{,}700 = 5.4}$$

3.2.3.3. Fatigue Analysis

The endurance limit for a smooth rotating bar (R= -1) of 4140 steel quenched and tempered at 1150 °F is 75 kpsi [10]. The stress concentration factor for rolled threads is 3.0 [11].

The formula for the component endurance limit (S_e) is

$$S_e = k_a\ k_b\ k_c\ k_d\ k_e\ S_e'$$

where

k_a = surface factor

k_b = size factor

k_c = load factor

k_d = temperature factor

k_e = miscellaneous affects factor

The calculation of S_e is presented in Table 3.1. The load factors were calculated using formulas from Shigley and Mischke [12].

Table 3.1: Calculation of the enduarance limit for the hardlink studs.

Parameter	Deffinition	Value	Comments	Se'	Se
ka	surface factor	1	Accounted for below		
kb	size factor	1	Axial loading		
kc	load factor	0.923	Axial loading		
kd	temp. factor	1	Room temperature		
ke	misc. affects factor	0.33	Stress conentration		
Effective k		0.307667		75	**23**

The peak nominal stress on the hardlink studs is

$$8700 \text{ lb} / .3730 \text{ in}^2 = 23{,}324$$

This is value is essentially equal to the effective endurance limit (23 kpsi). Considering this calculation conservatively assumes fully reversing stresses (R = -1) from the peak load 8700 lb, this component should have an infinite life.

3.2.4. Hardlink rod ends

The hardlink rod ends are high-strength alloy, precision rod ends made by Aurora Bearing Company (model # AB-16). The radial static load capacity of each bearings is 76,200 lbs. The peak estimated load on the hardlink is 8700 lbs. The rod end factor of safety for this load is

$$F.S._{rated} = 76{,}200 / 8700 = 8.8$$

Figure 3.4 displays the time series for the 25 m/s rigid, 0° to 180° rigid load case. I plotted the rigid load case because we have decided to not run the turbine in any condition which results in significant teeter impacts (all load cases with out teeter impacts have trends similar to this plot). The intent of including this plot is to demonstrate that the oscillations in the hardlink load are small compared to the mean load.

However, according to David Richard (an Aurora Bearing engineer) the rod ends can be considered to have an endurance limit of 10 –12 % of rod end ultimate strength. Thus the endurance limit for the rod end can be considered to be 7,620 lbs. This assumes that the load is oscillating between 0 lb and 7,620 lbs. Furthermore, when the rod end is in compression, there is essentially no fatigue affect on the rod ends. In order to meet the fatigue requirements for NASA, we will limit the tension loads on the hardlink to 7,620 lbs to ensure the hardlink rod ends have an infinite life.

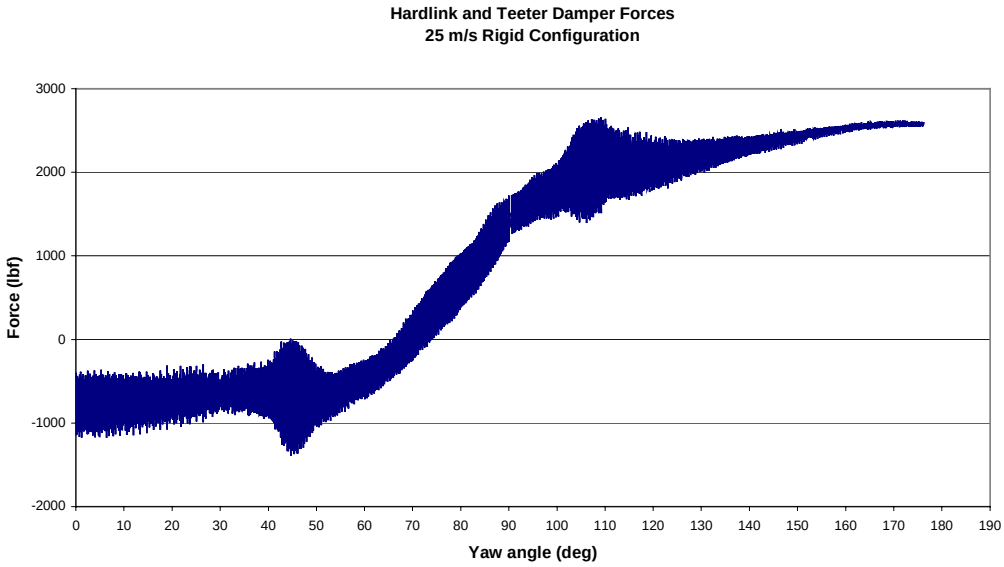

Figure 3.4: Hardlink Loads for the 25 m/s, Rigid, 0° to 180° Load Case.

3.2.5. Hardlink mount assembly

The hardlink mount assembly consists of the cheek plates, the cheekplate doublers, cheekplate stiffener, the 5/8" pins mounted in the cheek plate bushings, and the hardlink sleeves (see Figure 3.1). The hardlink loads are transferred from the rod ends to the hardlink sleeves, from the hardlink sleeves to the 5/8" pins, and from the pins to the cheekplates.

The cheekplate doublers distribute the loads to the cheek plates. The cheekplate doublers were constructed by welding steel disks to the cheekplates with continuos welds. The cheek plate stiffeners are bolted with 3/8" grade 8 screws between the two cheekplates. Drill bushings are pressed into the cheek plate doublers to hold the 5/8" pin. The 5/8" pin is pressed into the sleeve. There is .005" clearance between each sleeve end-face and the drill bushings which hold the 5/8" pin. The materials and strength properties for each component are listed in Table 3.2.

Table 3.2: Material properties for the hardlink mount assembly.

Component	Material	Yield tensile strength (kpsi)	Ultimate tensile strength (kpsi)
Cheek plate	A36 steel	36	58
Cheek plate doublers	A36 steel	36	58
Cheek plate welds	AWS E70XX electrode	53	70

Hardlink sleeve	4340 Q&T steel	162	182
Hardlink pin	17-4 H925 stainless	170	155
Cheek plate stiffener	6061 T6 AL	40	45

3.2.5.1. Hardlink mount FEA methodology

I performed a finite element analysis on the hardlink mount assembly. The assumption and loads I used in this analysis are presented below.

FEA Assumptions:

1) I cut the hub weldment solid model in half so I could analyze the front half of the hub weldment in greater detail.
2) I modeled the hardlink pin and hardlink sleeve as one solid. This is a valid assumption because the hardlink pin is pressed into the hardlink sleeve. I did included the .005" clearance that exists between each sleeve end-face and the bushings which hold the 5/8" pin.
3) I modeled the rectangular stiffener and the cheekplates as one solid piece of A36 steel. This is a valid assumption since the cheek plates are bolted to the stiffener and the loads on the stiffener are compressive loads.
4) I modeled the spherical rod end as a collar on the center of the hardlink sleeve.

FEA Loads:

1) We must limit the loads on the hardlink force sensor to 8,700 lbs to meet NASA requirements. To simulate this load, I applied a vertical load of 8,700 lb to the collar on the hardlink sleeve.
2) I constrained the cut section of the cheek plates to zero displacement.

3.2.5.2. Hardlink mount FEA results

The von Mises stress plot of the hardlink mount is presented in Figure 3.5. The von Mises stresses in the cheek are all less than 24,000 psi. The stresses in the doubler welds are computed in the next section. The peak stress in the hardlink sleeves is less than 48,000 psi. The stresses in the hardlink pin are less than 24,000 psi. The safety factors for these components are listed in Table 3.3.

Table 3.3 Safety factors for the hardlink mount assembly.

Component	n_{yield}	$n_{ultimate}$
Cheek plate	36,000 / 24,000 = 1.5	58,000 / 24,000 = 2.4
Hardlink sleeve	162,000 / 48,000 = 3.4	182,000 / 48,000 = 3.8

Hardlink pin	135,000 / 24,000 = 5.6	170,000 / 24,000 = 7.1
Cheek plate stiffener	40,000 / 20,000 = 2	45,000 / 20,000 = 2.3

Although the safety factors for the cheek plate and cheek plate stiffener do not meet the standard NFAC safety factor requirements ($F.S._{ultimate}$ is below 4.0), they meet the requirements for a class 3 load. ($F.S._{yield}$ = 1.5 and $F.S._{ultimate}$ = 2.0 * FB). FB for A36 steel in this condition is 1 because it's ductility is greater than 15% and FB for 6061-T6 aluminum is also 1 [13]. These components were statically tested when the hub weldment was tested. The results are presented in Chapters 3 and 4 of my thesis *The Mechanical Design, Analysis, and Testing of a Two-Bladed Wind Turbine Hub*.

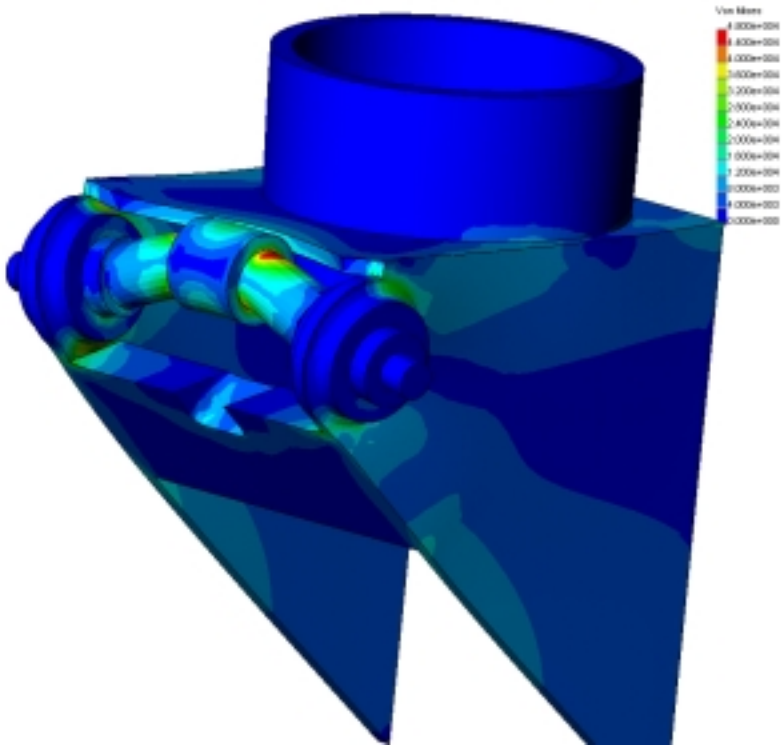

Figure 3.5: Von Mises stress plot of the hardlink mount (deflection x 75).

3.2.5.3. Doubler weld check

The finite element analysis of the cheekplate assumes that the doublers are attached to the cheekplate over their entire surface. I made this assumption because the FEA model was easier to make this way. I performed an analytical check on the cheekplate doubler welds. I considered the shear loads and bending loads on the welds.

The doublers have a 2" diameter and are .375 thick with .375" circumferential welds. Thus the weld area (A) of all four doubler welds is

$$A = 4\ (\pi\ D)\ \ .707 = 17.8\ in^2$$

The maximum teeter force is 8700 lb. The shear forces on the doubler welds are then 490 psi.

The doublers are space 6" apart (L). The bending moment on the doublers is

$$M = FL / 8 = 8700\ lb * 6" / 8 = 6525\ lb\text{-}in.$$

The unit second moment of area for two doublers is

$$I_u = 2(\pi r^3) = 2\pi 1^3 = 6.28\ in^3$$

The second moment of area for two doublers is then

$$I = .707 * h * I_u = .707 * .375\ in * 6.28\ in^3 = 1.66\ in^4$$

The bending stress in the welds is

$$\sigma = M * c / I = 6525\ lb\text{-}in * 1\ in / 1.66\ in^4 = 3931\ psi.$$

A simplified formula for the von Mises stress for combined shear and bending is given by Mischke [14] as

$$\sigma' = (\sigma_x^{\ 2} + 3\tau_{xy}^{\ 2})^{\frac{1}{2}}$$

where σ_x is the tensile stress due to bending and τ_{xy} is the shear stress thus

$$\sigma' = (3931^2 + 3 \times 490^2)^{\frac{1}{2}} = 4021 psi$$

This stress is significantly lower than the stresses surrounding the doublers for the cheek plates in the FEA results because the cheek plates are actually the weakest part. The cheek plates are only .25" thick and are subject to complex torsional and bending stresses.

According to AWS D1.1-98, the allowable stress in a fillet weld is .3 * the nominal tensile strength of the filler material. If 60 kpsi filler metal was used, the allowable tensile strength is 20 kpsi. The factor of safety against exceeding this allowable strength is

$$F.S._{allowable} = 20{,}000 / 4021 = 5$$

In addition, the AWS specifies a maximum fatigue stress range of 7000 psi [15] for an infinite life. The NFAC requires an additional safety factor of 2.0 on this stress range. The hardlink loads only vary significantly during teeter impacts. We plan to restrict the turbine during to wind speeds an yaw angles that don't cause extreme teeter impacts. An example of the allowable teeter impacts is shown in Figure 3.6. From this figure, it is evident that typically, the stress range is 25% of the peak value. Thus, I will assume that the typical stress range is 25% of 4,021 psi = 3,016 psi. Thus the safety factor against the AWS fatigue stress allowable is

$$F.S._{allowable} = 7{,}000 / 3{,}016 = 2.3$$

This meets the minimum NFAC requirement of 2.0.

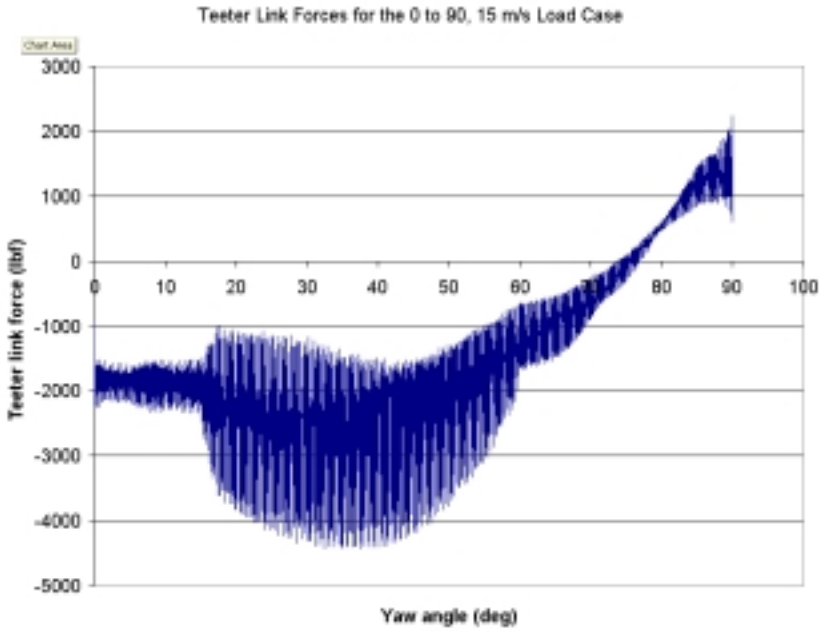

Figure 3.6: Typical teeter link forces.

3.2.5.4. Hardlink mount FEA validation

To check the FEA results, I computed the shear stress in the hardlink pin near the drill bushing supports. I assumed that the bending was negligible where the pin enters the end cap because the hardlink sleeve prevents the pin from deflecting significantly. Thus, the pins are in pure shear at this location and the stress is given by

$$\tau = \frac{F}{2(A_{Pincrosssectoin})} = \frac{8{,}700\,lb}{2\times .307\,in^2} = 14{,}169\,ksi$$

A simplified formula for the von Mises stress for combined shear and tension is given by Mischke [16] as

$$\sigma' = (\sigma_x{}^2 + 3\tau_{xy}{}^2)^{\frac{1}{2}}$$

where σ_x is the tensile stress (there is no tensile stress on this part) and τ_{xy} is the shear stress (11,075 psi) thus

$$\sigma' = (0^2 + 3\times 14{,}169^2)^{\frac{1}{2}} = 24{,}542\,psi$$

This value compares well with the von Mises stress determined in the FEA results of 24 kpsi. Thus, I conclude the FEA analysis is accurate.

3.2.5.5. Hardlink mount fatigue analysis

I analyzed the hardlink pin, hardlink sleeve, and cheekplate welds for fatigue. I used the technique presented by Shigley and Mischke [17] for these analyses. The hardlink pins are made from 17-4 H925 stainless steel. The endurance limit for the pins at 10^7 cycles is 88 kpsi [18]. The hardlink sleeve is made from cold finished 4140 steel. The endurance limit for quenched and tempered 4140 bars loaded in bending with R=-1 is 75 kpsi [19]. The cheekplate is made from A36 steel. The predicted endurance limit for buttwelded A36 steel plate with R=0 is 30 kpsi [20]

The formula for the corrected endurance limit for a field specimen (S_e) is

$$S_e = k_a\, k_b\, k_c\, k_d\, k_e\, S_e'$$

where

k_a = surface factor

k_b = size factor

k_c = load factor

k_d = temperature factor

k_e = miscellaneous affects factor

The calculation of S_e for the hardlink mount components is presented in Table 3.4.

Table 3.4: Calculation of S_e for the hardlink mount components.

Component	Parameter	Deffinition	Value	Comments	Se' kpsi	Se kpsi	Von Mises stress kpsi
Hardlink pin	ka	surface factor	0.87	Ground finish			
	kb	size factor	0.92	Bending and shear load; d = .625"			
	kc	load factor	1.00	Von Mises stress			
	kd	temp. factor	1.00	Room temp			
	ke	misc. affects factor	1.00	-			
	Effective k		0.80		88.0	**70.8**	24.7
Hardlink sleeve	ka	surface factor	0.86	Sanded finish			
	kb	size factor	0.87	Bending and shear load; d = .625"			
	kc	load factor	1.00	Von Mises stress			
	kd	temp. factor	1.00	Room temp			
	ke	misc. affects factor	1.00	-			
	Effective k		0.75		75.0	**56.3**	48
Cheek plate	ka	surface factor	0.79	Hot rolled plate			
	kb	size factor	1.00	-			
	kc	load factor	1.00	Von Mises stress			
	kd	temp. factor	1.00	Room temp			
	ke	misc. affects factor	1.00	-			
	Effective k		0.79		30.0	**23.7**	24

The predicted von Mises stresses in the hardlink pins and hardlink sleeve (24 kpsi and 48 kpsi respectively) are less than the component endurance limits (70.8 kpsi and 56.3 kpsi). Thus, fatigue is unlikely to cause a failure in the hardlink pins or sleeves.

The predicted von Mises stress in the cheek plates (24 kpsi) is higher than the component endurance limits (23.7 kpsi). However, this analysis assumed that a 8700 lb completely reversed loads is applied to the hardlink. In the worst case, the load actually fluctuates from 2000 to 8700 lb with a mean of 5350 lb and an alternating load component of ± 3350 lb. For fluctuating stresses, the Soderberg, Goodman, or Gerber equations are more realistic predictors of fatigue failure than assuming completely reversed stresses. The Soderberg criteria is the most conservative of these formulas [21]. However, the safety factor against

an infinite life is only .87. Thus, I performed this calculation using the Goodman criteria which is more liberal than the Soderberg criteria but more conservative than the Gerber criteria. The Goodman equation is

$$\frac{\sigma_a}{S_e} + \frac{\sigma_m}{S_{ut}} = \frac{1}{n}$$

where

σ_m is the mean stress component

σ_a is the alternating stress component

S_e is the component endurance limit

S_{ut} is the material ultimate strength

n is the factor of safety for fatigue (assuming an infinite life)

Because the FEA results are linear, the mean and alternating stress components are

σ_m = 24 kpsi * 5350 lb / 8700 lb = 14.8 kpsi

σ_a = 24 kpsi * 3350 lb / 8700 lb = 9.24 kpsi.

Thus the factor of safety against fatigue is

$$n = \frac{1}{\frac{\sigma_a}{S_e} + \frac{\sigma_m}{S_{yt}}} = \frac{1}{\frac{9.24}{23.7} + \frac{14.8}{58.0}} = 1.6$$

Thus the Goodman formula predicts an infinite life with a safety factor of 1.6. Therefore the component is unlikely to fail in fatigue.

3.3. Teeter encoders

The sole function of the each teeter encoders is to precisely measure the flap angle of each blade. The encoders are used for data acquisition only and are not necessary to run the turbine. The only failure of the encoders that could cause harm is if they flew off due to inertial loads.

Each encoder is mounted using four 10-32 screws. The largest significant load on the teeter encoders is due to the centrifugal forces of the rotor. The rotor spins at 72 RPM (7.54rad/sec). The formula for centrifugal force is

$$Force_{centripital} = \frac{mass \times \omega^2 \times r}{32.2 \frac{ft}{\sec^2}}$$

Thus, the inertial forces from the rotor rotation are 1.77 times as large as the part's mass for every foot the part is located from the center or

$$Force_{centripital} = 1.77 \times mass \times r$$

Equation 3-1: Centrifugal force for rotor components.

The teeter encoders are located 13" from the center of the rotor. Thus, the teeter encoder is only subjected to (1.77) (13/12 ft) (3lb) = 5.7 lb of force. This is negligible compared to the strength of the teeter encoder mounts.

3.4. Damper assembly

The teeter dampers consist of an elastomeric damper inside of a telescoping guide. Figure 3.7 displays a section view of the telescoping damper assembly. The telescoping guide uses a cleavis joint at each end to eliminate any side loading on the damper. The damper is an elastomeric damper made by Jarrett Inc. The damper is bolted to a stainless steel guide which slides inside of a copper bearing. The telescoping guide allows for free teeter until the flap angle reaches exceeds –1.49° from vertical. After –1.49°, the elastomeric damper compresses the button force sensor.

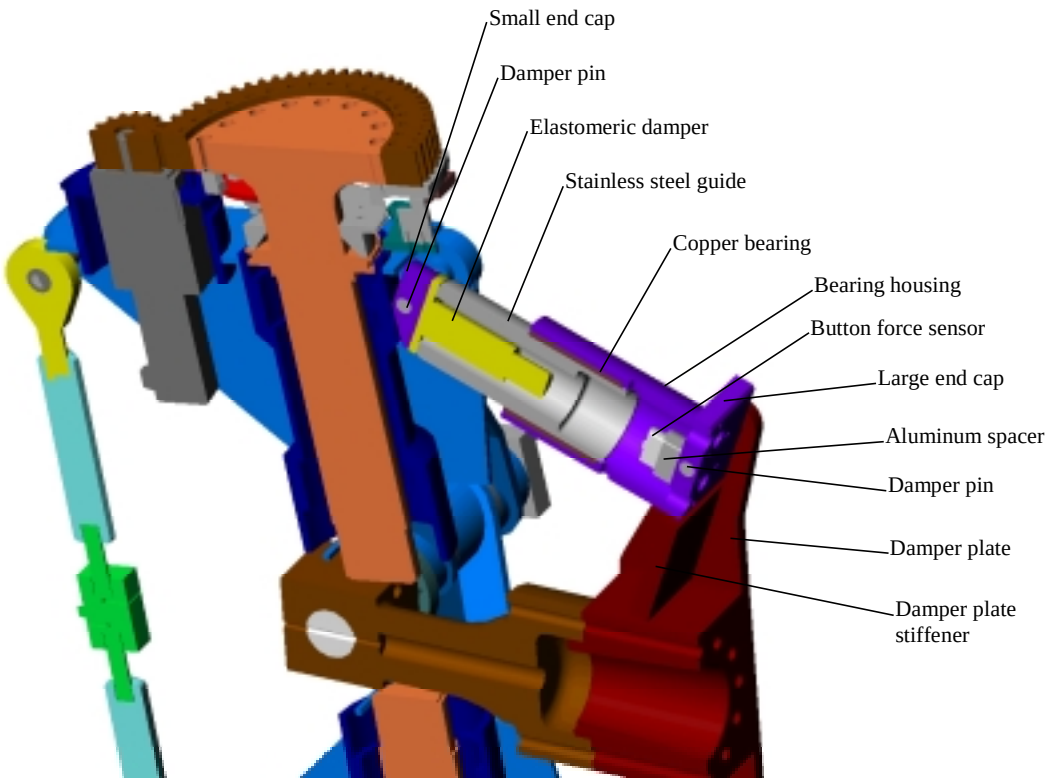

Figure 3.7: Section view of the telescoping damper assembly.

3.4.1. Critical components

The possible failure modes for the teeter damper are shear of the damper pins, failure of the screws which fasten the end caps, or failure of the teeter damper plates. Any of these failures would allow the hub to exceed its specified safe teeter range. Exceeding the safe teeter range would create the opportunity of the inboard section of the pitch shafts striking the hub shaft. Such an impact could create stress concentrations on the hub shaft and lead to eventual failure of the hub shaft. In addition, such a failure could allow a the blade to strike the tower.

3.4.1.1. Damper end cap, pin, bearing housing, and fasteners.

I performed a FEA analysis of the large end cap, pin, and bearing housing. I verified the FEA results for the damper pins using analytical methods. The deflection of the damper cap stresses the eight ¼-20 bolts used to fasten the bearing housing.

3.4.1.1.1. FEA analysis

Materials and construction:

The damper pins have been ground from aged 17-4 H925 stainless steel (155 kpsi yield, 170 UTS [22]). The damper pins are inserted through the damper plates and end caps with at most .003" clearance.

The end caps are made from 4150 steel quenched and tempered steel. The geometry of the end caps is such that the width of the large end cap is .050 smaller than the distance between the inside surfaces of the damper plates. Likewise, there is only .020 clearance between the small end cap and the mounts which hold the damper pins. The bearing housing is fastened to the end cap using ten ¼-20 L-9 grade (180 kpsi UTS) screws. The bearing housing is made from 6061-T6 Al and has helicoil inserts for the screws.

I performed stress analyses on the large end cap but not the small end cap because the small end cap is significantly stronger than the large end cap. The Jarret dampers have a ∅3" flange which distributes the load more evenly across the small end cap pin. On the large end cap, the button force sensor applies loads the large end cap via a ∅2" spacer attached to the center of the large damper plate. Furthermore, the large damper cap spans 6" between the damper plates while the small end cap only spans 4". The wider span of the large end cap makes it more susceptible to bending loads.

The FEA results for the large damper cap and pin are presented in Figure 3.8. The loads and assumptions I used are presented below.

FEA Loads:

1) I applied 9,000 lb to the same location as the damper spacer. This reduced load is necessary to meet the NFAC standard safety factors. We will not operate the turbine in conditions that exceed this load.
2) I restrained both ends of the damper pins (only one end of the pin is shown as restrained in Figure 3.8).

FEA assumptions:

1) I assumed that the bearing housing, damper pin, and the damper cap were made from one piece of 4150 quenched and tempered steel. This assumption was necessary to simplify the analysis.

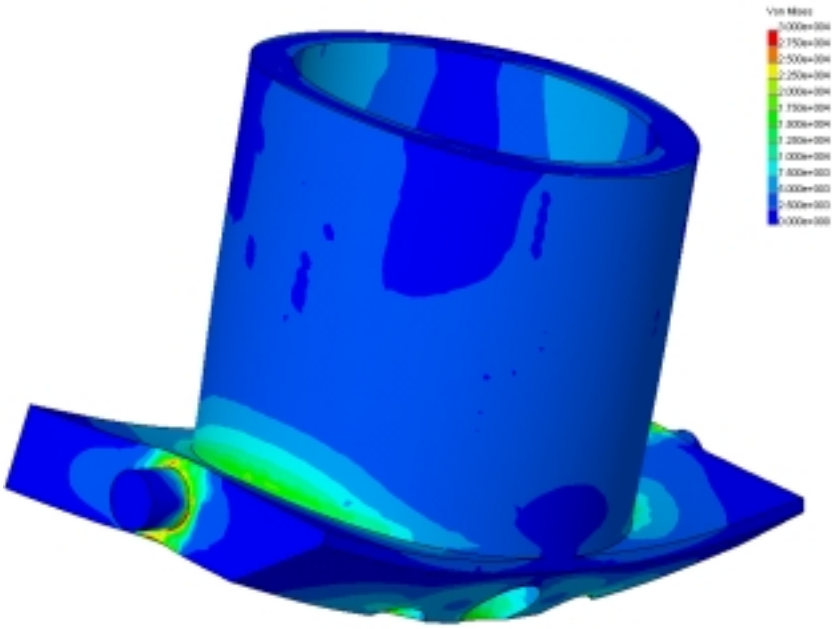

Figure 3.8: Large damper cap von Mises stress plot (deflection x183).

The peak stresses in the damper cap are near the damper pins. The peak von Mises stresses around the damper pins is 30 kpsi. The yield and ultimate stresses for the end cap steel (quenched and tempered 4150 steel) are 115 kpsi and 145 kpsi. The factors of safety for the damper cap are

$$F.S._{yield} = 115 / 30 = 3.8$$

$$F.S._{ultimate} = 145 / 30 = 4.8$$

The damper pins have stresses up to 30 kpsi. The damper pins were ground from 17-4PH SS H925 (131 kpsi yield, 153 UTS [23]). The safety factor for the damper pins are

$$F.S._{yield} = 131 / 30 = 4.4$$

$$F.S._{ultimate} = 153 / 30 = 5.1$$

To check the FEA results, I computed the shear stress in the damper pin near the end cap. I assumed that the bending was negligible where the pin enters the end cap because the deflection of the end caps prevent pins from deflecting significantly. Thus, the pins are in pure shear at this location and the stress is given by

$$\tau = \frac{F}{2(A_{Pincrosssectoin})} = \frac{9{,}000lb}{2 \times .307in^2} = 14.7ksi$$

The von-Mises equivalent stress for this shear stress is 25 kpsi. This value compares reasonably well with the von Mises stress determined in the FEA results of 30 kpsi considering no stress concentration factor was applied (I have not been able to find an applicable stress concentration factor).

3.4.1.1.2. Damper pin fatigue analysis

For the fatigue analysis of the damper pin, I used the technique presented by Shigley and Mischke [24]. The fatigue strength S_f' for a lab specimen of 17-4 steel PH steel aged to H925 for 10^7 cycles is 88 kpsi [25]. The formula for the corrected fatigue strength for a field specimen (S_e) is

$$S_f = k_a\, k_b\, k_c\, k_d\, k_e\, S_f'$$

where

k_a = surface factor

k_b = size factor

k_c = load factor

k_d = temperature factor

k_e = miscellaneous affects factor

The calculation of S_f is presented in Table 3.5.

Table 3.5: Calculation of Sf for the damper pin.

Parameter	Deffinition	Value	Comments	Se'	Se
ka	surface factor	0.485742	ground		
kb	size factor	1	-		
kc	load factor	1	Von Mises Stress		
kd	temp. factor	1	room temp		
ke	misc. affects factor	1	low cycle fatigue		
Effective k		0.485742		88,000	**42,745**

The predicted shear stress in the damper pins (30 kpsi) is significantly less than the component endurance limit (42.7 kpsi). Thus, fatigue is unlikely to cause a failure.

3.4.1.2. Damper plates

The teeter impact loads are transferred from the damper pins, through the damper plates to the hub shaft adapter (see Figure 3.18 for a descriptive picture of the damper plates). The damper plates are made from quenched and tempered 4150 steel. The damper plate stiffener is used to stiffen the damper plates in

torsion. We pressed two drill bushing into each plate to transfer the loads from the damper pins to the damper plates. We pressed the plates onto four ∅1" dowel pins.

I performed a numerical analysis on the damper plates. The results of the analysis are presented in Figure 3.9. I included both damper plates, the damper assembly, and the damper plate stiffener in the analysis to better simulate bending induced on the plates.

Loads and constraints:

1) I applied a 10,000 lb distributed load normal to the center of the end cap.
2) I restrained the 1" dowel pins bores (four are shown in Figure 3.9) to zero translation.

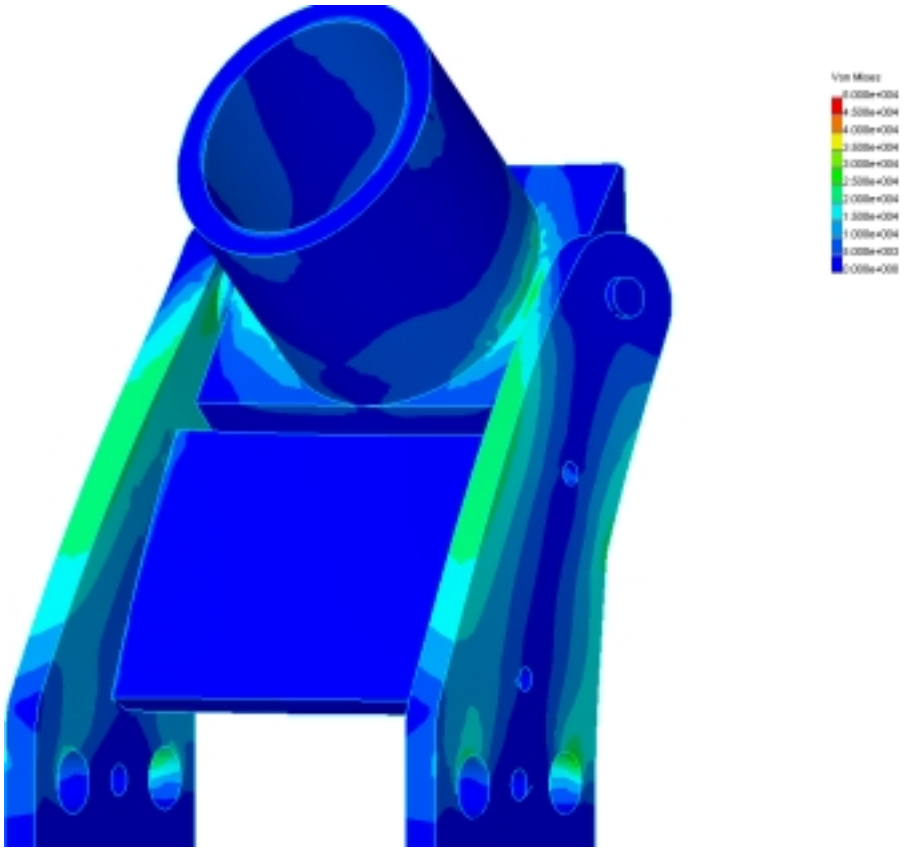

Figure 3.9: Damper plate von Mises stress plot (deflection X73).

The peak von Mises stresses (35 kpsi) occur in the damper plate at the dowel pin bores, the damper pin locations, and the edges of the damper plate. The yield and ultimate stresses for 4150 steel are 115 kpsi and 145 kpsi. The factors of safety for the damper plate are

$$F.S._{yield} = 115 / 35 = 3.3$$

$$F.S._{ultimate} = 145 / 35 = 4.1$$

The damper plate FEA analysis can be validated by comparing the analytically computed stresses at section A-A' in Figure 3.10. A stress element at "point A" in Figure 3.10 is subject to bending stresses

and torsional stress. If 5000 lb is applied to the damper plate shown, section A-A' is subject to a bending moment of (5000lb)(3.8")=19,000 lb-in. Assuming the damper plate is a rigid support for the 6" long damper pin, the torsional moment at the damper plate bushing is given by Shigley and Mischke as [26]

$$M = FL / 8 = 5000 \text{ lb} * 6" / 8 = 3750 \text{ lb-in.}$$

The bending stress is given by the flexure formula as

$$\sigma_x = My / I = 19{,}000*1.5 / 1.125 = 25{,}333 \text{ psi}$$

The torsional stress in a rectangular section is given by Shigley and Mischke as

$$\tau = \frac{T(3+1.8\frac{t}{w})}{wt^2} = \frac{3750(3+1.8\frac{.5}{3})}{8\times.5^2} = 6{,}187 \text{ psi}$$

The corresponding von Mises stress for these stress states is 27,500 psi. This stress value corresponds well to the FEA results of 20,000 to 25,000 psi.

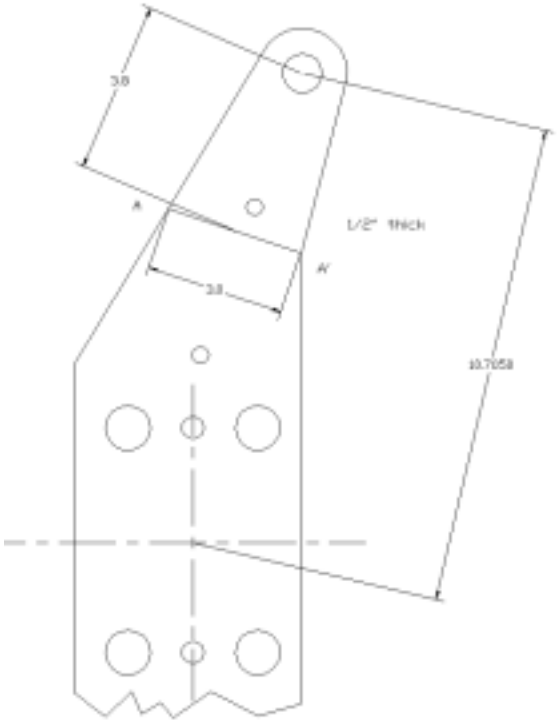

Figure 3.10: Damper plate section used to validate FEA results.

3.4.1.3. Damper plate dowel pins

The failure mode for the dowel pins is shear. The dowel pins are subject to a shear load 'V' and a moment load 'M'. Both of these loads create shear stresses in the dowel pins.

If I assume that a 10,000 lb teeter impact load is distributed evenly between the two Damper plates, then each plate is subject to a 5000 lb shear load and a (5000 lb)*(10.4 in) = 52,000 in-lb moment load.

The shear force on each bolt due to the shear load is 5000 lb / 4 = 1250 lb.

The shear force on each bolt due to the moment load is given by Shigley and Mischke as [27]

$$\frac{M}{4r} = \frac{52{,}000lb-in}{4\times 3in} = 4333lb$$

Assuming these forces add, the worst case load for one of the teeterpin bolts is

4333 + 1250 = 558l lb

The shear stress caused by this load is 5581 / (π .5^2) = 7106 psi.

The single shear strength of an American Standard hardened ground machine dowel pin is 130 kpsi [28]. Thus the factor of safety is at least

F.S. = 130,000/ 7106 = 18.3

3.4.2. Non-critical components

The Jarrett dampers, force sensors, and spacers are not critical components because they are failsafe. They are all loaded in compression during teeter impacts. Each of these components is solidly backed and will transfer the teeter impact load to the damper pins even if their rated loads are exceeded.

3.5. Blade assembly

Figure 3.11 presents the components in the blade #3 assembly. We have determined that the blade camera will not be used during the wind tunnel testing. Each blade is attached to the pitch shaft using eighteen ½-20 UNF B7 studs ($S_{y\,min}$ = 101 kpsi). The following sections analyze the blades, blade studs, pitch shaft, and camera mount.

We have determined that the blade camera will not be used during the wind tunnel testing. However, the blade camera mount bracket will be used on the non-instrumented blade to secure the weights used to balance the instrumented blade (see Figure 3.12).

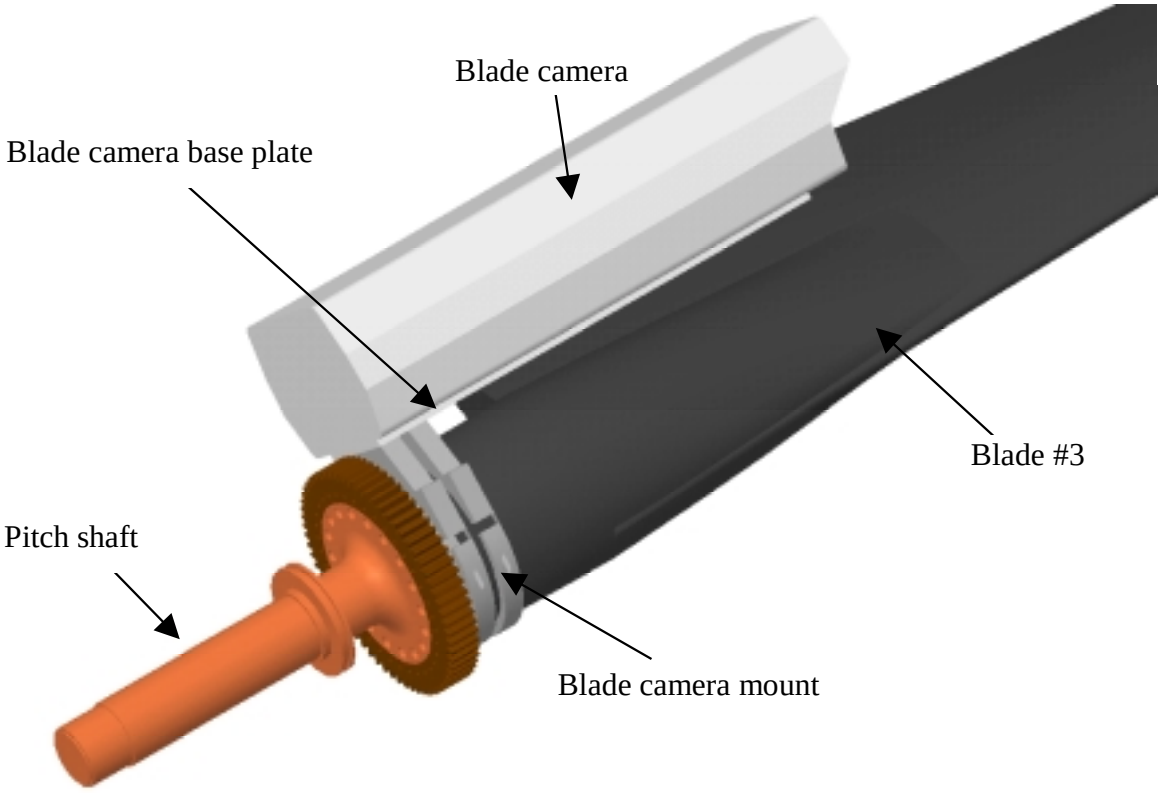

Figure 3.11: Phase V instrumented blade assembly.

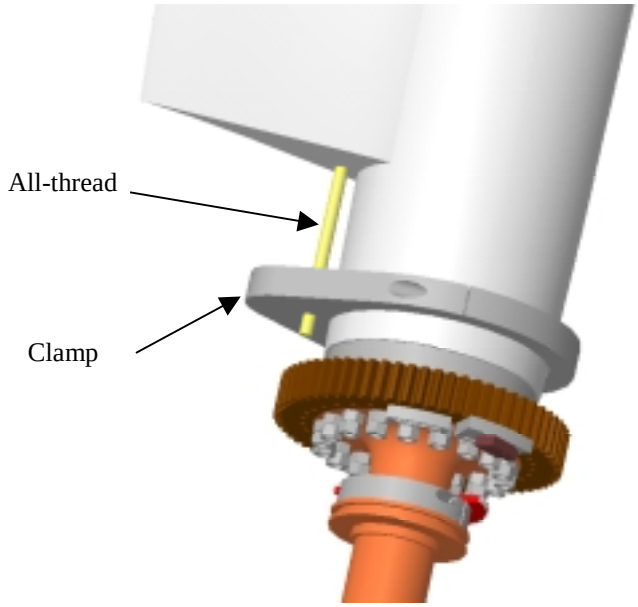

Figure 3.12: Phase VI non-instrumented blade assembly.

3.5.1. Fragmentation energy analysis

The blade and blade tip are the only two components I find necessary to include in the fragmentation energy analysis. The formula for the energy level is

$$e = W V^2/(1000^2 A)$$

where W = weight of unit (lb)

V = velocity at instant of separation (ft/sec)

A = Minimum cross sectional area, in^2

The weight of one blade is roughly 135 lbs. The center of gravity of each blade is roughly 6.56 ft (2 m) from the center of rotation. The velocity at the instant of separation is

$$V = r\,\omega = 6.56 \text{ ft } ((72 \text{ rev/min} * (2\pi \text{ rad/rev}) / (60 \text{ sec/min}))^2 = 49.5 \text{ ft / sec}$$

For the area, I used the plan area of the smallest airfoil on the blade (at the tip). The area of this section is 103.9 in^2. Thus the energy level is

$$e = 135 * 49.5^2 / (1000^2 * 103.9) = .0032$$

The corresponding thickness for steel armor plate is

$$t = 235.5/BHN * W/Ac * (V/1000)^2 = (235.5/300)\ (135/103.9)\ (49.5/1000)^2 = .002$$

It appears that this formula is not valid for such low energy assemblies.

3.5.2. Critical components

3.5.2.1. Blade weight clamp and all-thread

The blade weight clamp is used on the non-instrumented blade to secure the weights used to balance the instrumented blade (see Figure 3.12). The weights are screwed onto ½ UNC B7 all-thread ($S_{y\ min}$ = 101 kpsi). The clamp is made from 6061–T6 aluminum clamped together with two 3/8-16 UNC bolts with locking heli-coils.

The weights strung along the all-thread weigh approximately 35 lbs (15.9 kg). The center of gravity of these weights and the all-thread lies approximately 6.5 ft (2 m) from the rotor center. Thus, the centrifugal load applied to the clamp is

$$15.9 \text{ kg} * 2 \text{ m} * (72 \text{ rev/min} * 60 \text{ min/sec} * 2\pi / \text{rev})^2 = 1{,}812 \text{ N} = 407 \text{ lb.}$$

I analyzed the clamp to ensure it is capable of providing a sufficient moment reaction. In this analysis I made the following assumptions.

1) The moment applied to the clamp is resisted solely by the half of the clamp with the all thread. This is a reasonable assumption considering bending is unlikely to be transferred across the bolts while pre-load exists in the clamped surface.
2) The bending in the clamp is resisted by the load distribution shown in Figure 3.13. The load is distributed on the blue out-lined section. I assumed that the force is constant across the width of the clamp but varies linearly over the height of the clamp. "f(x)" represents the total force for a given "x" location. I arrived at this assumption by observing the clamps which had been

in service. The clamps have contact marks where they contacted the blades. These contact points were approximately 1.25" away from the hole for the all-thread.

3) The blue outlined section can be represented as a flat surface 1.25" away from the all-thread. This is a conservative assumption considering 1.25" is the furthest distance from the all-thread. The closest point of the blue surface is only .75" from the all-thread center. The further distance means that there will be more of a bending moment on that section from the all-thread.

4) The pre-load in each grade 8 bolt is 1/2 of the proof load (9,300 lbs) or 3,100 lbs. This is a conservative assumption because the aluminum has ½" heli-coils inserted in them. Heli-coil manufacturer literature indicates the heli-coil in 6061-T6 has an ultimate strength of over 15,000 lbs while the grade 8 bolt has only an ultimate strength of 11,620 lbs.

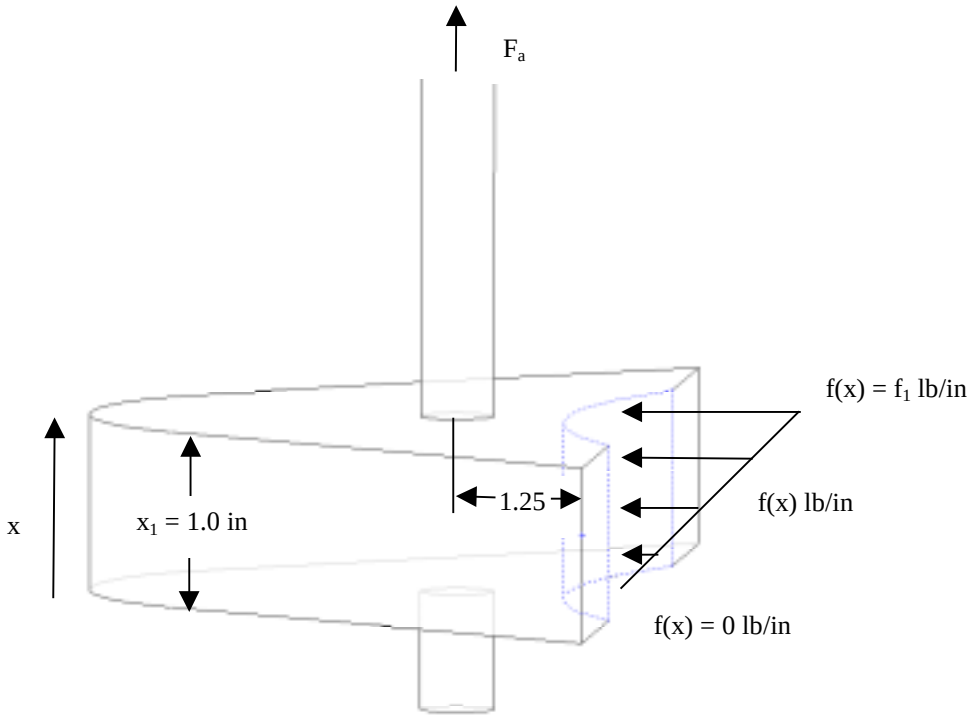

Figure 3.13: Force distribution on the blade weight clamp.

The function f(x) can be written as

$$f(x) = (f_1 / x_1) * x$$

The force f_1 can be found by integrating the function along X and setting it equal to the total bolt preload 2P.

$$½ f_1 x_1 = 2P$$

$$f_1 = 4P/x_1 = 4* 3{,}100 \ / 1 = 12{,}400 \text{ lb/in}$$

The maximum moment the clamp can support and still have the assumed force distribution is

$$M_{\max} = \int_0^{x_1} f(x)x\,dx = \int_0^{x_1} \frac{f_1}{x_1} x^2\,dx = \frac{f_1 x^3}{3x_1}\Big|_0^{x_1} = \frac{f_1 x^2}{3} = \frac{12{,}400 * 1^2}{3} = 4{,}133\ in-lb$$

The applied moment on the blue outlined section is

M = Fa * 1.25” = 407 lb * 1.25” = 509 lb-in

Thus the safety factor against exceeding this pre-load is

$F.S._{preload} = M_{max} / M_{applied} = 4{,}133 / 509 = 8.1$

All-thread strength check:

The all-thread strength should also be checked. B7 all-thread has a minimum yield strength of 700 MPa or 101kpsi.

The minimum yield strength for grade 5 bolts is 92 kpsi and grade 7 bolts is 115 kpsi. A grade 5 ½-13 bolt has a proof load of 12,050 lb. Assuming the all-thread is at least as strong as a grade 5 bolt, the safety factor against breaking the all-thread is

$F.S._{preload} = M_{max} / M_{applied} = 12{,}050 / 407\ lb = 29.6$

3.5.2.2. Blade

The phase V constant chord blades and phase VI tapered blades were designed and built by Composite Engineering in Concord, Massachusetts. The phase V and phase VI blades were engineered to the same strength standards. Composite engineering used a numerical code developed by Edward Van Dusen and Forrest Stoddard to determine the blade deflections and local strain at any specified position on the blade. They used the code to estimate the stresses in the spar and skin with the blades parked flapwise to 108 mph winds.

In this configuration, the code predicted a peak flap bending moment of 13,532 ft-lb[29]. The ADAMS results indicate that the peak bending moment and flapwise shear we will see during NFAC testing is 9,758 ft-lb and will occur during the 0° to 180° varied yaw testing. The loads Composite Engineering used to design the hub are 140% greater than the peak loads in the ADAMS simulations.

The design report written by Composite Engineering indicates that the peak stresses in the spar (33,956 psi) during the parked 108 mph loads case are less than half of the laminate strength. Thus, the spar has a safety factor of at least 2 for the 108 mph load case and 2* 140% = 2.8 for NFAC testing. The blades are gauged with strain gauges, thus they meet the requirements for a class 3 load.

The design report written by Composite Engineering indicates that the peak stresses in the skin (5,981 psi) during the parked 108 mph loads case are less than one quarter of the laminate strength at that section. Thus, the skin has a safety factor of at least 4 for the 108 mph loads case and an effective safety factor of 4 * 140% = 5.5 for NFAC testing.

3.5.2.3. Blade studs

The blade root is made from a 6061-T6 aluminum. The root is attached to the pitch shaft using eighteen ½" grade 8 studs. The studs have ½-13 UNC threads on one side and ½-20 UNF threads on the other. The coarse threads are inserted into 1" long, locking Heli-coils in the blade root. According to Heli-coil manufacture literature, the heli-coils have approximately a 37,500 lb pull out strength in 6061 T6 aluminum.

We turned a 1" length on each of the studs to ∅.400. This reduced section ensures that the stud will yield at the turned section rather than fail the blade root threads thereby ruining the blade. We performed a tensile test of a modified stud. The stud began to neck at 19,391 lb of tension. This result agrees reasonably well with an analytical prediction of when the stud will fail. A grade 8 bolt has a minimum yield strength of 130 kpsi. The minimum tensile forces necessary to yield a grade 8 steel, ∅.400, rod is

$$T = 130{,}000 \text{ psi} * \pi * .400^2 / 4 = 16{,}336 \text{ lb.}$$

The minimum tensile forces necessary to break a grade 8 steel, ∅.400, rod is

$$T = 150{,}000 \text{ psi} * \pi * .400^2 / 4 = 18{,}849 \text{ lb.}$$

3.5.2.3.1. Tensile strength check

According to the NFAC Test-Planning Guide, "the allowable stresses in threaded fasteners shall be based on the requirements for ductile materials…without consideration of preload" [30]. In this section, I calculate the stresses in the blade studs due to aerodynamic and centrifugal forces.

The forces on the pitch shaft which place tension on the studs are the edgewise and flapping moments (Mx and My receptively) and the centrifugal load Fz. The pitch moment Mz and the edgewise and flapwise forces (Fx and Fy) are shear loads on the studs. Table 3.6 lists magnitudes of these loads.

In the following analysis, I assume

1) The peak values of Mx, My, and Fz occur simultaneously.
2) I combined the moments Mx and My and assumed the resultant moment acted across the X-axis.
3) Tension and shear applied to the blade cap is applied evenly to all eighteen studs.
4) Moments applied to the blade cap create a linear load distribution and reaction as shown in Figure 3.14.

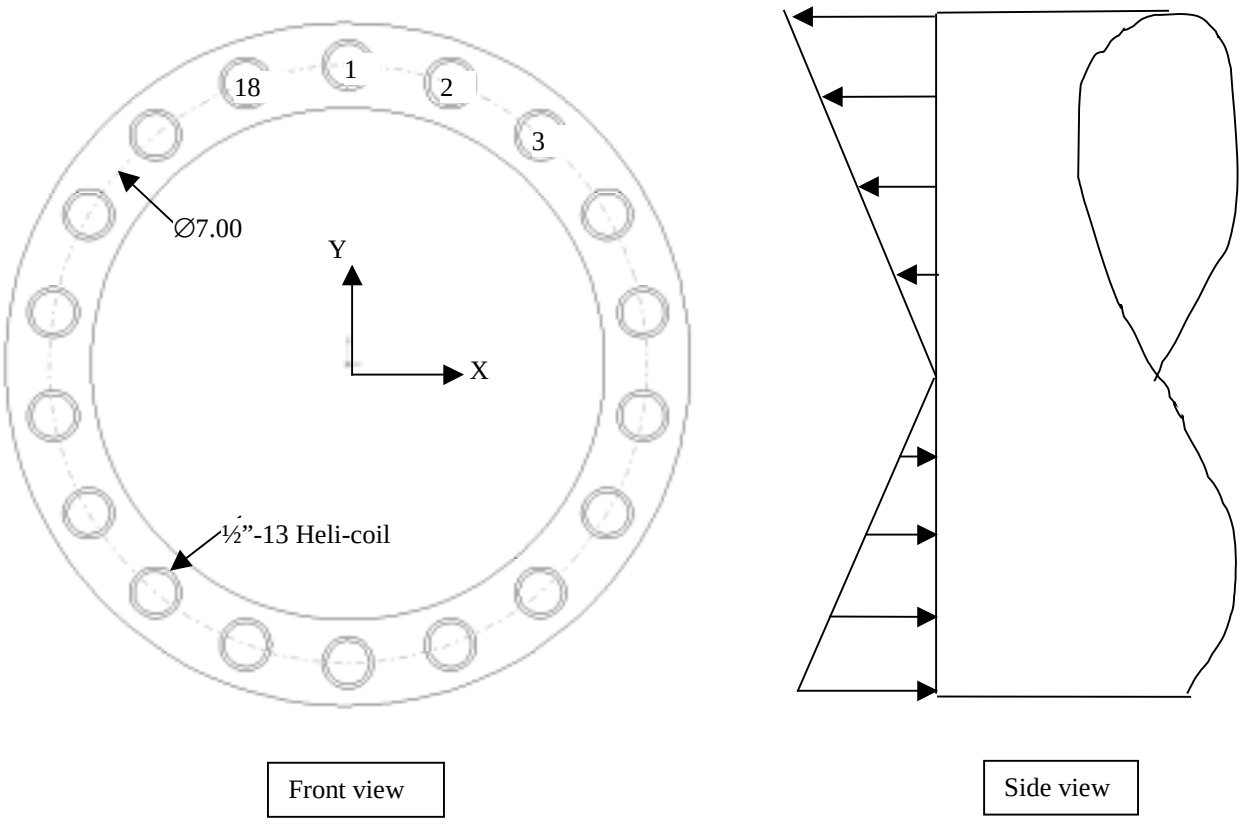

Figure 3.14: Bolt pattern geometry and tension distribution.

Table 3.6: Loads used in blade analyses.

Component	Maximum value (lb or ft-lb)
Fx (Thrust)	1,768
Fy (Edge)	565
Fz (Centrifugal)	4,493
Mx (Edgewise)	4,667
My (Flapwise)	9,758
Mz (Pitch)	249

Tension on stud 1 due to Fz:

$$Tension_{Fz} = Fz / 18 = 4{,}493 / 18 = 250 \text{ lb}$$

Tension on stud 1 due to Mx and My :

The resultant of Mx and My ($M_{x\&y}$) is $(4{,}667^2 + 9{,}758^2)^{.5} = 10{,}817$ ft-lb

The stress in the i^{th} stud can be found using the flexure formula for beams:

$$\sigma_i = (M)\,(y_i) / (I) = (M)\,(y_i) / \Sigma(y_i^2)\,dA$$

Thus the stud tension in the i^{th} stud is

$$\text{Stud tension}_i = (\sigma_i)\,(A_{stud}) = (M)\,(y_i)\,(A_{stud}) / A_{stud}\,\Sigma(y_i^2)$$

$$\mathbf{Tension_i = (M)\,(y_i) / \Sigma(y_i^2)}$$

(see Table 3.7 for y_i and Σy_i^2 values)

Therefore

$$\text{Tension}_{Mx\&y} = (Mx_{\&y})(y_1) / \Sigma(y_i^2)$$

$$\text{Tension}_{Mx\&y} = (10{,}817 * 12)(3.5) / 110.25 = 4{,}121 \text{ lb}$$

The total tension on bolt 1 due to $M_{x\&y}$ and Fz is

$$T_1 = 4121 + 250 = 4{,}371 \text{ lb}$$

As discussed previously, the theoretical yield point for the turned ∅.400 section is 16,336 lbs. The proof strengths of the ½-20 UNF and ½-13 UNC grade 8 threads on the stud are 19,200 lb and 17,050 lb respectively. Thus the turned section is the critical section. Thus the safety factors against the yield and ultimate strengths are

$$\boxed{F.S._{yield} = S_{yield} / \text{Tension}_{Mx\&y} = 16{,}336 / 4{,}371 = 3.7}$$

$$\boxed{F.S._{ultimate} = S_{ultimate} / \text{Tension}_{Mx\&y} = 18{,}849 / 4{,}371 = 4.3}$$

Table 3.7: Distance values for blade root analyses.

Stud	yi (in)	sum yi^2 (in^2)
1	3.50	12.25
2	3.29	10.82
3	2.68	7.19
4	1.75	3.06
5	0.61	0.37
6	-0.61	0.37
7	-1.75	3.06
8	-2.68	7.19
9	-3.29	10.82
10	-3.50	12.25
11	-3.29	10.82
12	-2.68	7.19
13	-1.75	3.06
14	-0.61	0.37
15	0.61	0.37
16	1.75	3.06
17	2.68	7.19
18	3.29	10.82
Sum		110.25

The NFAC Test Planning guide requires "the allowable stresses in threaded fasteners shall be based on the requirements for ductile materials…without consideration of preload" [31]. The safety factor against the ultimate strength is 4. Thus the blade cap studs have an acceptable safety factor for tension.

3.5.2.3.2. Shear strength check

The NFAC Test Planning Guide requires that the fasteners in critical structures which use friction to transfer the loads be designed to carry the full shear load without the benefit of friction. The pitch moment (Mz) and the edgewise and flapwise forces (Fx and Fy) are shear loads on the studs.

Assumptions:

1) Assume there is no friction in the blade which resists the shear loads.
2) Assume the shear loads are equally distributed among the eighteen studs.
3) Assume the peak values of Mz, Fx, and Fy occur simultaneously.

The resultant of Fx and Fy is $(Fx^2 + Fy^2)^{.5}$ = 1,856 lb

The shear load on each stud due to Fx and Fy is

$$V_{Fx\&y} = 1{,}856 \text{ lb} / 18 = 103 \text{ lb}$$

Shear in stud 1 due to Mz:

The load Mz represents the pitch torque on the pitch blade. The shear load on each bolt necessary to resist this torque is

(249 ft-lb * 12 in/ft) / (18 bolts * 3.5 in) = 47 lb.

Total shear in each bolt is

$V = V_{Fx\&y} + V_{Mz} = 103 + 47 = 150$ lb

This creates a shear stress in the ∅.400 section of

$\tau = V/A = 150 \text{ lb} / (.4^2 \pi / 4) = 1{,}197$ psi

The allowable ultimate strengths for a section in shear is 2/3 the of the material ultimate strength [32]. Thus the allowable shear for the studs is .667 * 150,000 psi = 100,000 psi

$F.S._{shear} = V_{allow} / V_1 = 100{,}000 / 1{,}197 = 84$

Combined shear and tension:

I calculated the von Mises stress to determine the factor of safety of a fastener in combined tension and shear. A simplified formula for the von Mises stress for combined shear and tension is given by Mischke [33] as

$$\sigma' = (\sigma_x^{\ 2} + 3\tau_{xy}^{\ 2})^{\frac{1}{2}}$$

where σ_x is the tensile stress and is equal to $T_1 / At = 4371 \text{ lb} / (.4^2 \pi / 4) = 34{,}783$ psi
and τ_{xy} is the shear stress (1,197 psi) thus

$$\sigma' = (34{,}783^2 + 3 \times 1{,}197^2)^{\frac{1}{2}} = 34{,}845 \, psi$$

$F.S._{\sigma'} = 150{,}000 / 34{,}845 = 4.3$

3.5.2.3.3. Joint preload check

According to the NFAC Test-Planning Guide, "A sufficient number of studs shall be provided with preloads so that the net joint preload for all loading is at least two times the operating loads. [34]". For the preload analysis, I assumed that the studs were preloaded to 50% of their proof load (.5 * 16,663 = 8,331 lb). The tensile strength check results indicate that the peak tension in the blade studs is 4,371 lb. The safety factor against exceeding the preload in a stud is

$F.S._{Tension\ preload} = 8{,}331 \text{ lb} / 4{,}371 \text{ lb} = 1.9$

Although this safety factor is slightly smaller than the required 2.0, it is satisfactory consider my conservative assumptions that the studs are only tensioned to half their preload and that the peak loads all occur simultaneously.

3.5.2.4. Pitch shaft

The pitch shaft is made from quenched and tempered cast 8630 steel (S_{ult} = 137 kpsi, S_y = 126 kpsi) [35]. The pitch shaft is subject to the same aerodynamic and centrifugal loads as the blade root (see Table 3.6). The bending and shear loads are resisted by a pair of roller bearings. The thrust load is resisted by thrust ball bearings.

3.5.2.4.1. Pitch shaft FEA methodology

I preformed an FEA analysis on the pitch shaft. Figure 3.15 displays the FEA loads on the pitch shaft. I included a part of the blade in the analysis to make the load application more realistic. I applied the same loads to the pitch shaft as in the blade stud calculations. However, I used a reduced value of My (flapwise bending) since we will not be running the turbine with extreme teeter impacts as we did in the simulations. I have listed these loads again in Table 3.8. The assumptions I made during the analysis are presented below.

FEA Assumptions:

1) I assumed that the clamping force was sufficient so that I could model the blade and the pitch shaft as one solid component.
2) I did not include in the analysis the spur gear which is pressed onto the pitch shaft flange. The spur gears directly transfer the pitch moment to the blades. The load path has no affect on the inboard section of the pitch shaft.

FEA load application:

1) I used a reduced value of My (flapwise) bending since we will not run the turbine in regimes where there are extreme teeter impacts (such as during 25 m/s wind at large yaw angles). I used the next largest My value 6,266 lb from the rigid 0 to 180 load case.
2) I used the blade coordinate system presented in the accompanying loads document.
3) I restrained the pitch shaft (see the green arrows in Figure 3.28) in the radial direction at radial bearing locations.
4) I restrained the pitch shaft in the axial and circumferential directions (see the green arrows in Figure 3.28) at location of the lock nut which restrains the blades radially.
5) I combined the loads Fx and Fy into a resultant force and the moments Mx and My into a resultant moment. I assumed these loads acted in the same direction.

Table 3.8: FEA loads for the pitch shaft analysis.

Component	Value	Notes on load application
Shear (Fx & Fy)	1,768 lb & 565 lb Resultant: $F_{x\&y}$ = 1,856 lb	Applied to pitch shaft flange
Centripetal (Fz)	4,493 lb	Applied to blade
Bending (Mx & My)	4,667 ft-lb & 6,266 ft-lb Resultant: $M_{x\&y}$ = 7,812 ft-lb	Applied to blade as a 31,251 lb force couple 3" apart
Pitch (Mz)	0 ft-lb	The bottom of the pitch shaft is not in the load path

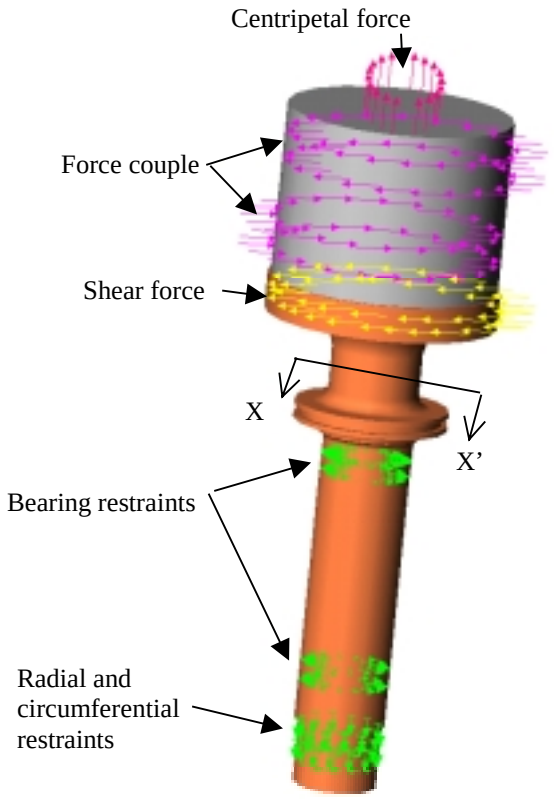

Figure 3.15: Loads applied to the pitch shaft.

3.5.2.4.2. Pitch shaft FEA results

The von Mises stresses in the pitch shaft are plotted in Figure 3.16. The peak stress (42,000 psi) occurs just above the outboard bearing restraint.

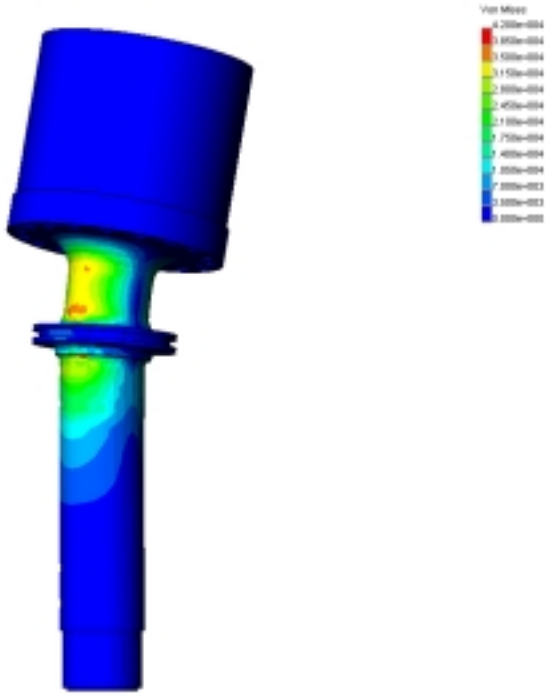

Figure 3.16: Von Mises stress plot for the pitch shaft.

The safety factor against yielding is

$$F.S._{yield} = S_{yield} / \sigma' = 128{,}000 / 42{,}000 = 3.0$$

and the safety factor against exceeding the ultimate strength is

$$F.S._{ultimate} = S_{ultimate} / \sigma' = 135{,}000 / 42{,}000 = 3.2$$

Although these safety factors do not meet the standard NFAC safety factor requirements ($F.S._{ultimate}$ is below 4.0), they meet the requirements for a class 3 load. ($F.S._{yield}$ = 1.5 and $F.S._{ultimate}$= 2.0 * FB). FB for 8630 steel is 1 because the reduction in area is greater than 15% [36].

In order to qualify for a class 2 load, the yaw shaft must be proof tested up to 125% of the peak load. The peak value of $M_{x\&y}$ used in this analysis was 6,266 ft-lb. 125% of this value is 7,832 ft-lb. The peak value of My measured in the field is 5,430 ft-lb. Although this value is significantly less than 7,832, we plan to obtain additional proof testing during the field testing before NFAC testing.

3.5.2.4.3. Pitch shaft FEA validation.

I validated the FEA results by showing agreement with a known analytical solution for the stresses at section X-X' in Figure 3.15. In this validation, I resolved the loads applied to the blade and flange at section X-X' (see Table 3.9). The section properties of section X-X' are listed in Table 3.10.

Table 3.9: Pitch shaft loads and reactions.

ADAMS load at the blade/ pitch shaft interface	Reactions at section X-X'
$F_{x\&y}$ = 1,856 lb	$R_{x\&y} = F_{x\&y}$ = 1,856 lb
$M_{x\&y}$ = 6,266 ft-lb	$MR_{x\&y} = M_{x\&y} + (2.8"/12)(F_{x\&y})$ = 6,699ft-lb

Table 3.10: Pitch shaft interface section properties.

Property	Formula	Value
Distance below hub shaft / blade interface	-	2.8"
Diameter (d)	-	3.125"
Cross sectional area (A)	$\pi (d^2) / 4$	7.670 in^2
Area moment of inertia (I)	$\pi (d^4) / 64$	4.681 in^4

Table 3.11: Stress calculations for the pitch shaft.

Stress	Formula	Calculation	Value (psi)
Bending	$\sigma_x = (MR_{x\&y})(d / 2) / I$	6,699 (12) (3.125 / 2) / 4.681	36,833
Shear	$\tau_{xy} = F_{x\&y} / A$	1,856 / 7.670	242

The shear stress at section X-X' is negligible compared to the bending stress. With this assumption, von Mises stress at section X-X' is equal to the bending stress (36.8 kpsi). This value agrees reasonably well with the FEA von Mises stress in that region of 31 to 35 kpsi. Thus, I conclude that the FEA analysis is accurate.

3.5.2.4.4. Pitch shaft fatigue analysis

The peak stresses in the pitch shaft occur at section X-X'. Here I calculate the endurance limit at this section and show that the stresses in the Pitch shaft are below this value.

According to Mischke, the endurance limit for steel can be related to the ultimate strength. The material endurance limit for 8630 steel in this condition is roughly 65 kpsi for a smooth specimen [37]. The formula for the component endurance limit (S_e) is

$$S_e = k_a k_b k_c k_d k_e S_e'$$

where

k_a = surface factor

k_b = size factor

k_c = load factor

k_d = temperature factor

k_e = miscellaneous affects factor

The calculation of S_e is presented in Table 3.12. The load factors were calculated using formulas from Shigley and Mischke [38].

Table 3.12: Calculation of the enduarance limit for the pitch shaft.

Parameter	Deffinition	Value	Comments	Se'	Se
ka	surface factor	0.733049	Machined finish		
kb	size factor	0.858251	Nonrotatating solid		
kc	load factor	1	Using von Mises stress		
kd	temp. factor	1	Room temperature		
ke	misc. affects factor	1	-		
Effective k		0.629139		65,000	**40,894**

The component endurance limit (41 kpsi) is slightly lower than the predicted peak stress (of 42 kpsi). This does not meet the criteria for an infinite life. However, I assumed a completely reversing load. The flap load Mx is responsible for most of the stress in the pitch shaft. When Mx peaks (at roughly 115° yaw angle), it has a mean component of roughly 3133 ft-lb. Thus the alternating component can be assumed as roughly 3133 ft-lbs. To find a more realistic endurance limit by using the Goodman equation, I can take into account the beneficial affect of the mean component. This equation is

$$\frac{\sigma_a}{S_e} + \frac{\sigma_m}{S_{ut}} = \frac{1}{n}$$

where

σ_m is the mean stress component

σ_a is the alternating stress component

S_e is the component endurance limit

S_{ut} is the material ultimate strength

n is the factor of safety for fatigue (assuming an infinite life)

Because the FEA results are linear, the mean and alternating stress components are

σ_m = 42 kpsi * 3100 lb / 6266 lb = 15.1 kpsi

$$\sigma_a = 50 \text{ kpsi} * 6258 \text{ lb} / 9758 \text{ lb} = 32.1 \text{ kpsi}.$$

Thus the factor of safety against fatigue is

$$n = \frac{1}{\frac{\sigma_a}{S_e} + \frac{\sigma_m}{S_{yt}}} = \frac{1}{\frac{32.1}{43.4} + \frac{17.9}{126}} = 1.1$$

Thus the Goodman formula predicts an infinite life with a safety factor of 1.1. Therefore the component is unlikely to fail in fatigue.

3.5.2.5. Pitch shaft lock nut

The pitch shafts are held in the barrels with a 3" AFBMA Standard Locknut (#AN-15). A typical steel for these locknuts is C1015 steel [39]. The minimum yield strength and tensile strengths for this steel in the cold drawn state is 54 and 64 kpsi. The pitch shaft is made from quenched and tempered cast 8630 steel (S_{ult} = 137 kpsi, S_y = 126 kpsi).

3.5.2.5.1. Pitch shaft thread shear strength check

The pitch shaft nut has a lower yield strength than the pitch shaft; thus, the pitch shaft nut is likely to fail first. I performed a shear strength check on the pitch shaft nut. I calculated the load capacity of the pitch shaft nut by dividing the allowable shear strength of pitch shaft nut by the thread shear area. The shear area of an internal thread given by the Machinery Hand Book as [40]

$$As = \pi \; n \; L \; D_{s\,Min}\left[\frac{1}{2n} + .57735\left(D_{s\,Min} - E_{n\,Max}\right)\right]$$

where

n = threads per inch = 12 tpi

L = length of engagement = .584 in

$D_{s\,Min}$= minimum major diameter of external thread = 2.933 in

$E_{n\,Max}$= maximum pitch diameter of internal thread = 2.8843 in

Thus the shear area is

$$A_s = \pi(12)(.584)(2.933)\,[(.5)/12 + .57735(2.933 - 2.8843)] = 4.506 \text{ in}^2$$

The allowable shear stress according to the Maximum Shear Stress failure theory is

$$\sigma_{allow} = (.667)\ 54 \text{ kpsi} = 36.0 \text{ kpsi}$$

The allowable tensile load on the pitch shaft nut is

$$P = \sigma_{allow} / A_s = 36{,}000 * 4.506 = 162{,}216 \text{ lb}$$

The peak centrifugal force on each blade was predicted using ADAMS to be 4,493 lb at 100 RPM.

The safety factor against exceeding the nut strength is

$$F.S._{ultimate} = 162{,}216 / 4{,}493 = 36$$

Clearly the tensile load is not an issue!

3.5.2.5.2. Pitch shaft thread preload check

According to the NFAC Test-Planning Guide, "A sufficient number of bolts shall be provided with preloads so that the net joint preload for all loading is at least two times the operating loads. [41]"

The alternating radial load component on the blades is due to gravity. Each blade weighs approximately 115 lb. This alternating load is negligible compared to the strength of a 3" AN-15 nut (162,216 lb). Thus, pre-load on this nut is not an issue.

3.5.3. Non-critical components

3.5.3.1. Pitch system

Figure 3.17 presents the components of the blade pitch system. The blades are pitched independently using a servo motor, gearhead, and a spur gear assembly. The limit switches are used to limit the blade pitch angle from -15° to 95° (90° is feathered into the wind). Failure of the pitch limit switches would result in the blade instrumentation wires being torn. The pitch hard stops are an added precaution to prevent damaging these wires.

The pitch system is not a critical structure because the hub was designed to withstand a malfunctioning pitch system. We simulated a pitch system failure using ADAMS (see the accompanying loads document). The simulation assumed that one blade pitches to feather while the other blade is still positioned in the run position. This failure induces loads in the hub shaft, blade root, yaw shaft, hardlink, and teeter dampers. The peak loads from this simulation have already been taken account in this document.

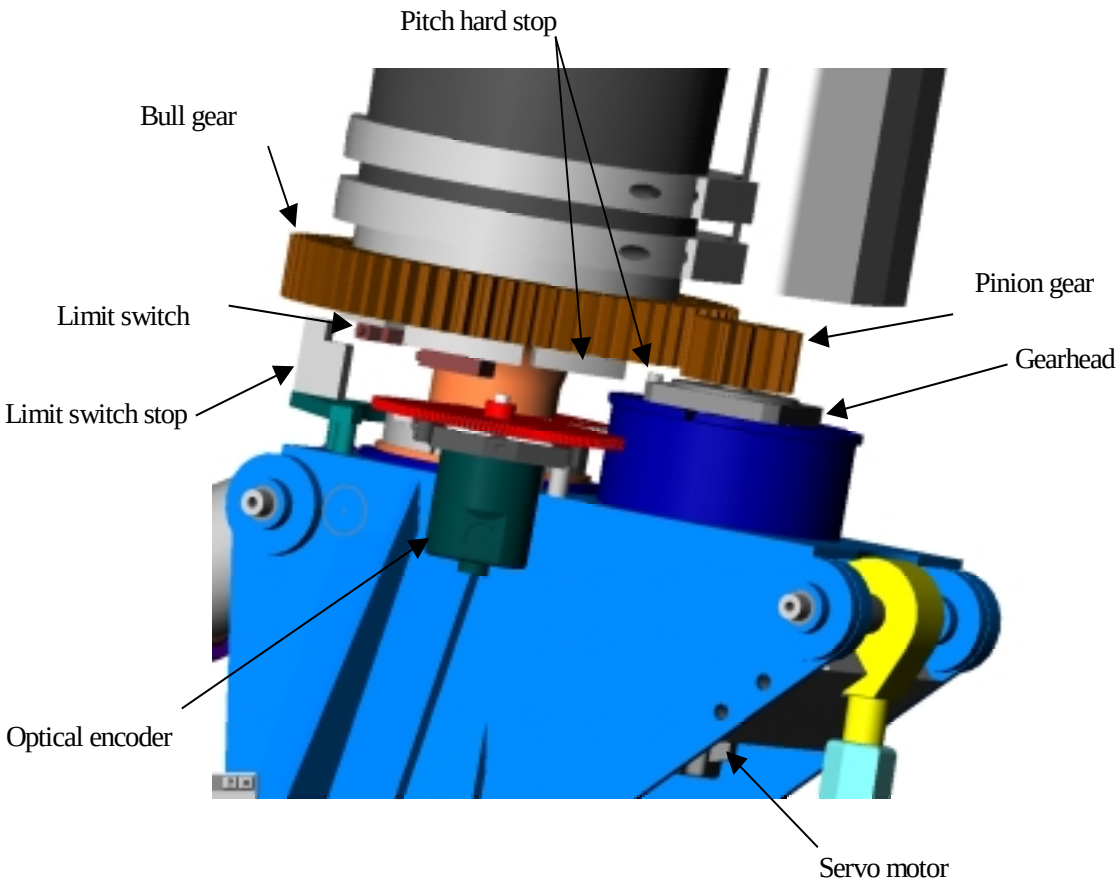

Figure 3.17: View of the blade pitch system.

3.6. Low speed shaft assembly

Figure 3.18 is a model of the low speed shaft assembly (LSS). The LSS assembly includes the hub shaft, teeterpin, teeterpin cap bolts, the adapter bolts, low speed shaft, and LSS main bearings. The loads are transferred to the hub shaft assembly through the teeterpin and the boom mount. The hub shaft then transfers the loads through the adapter to the low speed shaft. The adapter has a 1.5”/ft taper which fits on the LSS.

The adapter is fastened to the LSS with a AFBMA Standard Locknut #N-14. The hub shaft is fastened to the adapter via twelve 9” long ½-20 UNF grade 8 bolts. The teeterpin and boom spacer are clamped to the hub shaft by the teeterpin cap by eight 8.5” long ½-20 UNF L9 bolts. The boom spacer is clamped to the boom mount via eight 3.5” long 5/8-11 UNC grade 8 bolts. All nuts are stover locking nuts.

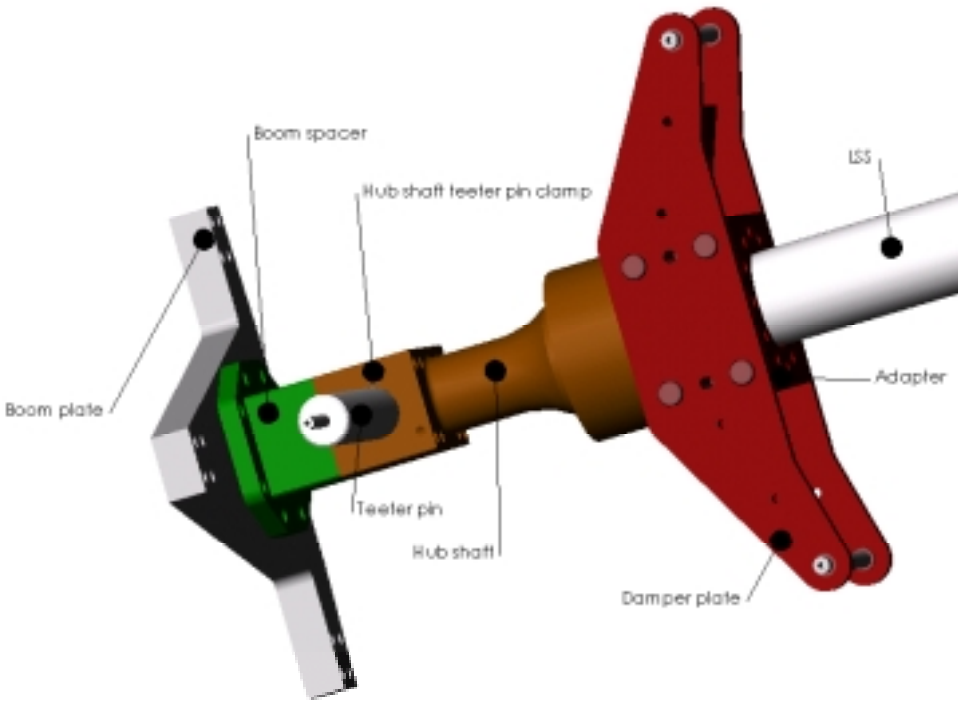

Figure 3.18: Low speed shaft assembly.

3.6.1. Hub shaft

This section presents the FEA results for the hub shaft. The hub shaft was recently redesigned for Phase VI of the Unsteady Aerodynamics Experiment. In addition to building the shaft from 15-5 stainless steel, slight geometry changes have be made to the hub shaft design to make it stronger.

The hub shaft was turned and milled from annealed 15-5 PH stainless steel round. After construction, the shaft was aged to H 1150. According to the Metals Handbook, the Typical yield strength for 15-5 PH stainless steel in this condition is 105 kpsi and the ultimate strength of the shaft is 135 kpsi [42].

3.6.1.1. Hub shaft FEA methodology.

Figure 3.19 displays the mesh used in the finite element analysis with the applied loads and restraints.

Assumption for the FEA load calculations:

1) I used the peak values from all of the ADAMS simulations for the six force components in Table 3.13. I assumed these components occur simultaneously which is an extremely conservative assumption.
2) I combined Fy and Fz as vectors to form Fyz.
3) I combined My and Mz as vectors to form Myz.
4) To simulate the moments, I applied force couples to the side faces of the teeterpin clamp. For example to simulate Myz, I applied a force couple (the pink arrows) shown in Figure 3.19.

5) I used the magnitudes of the forces and moments.
6) I applied the loads Fx and Fyz (the orange and olive arrows in Figure 3.19) to the round teeterpin surface inside the teeterpin clamp.
7) I assumed the hub shaft was rigidly fixed at the adapter interface (the light green arrows in Figure 3.19).

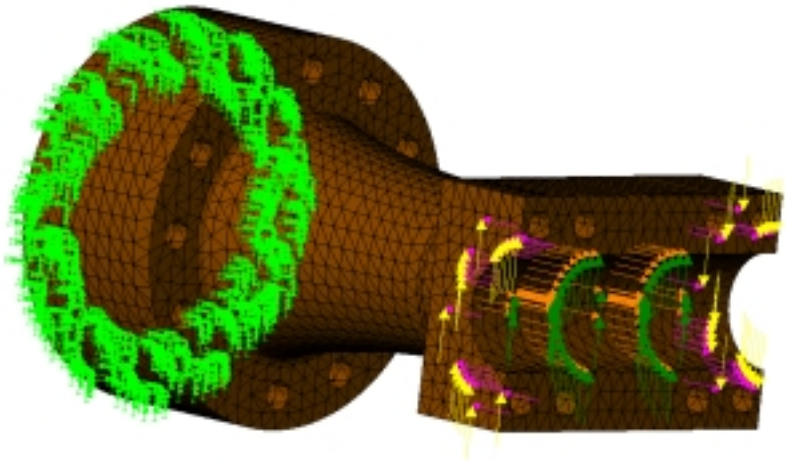

Table 3.13: Resolved FEA loads applied to the teeterpin clamp for the hub shaft analysis.

Component	Peak values (lb or ft-lb)	Description
Fx	8,585	Tension on hub shaft
Fy	1,869	Shear on hub shaft
Fz	4,498	Shear on hub shaft
Fyz	4,871	Combined shear on hub shaft
Mx	3,808	Torsion on hub shaft
My	4,881	Bending on hub shaft
Mz	2,155	Bending on hub shaft
Myz	5,336	Combined bending on hub shaft

Figure 3.19: Hub shaft FEA mesh and loads.

3.6.1.2. Hub shaft FEA results

Figure 3.20 is a plot of the von Mises stresses in the hub shaft. The peak stresses occur at the small fillet. The stresses at that location do not exceed 43 kpsi. The safety factor against exceeding the yield strength is

$$F.S._{yield} = S_{yield} / \sigma' = 105{,}000 / 43{,}110 = 2.4$$

The safety factor against exceeding the ultimate strength is

$$F.S._{ultimate} = S_{ultimate} / \sigma' = 135{,}000 / 43{,}110 = 3.1$$

Although these safety factors do not meet the standard NFAC safety factor requirements, they meet the requirements for a class 2 load ($F.S._{yield} = 2.0$ and $F.S._{ultimate} = 3.0 * FB$). FB for 15-5 VAR steel is at most 1 [43].

We have proof tested the hub shaft in the field up to 2680 ft-lb. This is roughly 50% of the peak load we observed in the ADAMS simulation. However, we plan to proof test this component further during field testing. Furthermore, we plan to not run the cases which result in excessive teeter impacts. These impacts are the primary contributor to the hub shaft stresses. Thus, we anticipate that the hub shaft loads will be significantly lower.

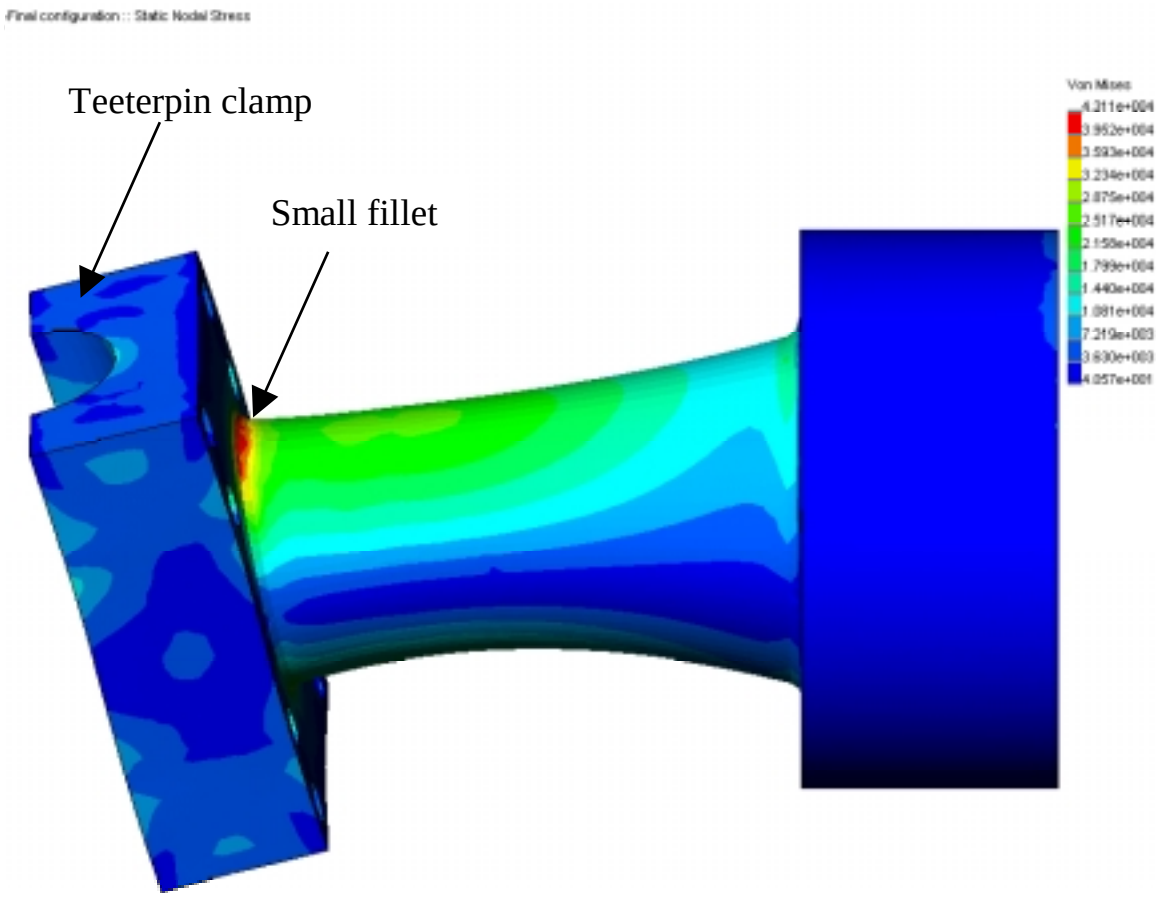

Figure 3.20: Hub shaft von Mises stress plot (distortion X150).

3.6.1.3. Hub shaft FEA validation.

I validated the FEA results by showing agreement with a known analytical solution at section F-F' (see Figure 3.21). The section properties at section F-F' are listed in Table 3.14. A two dimensional stress element on the circumference of the shaft at section F-F' is subjected shear, tension, torsion, and beam bending. The calculation of the principle stresses and the von Mises stresses on that element are presented in Table 3.15.

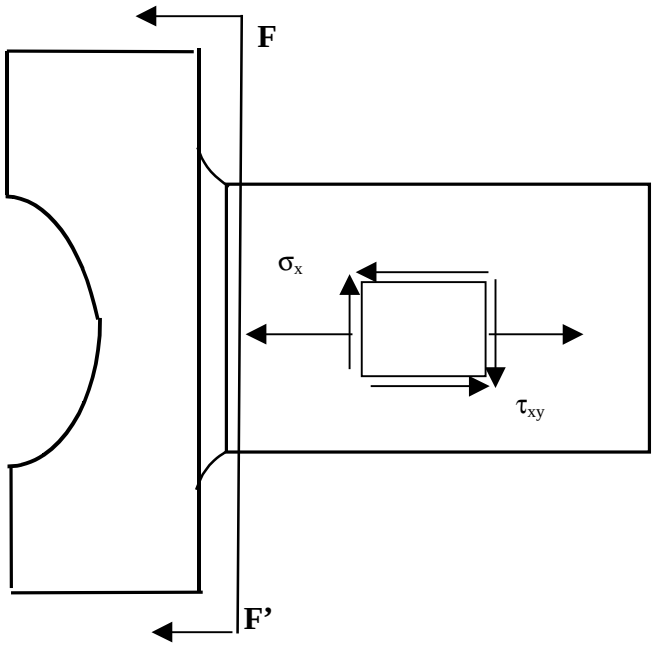

Figure 3.21: Hub shaft stress element.

Table 3.14: Hub shaft section properties.

Property	Formula	Value
Outside diameter	-	3.000"
Inside diameter	-	1"
Cross sectional area (A)	$\pi (d_o^2 - d_i^2) / 4$	6.283 in^2
Moment of area (I)	$\pi (d_o^4 - d_i^4) / 64$	3.927 in^4
Polar second moment of area (J)	$\pi (d_o^4 - d_i^4) / 32$	7.854 in^4

Table 3.15: Stress calculations for the hub shaft.

Stress	Formula	Value (psi)
Bending	$\sigma_x = (Myz) (d_o / 2) / I$	24,460
Tension	$\sigma_x = Fx / A$	775
Total for σ_x	-	25,235

Shear	$\tau_{xy} = Fy / A$	1,368
Torsion	$\tau_{xy} = (Mx)(d_o / 2) / J$	8,727
Total for τ_{xy}	-	10,095
Principle stresses (σ_1, σ_2)	$\sigma_1, \sigma_2 = (\sigma_x+\sigma_y)/2 \pm ((\sigma_x-\sigma_y) / 2)^2 + \tau_{xy}^2)^{.5}$	σ_1=18,985 σ_2=-5,368
Von Mises stress	$((\sigma_1- \sigma_2)^2+(\sigma_2-\sigma_3)^2+(\sigma_1-\sigma_3)^2) / 2)^{.5}$	22,158 psi

The calculated von Mises stress at section F-F' (22.1 kpsi) agrees with the FEA von Mises stress in that region (roughly between 21.5 and 25 kpsi). Thus, I conclude that the FEA analysis is accurate.

3.6.1.4. Hub shaft fatigue analysis.

We anticipate that the turbine will have been run no more than 50 hours before beginning the NFAC testing and at most another 150 hours in the NFAC for a total runtime of at most 200 hours. With the hub rotating at 72 RPM, the hub shaft will be subjected to roughly 8.6×10^5 cycles of fluctuating reversed loads. I designed the hub for an infinite life since because this number of cycles is considered high cycle fatigue.

The peak stresses in the hub shaft occur in the fillet near the teeterpin clamp. Below I calculate the endurance limit for the hub shaft and show that the stresses in the hub shaft are below this value.

17-4 stainless steel and 15-5 stainless steel have almost identical mechanical properties. The material endurance limit (S_e') for a lab specimen of 17-4 PH stainless steel in the H1150 aged condition is 90 kpsi [44]. 15-5 PH should have equal or better fatigue properties.

The formula for the component endurance limit (S_e) is

$$S_e = k_a k_b k_c k_d k_e S_e'$$

where

k_a = surface factor

k_b = size factor

k_c = load factor

k_d = temperature factor

k_e = miscellaneous affects factor

The calculation of S_e is presented in Table 3.5. The load factors were calculated using formulas from Shigley and Mischke [45]. The assumptions I made in determining the load factors are

1) Assume the size factor is .65. This is a conservative assumption because Shigley and Mischke claim the size factor varies from .60 to .75 for sections over ∅2".
2) The small fillet near the teeterpin clamp does not necessitate a geometry stress concentration factor because I am using the von Mises stress from the FEA analysis.

Table 3.16: Calculation of the enduarance limit for the hub shaft.

Parameter	Deffinition	Value	Comments	Se'	Se
ka	surface factor	1	Polished		
kb	size factor	0.65	Large diameter		
kc	load factor	1	Using von Mises stress		
kd	temp. factor	1	Room temperature		
ke	misc. affects factor	1	-		
Effective k		0.65		90	**59**

We monitor the von Mises stresses in the hub shaft during testing. We ensure that all testing is performed at stress levels beneath the endurance limit. This is a very conservative approach because it assumes that the cycling loads have a constant magnitude rather than a fluctuating magnitude. Using a more complex criteria such as the Modified Goodman Criteria or Soderberg Criteria would permit larger allowable loads.

The largest von Mises stresses was found to be 43.1 kpsi. This value is significantly less than the endurance limit (59 kpsi). Thus the fatigue loading will not fail the hub shaft.

3.6.2. Teeterpin

The teeterpin was re-made for Phase VI from 17-4 PH H1150 stainless steel (S_{yt} = 105 kpsi, S_{ut} = 135 kpsi). The teeterpin is 2" in diameter and is 24" long. I performed and finite element analysis and a fatigue analysis on the teeterpin. These analyses are described below.

3.6.2.1. Teeterpin FEA methodology

The loads on the pin are result from the rotor torque, thrust, and gravity (see Table 3.17) . The application of the loads is described below.

1) I used the loads reported at the hub shaft location in the ADAMS analysis. Some of the loads in the hub shaft aren't applicable to the teeter pin. For example, the bending moment Mz can be applied to the teeterpin because of the teetering degree of freedom. Similarly, the load My results from a boom load which is not transferred to the teeterpin. Finally, either Fy or Fz should be applied to the teeterpin, not both. This is a result of using the nacelle coordinate system to report the hub shaft loads. I chose to use the larger of the two loads (Fz).

2) The stresses in the teeterpin were slightly higher than NASA allowed. The thrust load proved to be the most significant load. The highest values of Fx occurred in the 15, 20, and 25 m/s wind cases. We have restricted the yaw angles were are going to run at these wind speeds. Thus, the peak thrust given these restrictions, the peak thrust (2590 lb) occurs in the 15 m/s wind speed. I used this value for Fx in the finite element analysis.
3) Fx is represented by the red arrows. The center-to-center distance between the middle teeterpin bearings is 16.5 inches. To simulate Mx, I applied a force couple (the pink arrows in Figure 3.22) of magnitude 3,808 ft-lb * 12 in/ft / 16.5 in = 2,770 lb (note: the orange load overlaps the other half of the pink force couple.)
4) I restrained the hub shaft to zero displacement. The green arrows in Figure 3.22 represent the hub shaft restraints.
5) There are six teeterpin bearings. The teeter bearings are Gar-max filament wound, high load, self-lubricating bearings. I distributed the thrust, torque, and gravity loads over the center-most teeterpin bearings (2^{nd} and 4^{th} bearings when counting from either end of the hub) because I could not determine how the loads were distributed among the teeterpin bearings.

Table 3.17: FEA loads applied to the teeterpin.

Component	Description	Magnitude
Fx (lb)	Thrust	2590*
Fy (lb)	Gravity	1,869
Fz (lb)	Edgewise load	4498
Mx (ft-lb)	LSS torque	3,808

* Peak load from the 15 m/s case.

3.6.2.2. Teeterpin FEA results

The highest von Mises stress in Figure 3.22 is 17,010 psi. The safety factor against yielding is

$$F.S._{yield} = S_{yield} / \sigma' = 105{,}000 / 21{,}990 = 4.8$$

and the safety factor against exceeding the ultimate strength is

$$F.S._{ultimate} = S_{ultimate} / \sigma' = 135{,}000 / 21{,}990 = 6.2$$

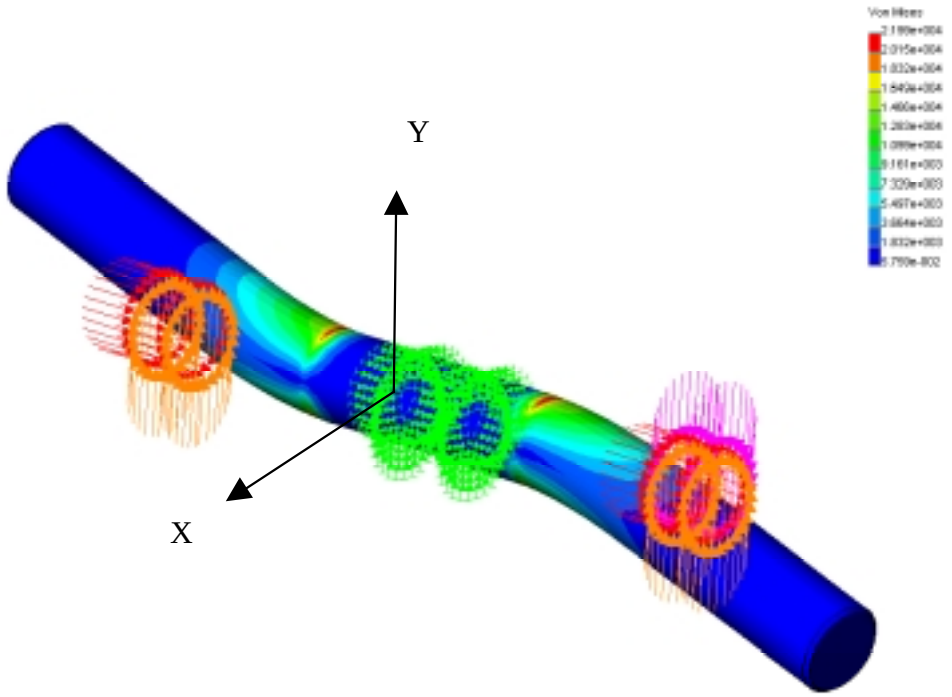

Figure 3.22: Teeterpin FEA loads and results.

3.6.2.3. Teeterpin FEA validation

To check the results of this analysis, I calculated the von Mises stress in the teeterpin analytically due to the bending moment and shear forces. At the teeterpin clamp interface, the teeterpin correctional area and area moment of inertia are 3.14 in^2 and .785 in^4. The distance from the center of the 2nd bearing and the edge of the teeterpin clamp is 4.75 in. The resultant moment at the edge of the teeterpin clamp is

$$M = (((F_x / 2)^2 + ((F_z + F_{Mx}) / 2)^2)^{.5}) * \text{Moment arm distance}$$

$$M = (((2590 / 2)^2 + ((2249 + 2{,}770) / 2)^2)^{.5} * 4.75 = 13{,}413 \text{ in-lb}$$

Thus, the bending stresses and shear stress on a 2-D element on the top of the teeterpin at the teeterpin clamp interface in Figure 3.22 are

$$\sigma_{bending} = M*y / I = 13{,}413 \text{ in-lb} * 1 \text{ in} / .785 \text{ in}^4 = 17{,}087 \text{ psi}$$

$$\sigma_{shear} = (((F_x / 2)^2 + ((F_z + F_{Mx}) / 2)^2)^{.5}) / A$$

$$\sigma_{shear} = (((2590 / 2)^2 + ((2249 + 2{,}770) / 2)^2)^{.5} / 3.14 \text{ in}^2 = 899 \text{ psi}$$

A simplified formula for the von Mises stress for combined shear and bending is given by Mischke [46] as

$$\sigma' = (\sigma_x^{\,2} + 3\tau_{xy}^{\,2})^{\frac{1}{2}}$$

where σ_x is the tensile stress due to bending and τ_{xy} is the shear stress thus

$$\sigma' = (17{,}087^2 + 3\times 899^2)^{\frac{1}{2}} = 17.2ksi$$

This value is relatively close to the value predicted in the FEA analysis of 22 kpsi considering I did not apply a stress concentration factor to the analytical results. Thus, the I conclude the results of the FEA analysis are accurate.

3.6.2.4. Teeterpin fatigue analysis

17-4 H1150 stainless has an endurance limit (S_e') for a lab specimen with R= -1 of 90 kpsi [47]. The formula for the component endurance limit (S_e) is

$$S_e = k_a\, k_b\, k_c\, k_d\, k_e\, S_e'$$

where

k_a = surface factor

k_b = size factor

k_c = load factor

k_d = temperature factor

k_e = miscellaneous affects factor

The calculation of S_e is presented in Table 3.18. The load factors were calculated using formulas from Shigley and Mischke [48]. The miscellaneous affects factor I used (k_e) was due to the chromium plating on the teeterpin. Shigley and Mischke claim that chromium plating can reduce the endurance limit by as much as 50%. Thus, I conservatively let k_f =.5.

Table 3.18: Calculation of the enduarance limit for the teeterpin.

Parameter	Deffinition	Value	Comments	Se'	Se
ka	surface factor	1	Machined		
kb	size factor	0.806587	Large diameter		
kc	load factor	1	Using von Mises stress		
kd	temp. factor	1	Room temperature		
ke	misc. affects factor	0.5	Chromium plated		
Effective k		0.403293		90,000	**36,296**

The peak von Mises stress in the teeterpin is predicted to be 17.0 kpsi. This value is significantly less than the endurance limit (24.4 kpsi). Thus the fatigue loading will not fail the teeterpin.

3.6.3. Teeterpin cap bolts

The teeterpin cap bolts fasten the boom and teeterpin to the hub shaft. There are eight teeterpin cap bolts. They are L9 grade ½-20 UNF. They have a minimum proof strength of 156 kpsi (24,900 lb proof load) and a tensile strength of 28,780 lb. SAE washers are used under the nut and head of each bolt. The nuts are L9 grade stover lock nuts.

3.6.3.1. Elongation calculations and torque requirements

We measured the elongation of each teeterpin cap bolt to ensure the proper preload was applied. To measure the elongation we had to mill each end of the bolts (approximately .020") to obtain a flat faces. We then used dial-calipers to measures the lengths of the bolts before and after installation. According to the Machinery Hand Book [49], measuring the bolt elongation in this manner yields ± 3%-5% preload accuracy. In contrast, using a torque wrench and torque prediction formulas yields ± 25% accuracy.

We torqued the bolts to 90% ± 5% of their proofload strengths. To determine the elongation necessary to obtain this pre-load, I used the relationship between elongation and preload given in the Machinery Hand Book as

$$\delta = Fi \times \frac{Ad \times Lt + At \times Ld}{Ad \times At \times E}$$

The parameter definitions and values are given in Table 3.19.

Table 3.19: Paramaters and values for the teeterpin clamp bolt torque calculations.

Parameter	Symbol	Value
Proof strength (lb)	Sp	24,944
Shank area (in^2)	Ad	.1924
Tensile stress area (in^2)	At	.1599
Thread length (in)	Lt	1.125
Shank length (in)	Ld	6.375
Modulus of elasticity (psi)	E	29×10^6
Elongation (in) for	δ	
Fi = Sp		**.034**
Fi = 90% Sp		**.031**
Preload (lb) for	Fi	
Fi = Sp		**24,944**
Fi = 90% Sp		**22,450**

3.6.3.2. Tensile strength check

According to the NFAC Test-Planning Guide, "the allowable stresses in threaded fasteners shall be based on the requirements for ductile materials…without consideration of

preload" [50]. In this section, I calculate the effect of the loads applied by the boom and the rotor on the teeterpin clamp bolts.

Table 3.20 presents the peak loads in the hub shaft obtained from the ADAMS simulations. The forces on the teeterpin clamp which stress the bolts are My, Mz, and Fx (see Figure 3.23).

In the following analysis, I assume the following

5) The peak values of My, Mz, and Fx occur simultaneously.
6) The ADAMS loads were given in the nacelle coordinate system. That is, it does not rotate with the hub shaft. I assumed the coordinate system is position as shown in Figure 3.23. This ensured that My (which is larger than Mz) acts across the axis with the smallest inertia which results in the highest tensile load. When the hub shaft is positioned as shown in Figure 3.23, then the upper left bolt (bolt 1) will have the highest tensile force.
7) Tension and shear applied to the teeterpin cap is applied evenly to all eight bolts.
8) Moments applied to the teeterpin cap create a linear load distribution and reaction as shown in Figure 3.24.

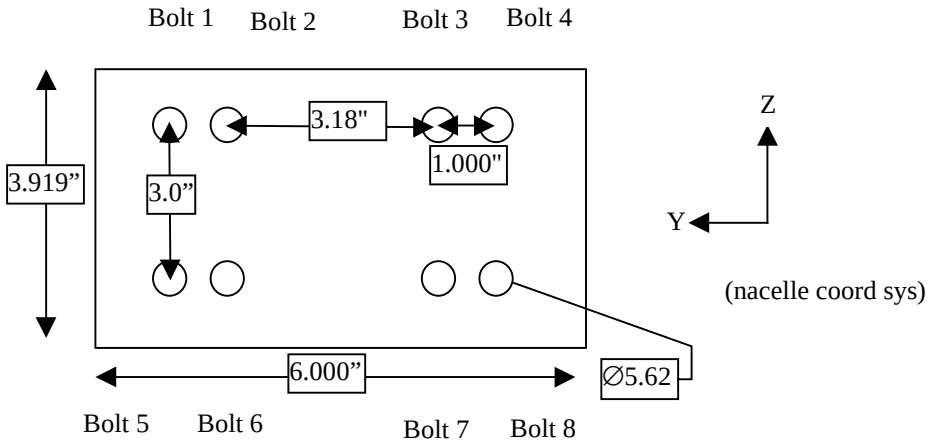

Figure 3.23: Teeterpin clamp geometry.

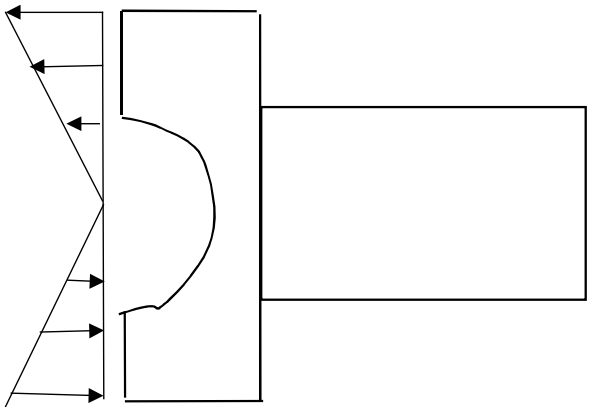

Figure 3.24: Bolt tension distribution.

Table 3.20: Loads used in teeterpin clamp analyses.

Component	Maximum value (lb or ft-lb)
Fx	8,585
Fy	1,869
Fz	4,498
Mx	3,808
My	4,881
Mz	2,155

Tension on bolt 1 due to Fx:

$$Tension_{Fx} = Fx / 8 = 8,585 / 8 = 1,073 \text{ lb}$$

Tension on bolt 1 due to My :

The stress in the i^{th} bolt can be found using the flexure formula for beams:

$$\sigma_i = (M)\,(y_i) / (I) = (M)\,(y_i) / \Sigma(y_i^2)\,dA$$

Thus the bolt tension in the i^{th} bolt is

$$\text{Bolt tension}_i = (\sigma_i)\,(A_{bolt}) = (M)\,(y_i)\,(A_{bolt}) / A_{bolt}\,\Sigma(y_i^2)$$

$$\mathbf{Tension_i = (M)\,(y_i) / \Sigma(y_i^2)}$$

(see Table 3.21 for y_i and $\sum y_i^2$ values)

Therefore

$$Tension_{My} = (My)(y_1) / \Sigma(y_i^2)$$

$$Tension_{My} = (4,881 * 12)(1.5) / 18 = 4,881 \text{ lb}$$

Table 3.21: Distance values for teeterpin cap analyses.

Bolt	y_i (Y distance to centerline)	Σy_i^2 (Y distance to centerline)^2	z_i (Z distance to centerline)	Σz_i^2 (Z distance to centerline)^2
1	1.5	2.25	2.59	6.71
2	1.5	2.25	1.59	2.53
3	1.5	2.25	1.59	2.53
4	1.5	2.25	2.59	6.71
5	1.5	2.25	2.59	6.71
6	1.5	2.25	1.59	2.53
7	1.5	2.25	1.59	2.53
8	1.5	2.25	2.59	6.71
Cumulative		18		37

Tension in bolt 1 due to Mz:

$$Tension_{Mz}=(Mz)(z_1) / \Sigma(z_i)^2$$

$$Tension_{Mz}=(2{,}155 * 12)(2.53) / 37 = 1{,}768 \text{ lb}$$

Total tension in bolt 1 = $T_1 = Tension_{Fx} + Tension_{My} + Tension_{Mz} = 1{,}073 + 4{,}881 + 1{,}768 = 7{,}722$ lb
The tensile strength of a ½-20 UNF grade L-9 bolt is 28,780 lb. Thus the safety factor against exceeding the tensile strength of the bolt is

$$F.S._{tension} = S_{tensile\ strength} / T_1 = 28{,}780 / 7{,}722 = 3.7$$

The NFAC Test Planning guide requires "the allowable stresses in threaded fasteners shall be based on the requirements for ductile materials…without consideration of preload" [51]. The safety factor against the ultimate strength is 3.7. The loads in the hub shaft are monitored. The NFAC requires a minimum safety factor of 2.0 on components with monitored loads. Thus, this safety factor is adequate.

3.6.3.3. Shear strength check

The NFAC Test Planning Guide requires that the fasteners in critical structures which use friction to transfer the loads be designed to carry the full shear load without the benefit of friction. The shear applied to the teeterpin cap bolts results from Fy and Fz and the low speed shaft torque (Mx).

Assumptions:

1) Assume that the load path for the rotor shear forces travel from the teeterpin, to the teeterpin cap, and finally to the hub shaft. This is an extremely conservative assumption since the teeterpin sits half in the hub shaft and half in the removable clamp. Thus, part of the load actually travels directly from the teeterpin to the hub shaft relieving the loads on the teeterpin clamp bolts.
2) Assume there is no friction in the teeterpin clamp which resists the shear loads. This is also a conservative assumption since approximately 16,000 lb of friction exits between the teeterpin clamp faces assuming a coefficient of friction of .1.
3) Assume the shear load is equally distributed among the eight bolts.

With these assumptions the shear load on bolt 1 due to Fy and Fz is

$$V_{Fx\&y} = (Fy^2 + Fz^2) / 8 = (1{,}869^2 + 4{,}498^2) / 8 = 609 \text{ lb}$$

Shear in bolt 1 due to Mx:

The load Mx represents the torque on the hub shaft. This torque load is transferred from the rotor to the teeterpin and from the teeterpin to the hub shaft and the head of the teeterpin clamp.

Assumptions:

1) Assume that half of the torque load (Mx) is applied directly to the hub shaft while the other half is applied to the teeterpin clamp head and bolts. Thus, the torque applied to the teeterpin clamp bolt pattern is Mx / 2 = 3,808 ft-lb / 2 = 1,904 ft-lb.
2) Assume there is no friction in the teeterpin clamp which resists the shear loads. This is also a conservative assumption since approximately 16,000 lb of friction exits between the teeterpin clamp faces if I assume a coefficient of friction of .1.
3) Assume the shear load is equally distributed among the eight bolts.

The shear load on bolt 1 due to Mx can be represented as [52]

$$V_{Mtx} = \frac{\frac{M_{tx}}{2} \times r_1}{r_1^2 + r_2^2 + \ldots + r_8^2}$$

Where r_i is the distance from the center of the teeterpin cap centriod to the i^{th} bolt. The values for the equation above are presented in Table 3.22. Thus the shear load on bolt 1 is equal to

$$V_{Mtx} = \frac{\frac{3{,}808}{2} \times 12 \times 2.996}{20.736} = 3{,}301\, lb$$

Total shear in bolt 1 = $V_1 = V_{Fy} + V_{Mx}$ = 608 + 3,301 = 3,909 lb

The allowable shear strength for a bolt in single shear is roughly 2/3 of the bolt's ultimate strength [53]. Thus the allowable shear for the teeterpin cap bolts is .667*28,780 = 19,196 lb

$F.S._{shear} = V_{allow} / V_1 = 19{,}196 / 3{,}909 = 4.9$

Table 3.22: Radial distances to the teeterpin cap centriod for the teeterpin bolt shear calculation.

Bolt	r_i (distance to the center of the teeterpin cap)
1	2.996
2	2.188
3	2.188
4	2.996
5	2.996
6	2.188
7	2.188
8	2.996
Cumulative	20.736

Combined shear and tension:

I calculated the von Mises stress to determine the factor of safety of a fastener in combined tension and shear. A simplified formula for the von Mises stress for combined shear and tension is given by Mischke [54] as

$$\sigma' = (\sigma_x{}^2 + 3\tau_{xy}{}^2)^{\frac{1}{2}}$$

where σ_x is the tensile stress and is equal to T_1 / At =7,722 / .1599 = 48,292 psi

and τ_{xy} is the shear stress and is equal to V_1/ Ad = 3,909 / .192 = 20,359 psi thus

$$\sigma' = (48{,}292^2 + 3 \times 20{,}359^2)^{\frac{1}{2}} = 59{,}797\, psi$$

The ultimate tensile strength for grade L9 material is 180,000 psi. Thus, the factor of safety against exceeding the von Mises stress in the bolt is

$$F.S._{\sigma'} = 180{,}000 / 59{,}797 = 3.0$$

The NFAC requires a minimum safety factor of 2.0 on components with monitored loads. Thus, this safety factor is adequate.

3.6.3.4. Joint preload check

According to the NFAC Test-Planning Guide, "A sufficient number of bolts shall be provided with preloads so that the net joint preload for all loading is at least two times the operating loads. [55]" The teeterpin clamp preload must be checked for shear and tension.

For the preload analysis, I assumed that the bolts were preloaded to 75% of their proof load (.75 * 24,900 =18,675 lb. This is a conservative assumption since we preloaded the bolts to 90 ± 5% of their proof load.

The tensile strength check results (section 3.6.3.2) indicate that the peak tension in the teeterpin cap bolts is 7,722 lb. The safety factor against exceeding the preload in this bolt is

$$F.S._{\text{Tension preload}} = 18{,}675 / 7{,}722 = 2.4$$

The shear strength check results (section 3.6.3.3) indicate that the peak shear load in the teeterpin cap is 3,909 lb. The safety factor against exceeding the preload in this bolt is assuming a coefficient of friction of .1 between the teeterpin cap faces, the friction generated by the preload is .1 *8 * 18,675 = 14,940 lb.

$$F.S._{\text{Tension preload}} = 14{,}940 / 3{,}909 = 3.8$$

These safety factors are greater than 2, thus the joint has adequate preload.

3.6.4. Adapter

This section presents the stress analysis of the adapter. The adapter was turned and milled from annealed 4140 SAE steel round (see Figure 3.25). The Typical yield strength for Annealed 4140 steel is 61 kpsi and the ultimate strength of the shaft is 90 kpsi [56]. The adapter has a tapered bore which mounts to the LSS shaft. Eight ∅1" dowel pins used to mount the adapter plates are pressed into either side of the adapter.

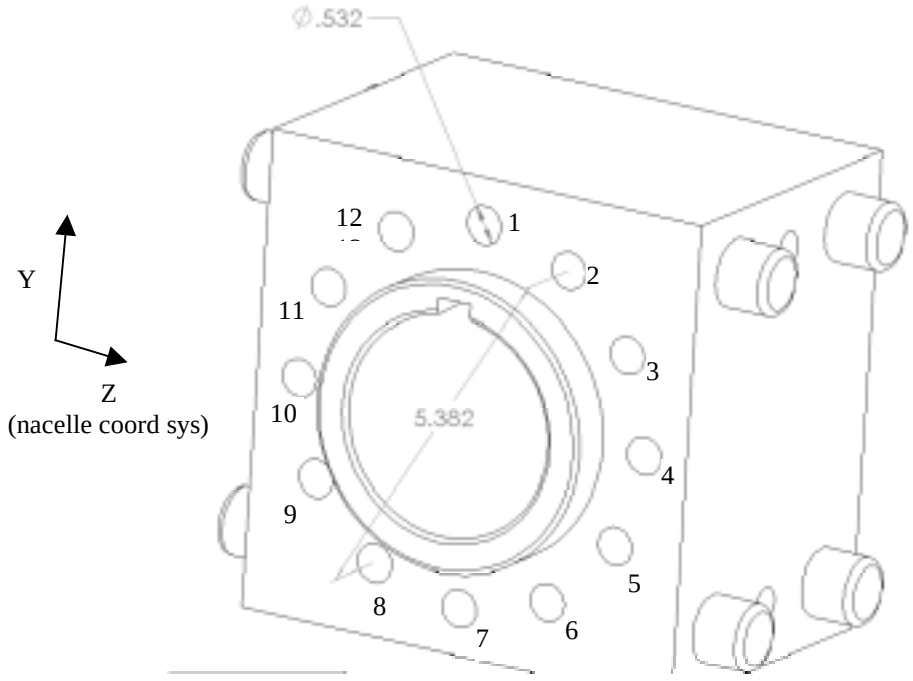

Figure 3.25: Adapter geometry.

3.6.4.1. Adapter FEA methodology

I performed an FEA analysis on the adapter. Figure 3.26 displays the FEA loads and von Mises stresses in the adapter. I included the hub shaft with in the analysis to make the load applications more realistic. I applied the same loads as in the hub shaft analysis. I have listed these loads again in Table 3.23. The assumptions I made during the analysis are presented below.

1) To simulate the moments, I applied force couples to the faces of the teeterpin clamp.
2) I applied the loads Fx, Fy, and Fz (the pink arrows in Figure 3.26) to the front teeterpin clamp face. I altered the direction of the forces so the moments caused by the forces Fx, Fy, and Fz act in the same direction as Mx, My, and Mz.
3) I assumed the adapter was rigidly fixed (the green arrows in Figure 3.26) on the low speed shaft.
4) I assumed that the clamping force was sufficient so that I could model the hub shaft and adapter as one solid component.

Table 3.23: FEA loads for the hub shaft and adapter.

Component	Maximum value (lb or ft-lb)	Notes on load application
Fx	8,585	Applied to teeterpin cap
Fy	1,869	Applied to teeterpin cap
Fz	4,498	Applied to teeterpin cap
Mx	3,808	3,808 ft-lb *12 / 6 in = 7,616 lb couple applied to teeterpin cap
My	4,881	ft-lb * 12 / 6.000 in = 9,762 lb couple applied to teeterpin cap
Mz	2,155	ft-lb * 12 / 3.919 in = 6,599 lb couple applied to teeterpin cap

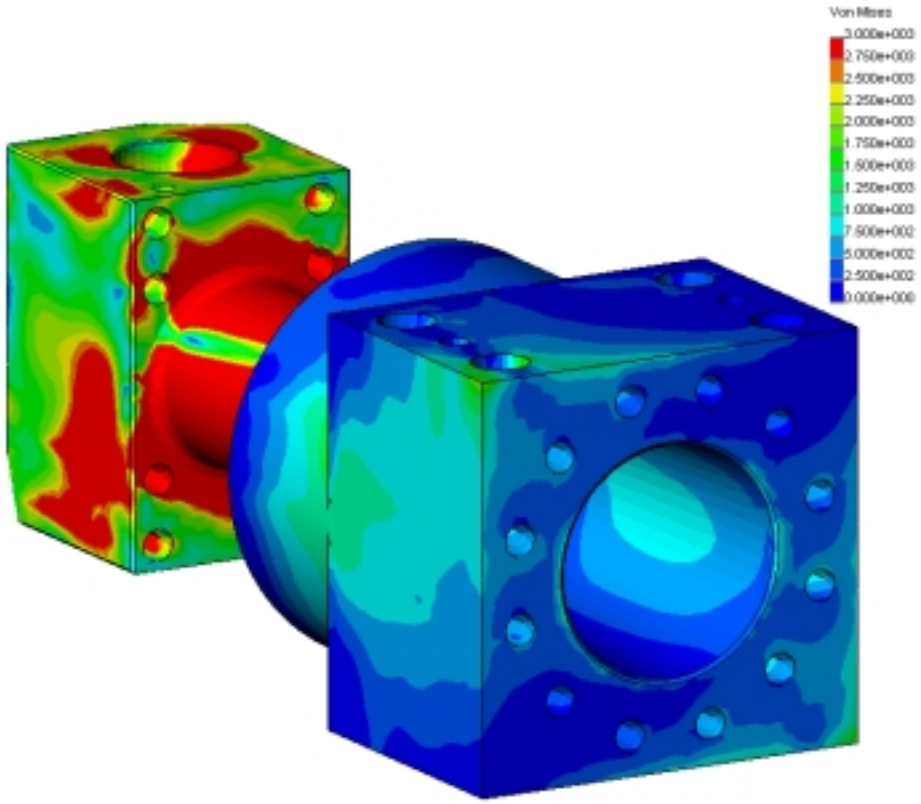

Figure 3.26: Von Mises stresses and loads on the adapter.

3.6.4.2. Adapter FEA results

The stresses in the adapter are negligible compared to the hub shaft. The peak stress in the adapter occurs at the interface of the hubshaft and the adapter and is less than 2000 psi. The safety factor against yielding is

$$F.S._{yield} = S_{yield} / \sigma' = 61{,}000 / 2{,}560 = 24$$

and the safety factor against exceeding the ultimate strength is

$$F.S._{ultimate} = S_{ultimate} / \sigma' = 90{,}000 / 2{,}560 = 35$$

These safety factors are sufficiently high that the component can be considered to have an infinite life.

3.6.4.3. Adapter FEA validation.

I validated the FEA results by showing agreement with a known analytical solution for the stresses in the adapter at the hub-shaft / adapter interface. The section properties of this interface are listed in Table 3.25. I also altered the direction of the forces Fy and Fz so that the moments caused by these forces acted in the same direction as My and Mz. I made this same conservative assumption in the FEA analysis.

Table 3.24: Hub shaft loads and adapter reactions.

Component	ADAMS loads on the hub shaft
Fx (lb)	8,585
Fy (lb)	1,869
Fz (lb)	4,498
Mx (ft-lb)	3,808
My (ft-lb)	4,881
Mz (ft-lb)	2,155

Table 3.25: Hub shaft / adapter interface section properties.

Property	Formula	Value
Outside diameter	-	6.000”
Inside diameter	-	4.083”
Cross sectional area (A)	$\pi (d_o^2 - d_i^2) / 4$	15.203 in^2
Moment of area (I)	$\pi (d_o^4 - d_i^4) / 64$	50.015 in^4
Polar second moment of area (J)	$\pi (d_o^4 - d_i^4) / 32$	102.102 in^4

Table 3.26: Stress calculations for the adapter.

Stress	Formula	Calculation	Value (psi)
Bending	$\sigma_x = (Mz) (d_o / 2) / I$	(2,155)(12)(6.0/2) / 50	1551
Tension	$\sigma_x = Fx / A$	8,585 / 15.203	564
Total for σ_x	-	-	2116
Shear	$\tau_{xy} = Fy / A$	4,498 / 15.203	296
Torsion	$\tau_{xy} = (Mx) (d_o / 2) / J$	(3,808)(12)(6/2) / 102.1	1,342
Total for τ_{xy}	-	-	1,638
Principle stresses (σ_1, σ_2)	$\sigma_1, \sigma_2 = (\sigma_x+\sigma_y)/2 \pm ((\sigma_x-\sigma_y) / 2)^2 + \tau_{xy}^2)^{.5}$		σ_1= 3,000 σ_2= -892
Von Mises stress	$((\sigma_1- \sigma_2)^2+(\sigma_2-\sigma_3)^2+(\sigma_1-\sigma_3)^2) / 2)^{.5}$		3536 psi

The calculated von Mises stress at section X-X' (2.56 kpsi) is in somewhat poor agreement with the FEA von Mises stress in that region of 3.5 kpsi. However, the stresses are so low that the FEA analysis is accurate enough.

3.6.5. Adapter bolts

The adapter bolts fasten the hub shaft to the adapter. There are twelve grade 8 ½-20 UNF adapter bolts. They have a minimum proof strength of 120 kpsi (19,200 lb proof load) and a tensile strength of 23,980 lb. Hardened SAE washers are used under the nut and head of each bolt. The nuts are grade 8 stover lock nuts.

We lubricated the nuts with motor oil and torqued the bolts to the rating specified by the bolt manufacturer Bowman Distribution. This torque specification preloads the bolts to 75% of proof load. According to the Machinery Hand Book [57], using a torque wrench and torque prediction formulas we can expect ± 25% preload accuracy.

3.6.5.1. Tensile strength check

The loads on the adapter which create tension in the bolts are My, Mz, and Fx. The loads which stress the bolts in shear are Fy and Fz. The magnitude of these loads is listed in Table 3.24. In the following analyses, I calculate the tensile and shear stresses necessary to find the von Mises stress in the bolts.

In the tensile strength analysis I assume

1) The thrust load is applied evenly to all twelve bolts.
2) Moments applied to the teeterpin cap create a linear load distribution on the bolts as shown in Figure 3.27.
3) The moment My and Mz combine to form the resultant moment

$$MR_{y\&z} = (My^2 + Mz^2)^{.5} = (4{,}881^2 + 2{,}155^2)^{.5} = 5{,}335 \text{ ft-lb}$$

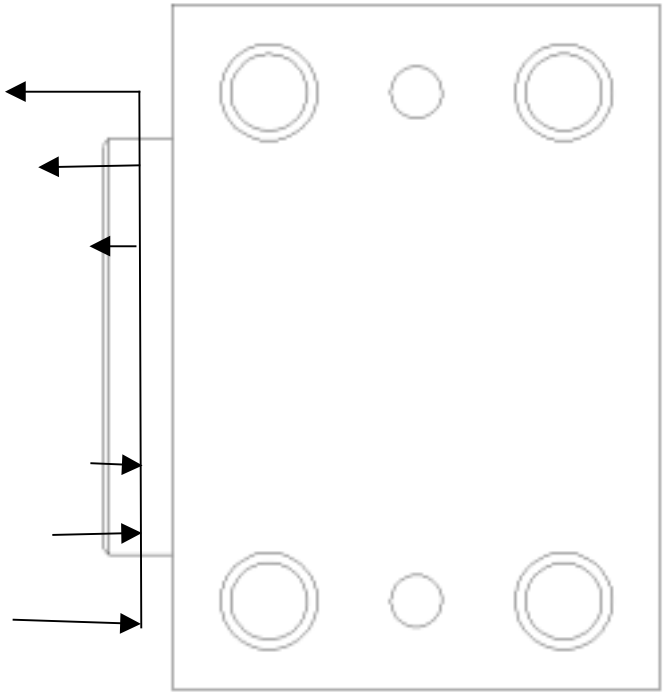

Figure 3.27: Bolt tension distribution in the adapter.

Tension on bolt 1 due to Fx:

$$Tension_{Fx} = Fx/12 = 8,585 / 12 = 715 \text{ lb}$$

Tension on bolt 1 due to $M_{y\&z}$:

The stress in the i^{th} bolt can be found using the flexure formula for beams:

$$\sigma_i = (M)\,(y_i) / (I) = (M)\,(y_i) / \Sigma(y_i^2)\,dA$$

Thus the bolt tension in the i^{th} bolt is

$$\text{Bolt tension}_i = (\sigma_i)\,(A_{bolt}) = (M)\,(y_i)\,(A_{bolt}) / A_{bolt}\,\Sigma(y_i^2)$$

$$\mathbf{Tension_i = (M)\,(y_i) / \Sigma(y_i^2)}$$

(see Table 3.27 for y_i and $\mathbf{\Sigma y_i^2}$ values)

Therefore

$$Tension_{MRy\&z} = (M_{y\&z})(y_1) / \Sigma(y_i^2)$$

$$Tension_{My} = (5,335*12)(2.776) / 46.247 = 3,843 \text{ lb}$$

Table 3.27: Component distances from the adapter center.

Bolt	yi	yi^2
1	2.776	7.708
2	2.404	5.781
3	1.388	1.927
4	0.000	0.000
5	1.388	1.927
6	2.404	5.781
7	2.776	7.708
8	2.404	5.781
9	1.388	1.927
10	0.000	0.000
11	1.388	1.927
12	2.404	5.781
	20.723	46.247

Total tension in bolt 1 = T_1 = $Tension_{Rx}$ + $Tension_{MRy\&z}$ = 715 + 3,843 = 4,559 lb

$F.S._{tension} = S_{ultimate} / T_1 = 23,980 / 4,559 = 5.26$

3.6.5.2. Shear strength check:

The hub shaft is pressed onto a pilot on the adapter (see Figure 3.25). All shear loads except those due to the LSS torque (Mx) are transferred directly to the pilot and are not resisted by the adapter bolts. I made the following assumptions while calculating the shear on the adapter bolts.

Assumptions:

1) Assume there is no friction between the adapter and the hub shaft. This is a conservative assumption since the approximate preload clamping force of 115,000 lb in the joint creates roughly 11,500 lb of friction between faces. This friction creates a torque of approximately

   11,500 lb * 2.776 = 31,924 in-lb = 2,660 ft lb.

2) Assume the shear load is equally distributed among the twelve bolts.

The bolt circle diameter is 2.776". The torque Mx subjects each bolt to a shear force of

Shear force = Mx / (12 r) = (3,808 ft-lb * 12in /ft) / (12 * 1.388 in) = 2,743 lb

The allowable shear strength for a bolt in single shear is roughly 2/3 of the bolt's ultimate strength [58]. Thus the allowable shear for the adapter bolts is .667 * 23,980 lb = 15,987 lb

$F.S._{shear} = V_{allow} / V_1 = 15,987 / 2,743 = 5.8$

3.6.5.3. Combined shear and tension strength check

I used the von Mises stresses to determine the factor of safety for a fastener in combined tension and shear. A simplified formula for the von Mises stress for combined shear and tension is given for a bolt (with the tensile stress area A_t and a nominal area A_d) by Shigley and Mischke [59] as

$$\sigma' = (\sigma_x{}^2 + 3\tau_{xy}{}^2)^{\frac{1}{2}}$$

where σ_x is the tensile stress and is equal to T_1 / At = 3,843 / .1599 = 24,033 psi.

and τ_{xy} is the shear stress and is equal to V_1/ Ad = 2,743 / .192 = 14,286 psi. The von Mises stress is

$$\sigma' = (24{,}033^2 + 3 \times 14{,}286^2)^{\frac{1}{2}} = 34{,}494\, psi$$

The material ultimate strength for a grade 8 bolt is 150,000 psi. The safety factor against exceeding this strength is

$$F.S._{\sigma' \text{ ultimate}} = 150{,}000 / 34{,}494 = 4.3$$

3.6.5.4. Joint preload check

According to the NFAC Test-Planning Guide, "A sufficient number of bolts shall be provided with preloads so that the net joint preload for all loading is at least two times the operating loads. [60]" The cleavis mount preload must be checked for shear and tension.

For the preload analysis, I assumed that the bolts were torqued to 50% of their proof load (.5 * 19,200 = 9,593 lb). This is a conservative assumption since we preloaded the bolts using a torque wrench to 75% ± 25% of their proof load.

The tensile strength check results indicate that the peak tension in the adapter bolts is 3,843 lb. The safety factor against exceeding the preload in this bolt is

$$F.S._{\text{Tension preload}} = 9{,}593 / 3{,}843 = 2.5$$

The hub shaft is pressed onto a pilot on the adapter (see Figure 3.25). All shear loads except those due to the LSS torque (Mx) are transferred directly to the pilot and are not resisted by the adapter bolts. Assuming a coefficient of friction of .15 in the joint, the friction generated by the preload is .15 *12 * 9,593 = 17,267 lb. The bolt pattern diameter is 5.382". The torque created by the preload can be estimated as

$$T_{\text{friction}} = 17{,}267 \text{ lb} * 5.382" = 92{,}933 \text{ in-lb} = 7{,}744 \text{ ft-lb}$$

The peak LSS torque Mx was estimated to be 3,808 ft-lb. Thus the safety factor against exceeding the torque pre-load is

$$F.S._{\text{Shear preload}} = 7{,}744 / 3{,}808 = 2.0$$

These safety factors are greater than 2, thus the joint has adequate preload.

3.6.6. Low speed shaft

The low speed shaft was designed and built by Grumman Aerospace Corporation. The shaft was turned and ground from 15-5 PH cold rolled electric stainless steel that has been heat treated to H1025. This heat treatment results in a minimum yield strength = 145 kpsi and a minimum tensile strength of 155 kpsi. The low speed shaft is supported by two bearings 27.9" apart. The bearing closest to the rotor is a spherical roller bearing. The other bearing is a standard tapered roller bearing.

3.6.6.1. Low speed shaft FEA methodology

I preformed an FEA analysis on the low speed shaft. Figure 3.28 displays the FEA loads on the shaft. I included the hub shaft in the analysis to make the load application more realistic. I applied the same loads as in the hub shaft analysis. I have listed these loads again in Table 3.28. The assumptions I made during the analysis are presented below.

FEA Assumptions:

1) I assumed the adapter was rigidly fixed on the low speed shaft so that they could be modeled as one solid component.
2) I only modeled a section of the LSS (from the adapter to the upwind bearing).

FEA load application:

1) I applied the peak ADAMS loads to the LSS assembly. These loads are presented in Table 3.28 and Figure 3.28. I have only displayed the loads in the X-Z plane in Figure 3.28 for clarity.
2) I restrained the LSS to zero displacement in all three directions at the location of the upwind bearing (the green arrows in Figure 3.28 represent these constraints).
3) I applied the loads Fx, Fy, and Fz to the upwind face of the adapter (the orange arrows in Figure 3.28 represent Fz).
4) I applied a the moments Mx, My, and Mz as force couples on the side faces of the adapter (the pink arrows in Figure 3.28 represent the My force couple). The magnitude of these couples is calculated using

$$Mx\_couple := \frac{Mx}{6.7\ in} \qquad Mx\_couple = 6.808 \cdot 10^{3} \cdot lb$$

$$My\_couple := \frac{My}{6.7 \cdot in} \qquad My\_couple = 2.333 \cdot 10^{4} \cdot lb$$

$$Mz\_couple := \frac{Mz}{6.7 \cdot in} \qquad Mz\_couple = 9.702 \cdot 10^{3} \cdot lb$$

5) The downwind bearing is a spherical roller bearing which can only apply a radial force to the LSS. The components of this force can be calculated by summing the moments about the upwind bearing. The results are

$$RFz := \frac{My + Fz \cdot Adapter\_dist}{Bearing\_dist}$$

$$RFy := \frac{Mz + Fy \cdot Adapter\_dist}{Bearing\_dist}$$

$Adapter\_dist = 30.331 \cdot in$

$Bearing\_dist = 25.705 \cdot in$

$RFz = 9.808 \cdot 10^3 \cdot lb$

$RFy = 4.031 \cdot 10^3 \cdot lb$

Table 3.28: Low speed shaft loads.

Component	Maximum value	Notes on load application
Fx (Thrust)	1768 lb	Applied to adapter downwind face
Fy	1273 lb	Applied to adapter downwind face
Fz	3158 lb	Applied to adapter downwind face
Mx (torque)	3801 ft-lb	3,801ft-lb *(12 in/ft) / 6.7 in = 6,808 lb couple applied to adapter
My	13027 ft-lb	13,027 ft-lb * (12 in/ft) / 6.7 in = 23,333 lb couple applied to adapter
Mz	5417 ft-lb	5,417 ft-lb * (12 in/ft) / 6.7 in = 9,702 lb couple applied to adapter

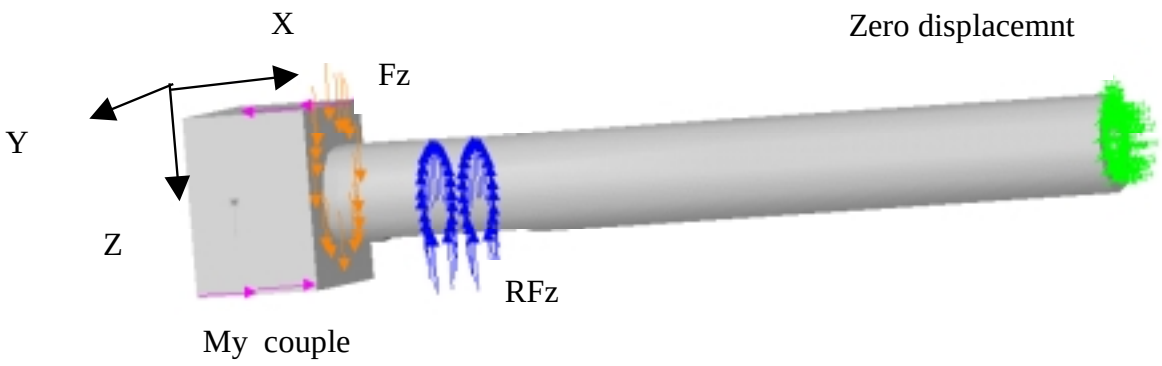

Figure 3.28: LSS FEA loads in the X-Z plane.

3.6.6.2. Low speed shaft FEA results

The von Mises stresses in the low speed shaft are plotted in Figure 3.29. The peak stress (46,460 psi) occurs in the ground flat.

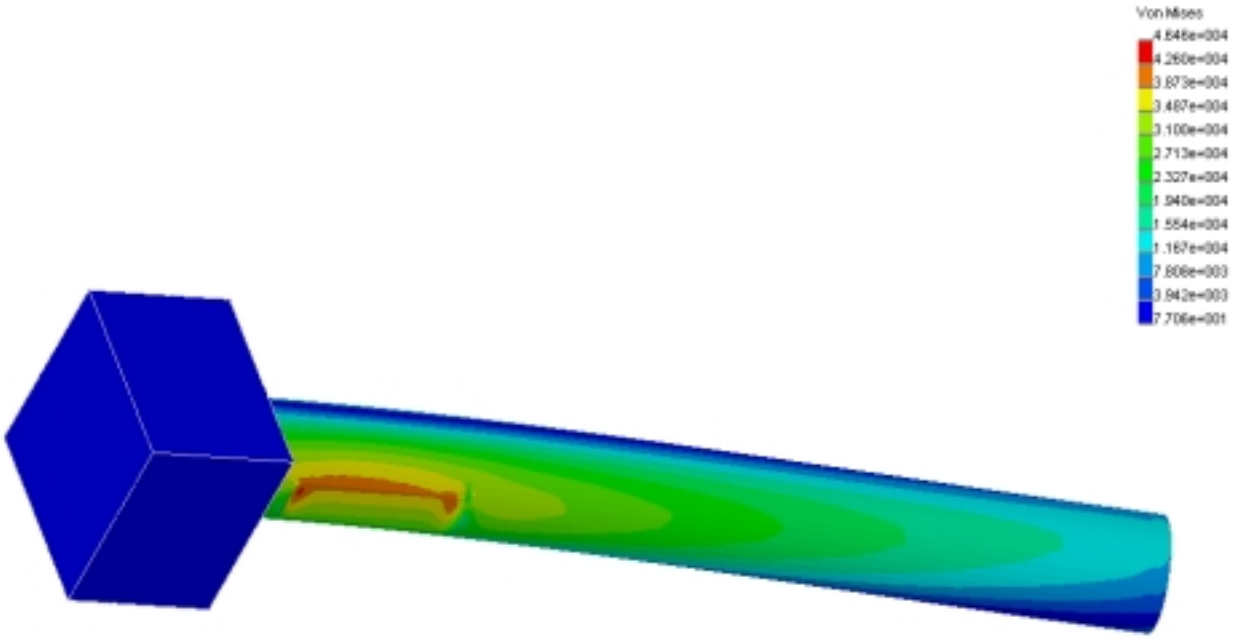

Figure 3.29: Von Mises stress plot for the low speed shaft.

The safety factor against yielding is

$$F.S._{yield} = S_{yield} / \sigma' = 145{,}000 / 46{,}460 = 3.1$$

and the safety factor against exceeding the ultimate strength is

$$F.S._{ultimate} = S_{ultimate} / \sigma' = 155{,}000 / 46{,}460 = 3.3$$

Although these safety factors do not meet the standard NFAC requirements ($F.S._{ultimate}$ is below 4.0) the LSS does meet the safety factor requirements to qualify for a class 3 NASA load case ($F.S._{yield}$ = 1.5 and $F.S._{ultimate}$=2.5 * FB). FB for 15-5 VAR stainless steel is at most 1 [61].

We have LSS field loads during the phase IV experiment of LSS bending loads up to 10,671 ft-lb (14,471 N-m). In order to qualify for a class 3 load, the LSS must be proof tested up to 125% of the peak load. We will limit the load cases we run so that the LSS loads remain under 7,989 ft-lb. This is the value that corresponds to the -90° yaw release load case. 125% of 7,989 is 9,986 ft-lb. Thus the LSS meets the requirements for a class 3 load case.

3.6.6.3. Low speed shaft FEA validation.

To validate the FEA results, I calculated the stresses in the LSS assembly analytically. I do not have an accurate stress concentration factor for the stress concentration caused by the flat in the LSS; thus, my calculations assumed that the shaft did not have a flat.

I compared these analytical results to an FEA analysis of a shaft with no flat. The section I compared these values at the center of the ground flat. I chose this location because that is the location of the peak bending moment. The properties at this section X-X' are listed in Table 3.29. The analytical results are presented in Table 3.30 and the FEA results are presented in

Table 3.29: Hub shaft / low speed shaft interface section properties.

Property	Formula	Value
Outside diameter	-	3.682"
Inside diameter	-	1.5"
Cross sectional area (A)	$\pi (d_o^2 - d_i^2) / 4$	8.890 in^2
Moment of area (I)	$\pi (d_o^4 - d_i^4) / 64$	8.783 in^4
Polar second moment of area (J)	$\pi (d_o^4 - d_i^4) / 32$	17.566 in^4

Table 3.30: Stress calculations for the low speed shaft.

Stress	Formula	Calculation	Value (psi)
Bending	$\sigma_x = (My^2 + Mz^2)^{.5} (d_o / 2) / I$	$(13027^2 + 3801^2)^{.5} *$ (12)(3.682 / 2) / 8.783	34,133
Tension	σ_x = Fx / A	1768 / 8.890	199
Total for σ_x	-	-	34,332
Shear	τ_{xy} =	$[(9808^2 + 4031^2)^{.5} - (1273^2$	742

	$[(RFy^2+RFz^2)^{.5} - (Fy^2+Fz^2)^{.5}] / A$	$+ 3801^2)^{.5}] / 8.890$	
Torsion	$\tau_{xy} = (Mx) (d_o / 2) / J$	(3801)(12)(3.682 / 2) / 17.566	4,780
Total for τ_{xy}	-	-	5,522
Principle stresses (σ_1, σ_2)	$\sigma_1, \sigma_2 =$ $(\sigma_x+\sigma_y)/2 \pm ((\sigma_x -\sigma_y) / 2)^2 + \tau_{xy}^2)^{.5}$		σ_1= 35,198 σ_2= -866
Von Mises stress	$((\sigma_1- \sigma_2)^2+(\sigma_2-\sigma_3)^2+(\sigma_1-\sigma_3)^2) / 2)^{.5}$		35,634 psi

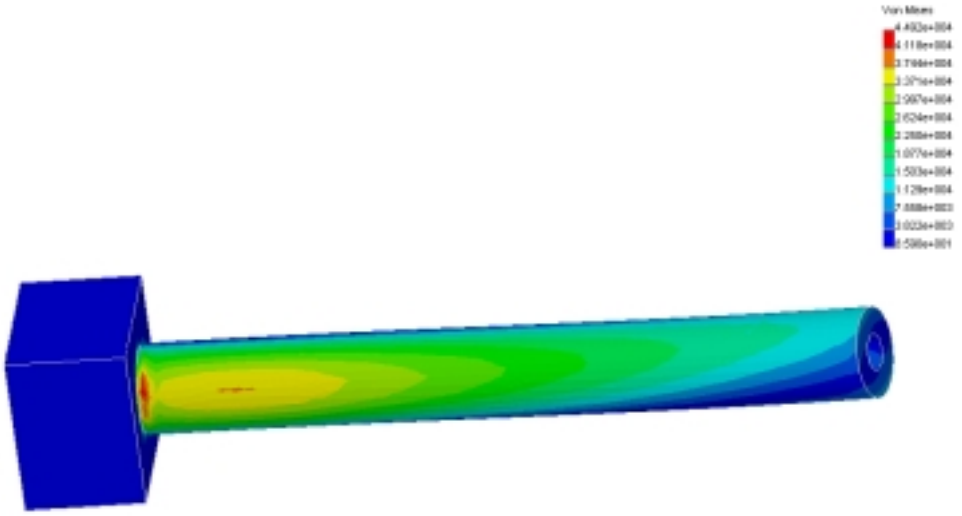

Figure 3.30: LSS FEA results without a flat ground in the shaft.

The calculated von Mises stress at the section of interest (35 kpsi) agrees reasonably well with the FEA von Mises stress in that region of 37 to 41 kpsi. Thus, I conclude that the FEA analysis for the LSS without a flat is accurate. The FEA results for the LSS with a flat resulted in a stress of 46.4 kpsi. Thus, the stress concentration caused by the flat is 46.4 / 37 kpsi = 1.25.

3.6.6.4. Low speed shaft fatigue analysis

The peak stresses in the low speed shaft occur at section X-X'. Here I calculate the endurance limit at this section and show that the stresses in the Low speed shaft are below this value. 17-4 stainless steel and 15-5 stainless steel have almost identical mechanical properties. The material endurance limit (10^8 cycles) (S_e') for a lab specimen of 17-4 PH stainless steel in the H1025 aged condition is 80 kpsi [62]. 15-5 PH should have equal or better fatigue properties.

The formula for the component endurance limit (S_e) is

$$S_e = k_a\, k_b\, k_c\, k_d\, k_e\, S_e'$$

where

k_a = surface factor

k_b = size factor

k_c = load factor

k_d = temperature factor

k_e = miscellaneous affects factor

The calculation of S_e is presented in Table 3.31. The load factors were calculated using formulas from Shigley and Mischke [63].

Table 3.31: Calculation of the enduarance limit for the low speed shaft.

Parameter	Deffinition	Value	Comments	Se'	Se
ka	surface factor	0.914101	Ground		
kb	size factor	0.65	Large diameter		
kc	load factor	1	Using von Mises stress		
kd	temp. factor	1	Room temperature		
ke	misc. affects factor	1	-		
Effective k		0.594166		77,500	**46,048**

The component endurance limit (46 kpsi) is roughly equal to the predicted peak stress (46 kpsi). Thus the component can be considered to have an infinite life for our application.

3.6.7. Low speed shaft locknut

The adapter is fastened to the LSS with a AFBMA Standard Locknut #N-14. A Typical steel for these locknuts is C1015 steel [64]. The minimum yield strength and tensile strengths for this steel in the cold drawn state is 54 and 64 kpsi. The low speed shaft was turned and ground from 15-5 PH cold rolled electric stainless steel that has been heat treated to H1025. This heat treatment results in a minimum yield strength = 145 kpsi and a minimum tensile strength of 155 kpsi.

3.6.7.1. LSS thread shear strength check

The LSS has a significantly higher yield strength than the LSS nut; thus, the nut is likely to fail before the shaft threads. I performed a shear strength check on the nut threads and a tensile strength check on the shaft. I calculated the load capacity of the nut threads by dividing the allowable shear strength of threads by the thread shear area. The LSS thread form is a 2 ¾ UNS – 18. The shear area of an internal thread given by the Machinery Hand Book as [65]

$$As = \pi\, n\, L\, D_{s\,Min}\left[\frac{1}{2n} + .57735\left(D_{s\,Min} - E_{n\,Max}\right)\right]$$

where

n = threads per inch = 18 tpi

L = length of engagement = .553 in

$D_{s\,Min}$= minimum major diameter of external thread = 2.7397 in

$E_{n\,Max}$= maximum pitch diameter of internal thread = 2.7208 in [66]

Thus the shear area is

$$A_s = \pi(18)(.553)(2.7397)\,[(.5)/18 + .57735(2.7397 - 2.7208)] = 3.315\ in^2$$

The allowable shear stress according to the Maximum Shear Stress failure theory is

$$\sigma_{allow}=(.667)\ 54\ kpsi = 36\ kpsi$$

The allowable tensile load on the LSS thread is

$$P = \sigma_{allow} * A_s = 36{,}000 * 3.315 = 119{,}340\ lb$$

The peak thrust from the ADAMS simulations (Fx) is 1,768 lb. Thus the safety factor against the thrust loads shearing the LSS threads is

$$\boxed{F.S._{tension} = P / Fx = 119{,}340 / 1{,}768 = 67.5}$$

3.6.7.2. LSS thread tensile strength check

The direct tensile load P to break the threaded portion of a screw or bolt (assuming no shearing or torsional stress are acting) can be determined from [67]

$$P=S_{uts}A_t$$

where

S_{uts} = the ultimate strength of the screw = 145 kpsi

A_t = tensile-stress area of the threads.

A_t can be found using

$$A_t = .7854(D - .9743 / n)^2 = .7854\ (2.75 - .9743 / 18)^2 = 5.71$$

where

D = the basic major diameter of the screw = 2.75”

n = the threads per inch = 18

The direct tensile load is $P=S_{uts}A_t = 145{,}000*5.71 = 827{,}950$. The safety factor against breaking the shaft threaded section in tension is

$$\boxed{F.S._{tension} = P / Fx = 827{,}950 / 1{,}768 = 468}$$

Clearly the tensile load is not an issue!

3.6.7.3. LSS thread preload check

According to the NFAC Test-Planning Guide, “A sufficient number of bolts shall be provided with preloads so that the net joint preload for all loading is at least two times the operating loads. [68]”
I calculated the LSS preload using the following formula [69]

$$T=K\ F_i\ d$$

where

T = wrench torque = 350 ft-lb = 4,200 in-lb

K = constant that depends on the bolt material and size = .2 (for unplated threads)

d = nominal bolt diameter = 2.75in

With these values, the pre-load on the nut is

$$F_i = T / (K\ d) = 4{,}200 / (.2*2.75) = 7{,}636\ lb$$

The peak thrust load obtained in the ADAMS simulations is 1,768 lb. Thus, we have 7,636 / 1,768 = 4.3 times the preload necessary in the joint.

3.6.8. Low speed shaft main bearings

The LSS is supported by two main bearings 24" apart. The down wind low speed shaft bearing is a 3 11/16" spherical roller bearing. The upwind bearing is a 3 7/16" tapered roller bearing. The upwind bearing resists the thrust loads, radial loads, and some bending. The front shperical roller bearing rotates 1.5° to relieve any bending. This design allows most of the rotor moment to be resisted by a force couple at the two bearings. Thus, the primary loads on the bearings are radial.

The ADAMS simulations loads on the low speed shaft are listed in Table 3.32. The resultant moment from My and Mz is $(13{,}027^2 + 5{,}417^2)^{.5}$ = 14,108 ft-lb. The bearings are 2 ft apart, thus the force couple between the two bearings is then 14,108 / 2 = 7,054 lb on each bearing. The peak thrust load on the LSS is 1,768 lb.

The bearings are made by Browning Emerson Power Transmission Corporation. The upwind bearing (model number 3 7/16" C 950) is a tapered roller bearing. The manufacture claims a thrust load rating of 7,410 lb and a radial load L10 life of 17,279 lb for 5000 hours at 100 RPM. The safety factor against exceeding the loads for an L10 life of 5000 hours is

$$F.S._{\text{fatigure radial}} = 17{,}279 / 7{,}054 = 2.4$$

$$F.S._{\text{fatigure thrust}} = 7{,}410 / 1{,}768 = 4.2$$

The downwind bearing (model number 3 11/16" SFB 1000 E) is a spherical roller bearing. The manufacture claims a radial load L10 life of 20,590 lb for 5000 hours at 100 RPM. Using this rating as the fatigue strength, the safety factor against fatigue for the downwind bearing is

$$F.S._{\text{fatigure radial}} = 20{,}590 / 7{,}054 = 2.9$$

These safety factors are for a 5000 hour life. The manufacture does not provide the instantaneous peak load ratings. The instantaneous peak load ratings should be significantly higher.

Table 3.32: Predicted peak loads on the low speed shaft during testing.

Component	Maximum value (lb or ft-lb)
Fx	1,768
Fy	1,273

Fz	3,156
Mx	3,801
My	13,027
Mz	5,417

3.7. Nacelle assembly

The nacelle assembly is displayed in Figure 3.31. The assembly components include the mainframe, mainframe mount, bed plate, transmission, High speed shaft, generator, and rotor brake.

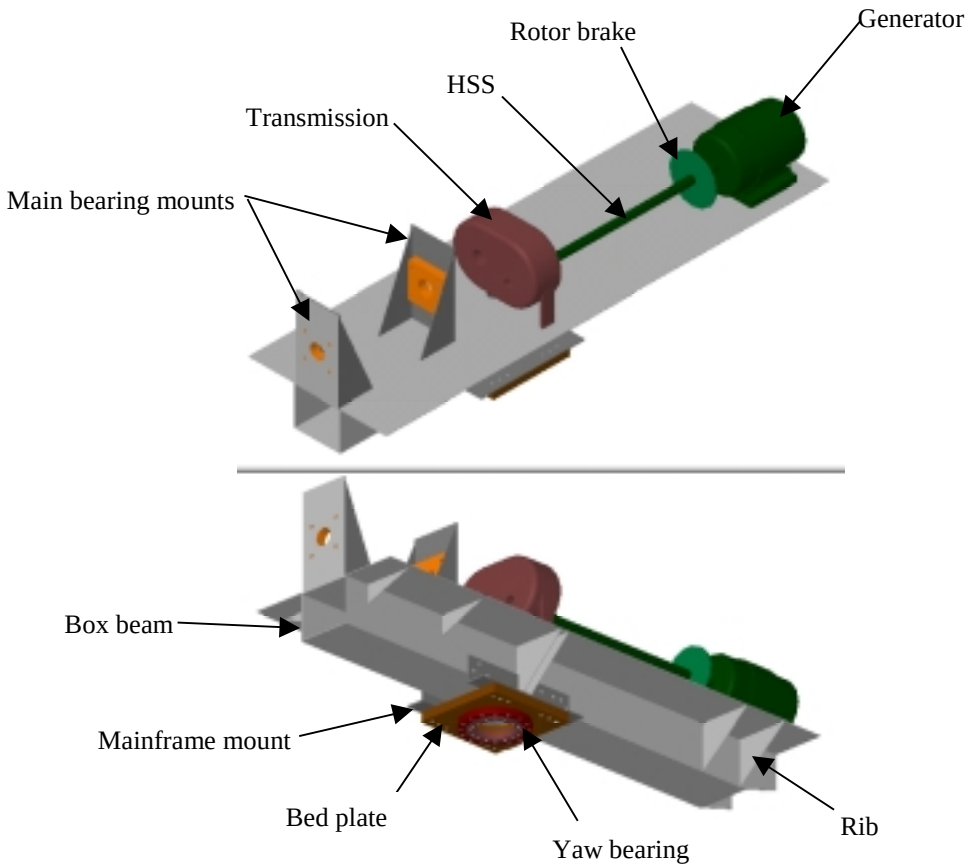

Figure 3.31: Two views of the nacelle assembly (nacelle cover not shown).

3.7.1. Critical components

3.7.1.1. Main bearing mounts, mainframe, mainframe mount, and bed plate

The main bearing mounts, mainframe, mainframe mount, and bed plate are the critical structural components. The main bearings are self aligning. The upwind main bearing is a tapered roller bearing which transmits radial and thrust loads to the mainframe. The down wind bearing transmits only radial loads to the mainframe. The mainframe carries these loads to the mainframe mount, bedplate, yaw bearing and finally to the tower.

The primary load bearing structure of the main frame is a 10" X 12" box beam. I assumed the steel is A36 steel. A 3/16" steel plate is welded to top of the beam and braced with 3/16" thick webs.

The mainframe mount is bolted and welded to the box beam. Five grade 8, ¾" diameter bolts are used to fasten each half of the mainframe mount to the mainframe. In addition to the bolts, each mount has continuous weld beads around the edges of the mainframe mount. I assumed the mainframe mount and other mainframe parts are made from are made from A-36 steel. The mainframe mount bolts to the bedplate with six ¾-UNC grade 8 bolts.

The bed plate is made from 2" thick steel. The yaw bearing bolts to the bedplate with sixteen ½-13 UNC grade 8 bolts. I present the analysis of the main frame mount and the yaw bearing bolts in the next section.

Table 3.33: Material properties for the hardlink nacelle assembly.

Component	Material	Material thickness	Yield tensile strength (kpsi)	Ultimate tensile strength (kpsi)
Main bearing mount	A36 steel	3/8"	36	54
Mainframe box beam	A36 steel	¼"	36	54
Mainframe sheet metal	A36 steel	3/16"	36	54
Mainframe mount	A36 steel	3/8"	36	54
Bed plate	A36 steel	2"	36	54
Yaw bearing bolts	Grade 8	½-13 UNC	17,050 lb proof load	21,280 ultimate tensile load
Main frame mount bolts	Grade 8	¾-10 UNC	40,100 lb proof load	50,100 ultimate tensile load

3.7.1.1.1. FEA methodology

I performed a finite element analysis on the nacelle assembly. The assumption and loads I used in this analysis are presented below. The application of the loads is shown in Figure 3.32.

FEA Assumptions:

1) I assumed that the bolt preload and welds sufficiently joined the main frame mount to the main frame so that I could model both components as one unit.
2) I assumed that the bolt preload joined the main frame mount to the bed plate so that I could model both components as one unit.
3) I assumed that the bolt preload joined the bedplate to the yaw bearing so that I could model both components as one unit.
4) I modeled the welds on the bearing mounts and stiffeners near the transmission but I did not model the other welds. I modeled these welds because the metal is relatively thin and the welds help distribute the loads.
5) I modeled only the front half of the nacelle assembly to reduce the size of the problem.

FEA Loads:

1) We used ADAMS to approximate the loads on the LSS. These largest reactions in the low speed shaft at the adapter are listed in Table 3.32. I assumed that the reactions all occur simultaneously.
2) I distributed the force Fz (3,156 lb) on the main bearing mounts as 3,156 / 2 =1578 lb to each bearing mount. I applied Fx (1,768 lb) to the rear bearing mount.
3) The peak value of My is 13,027 ft-lb. The mainframe does not meet the NASA load safety factor requirements using this load. Thus, we will have to limit the LSS bending loads. We are not going to run the turbines in situations that result in severe teeter impacts (such as the 25 m/s, teetered, off yaw conditions). We will use the 90° yaw release simulation results as the limit for the LSS My load to 7989ft-lb. Thus, in all loads cases, we will be required to monitor the LSS My and limit it to 7989 ft-lb. All other loads in this FEA analysis were conservatively taken from the peak values of the all the ADAMS simulations at 25 m/s.
4) I applied the moments My and Mz as force couples on the main bearings. The bearings are 2 ft apart, thus the force couple representing My between the two bearings is then 7,989 / 2 = 3,995 lb on each bearing. The peak value of Mz is 5417 ft-lb. I applied this as a force couple of 2708 lb.
5) I assumed that the peak moment occurred about the nacelle Y-axis. This is a reasonable assumption since the peak moment was due to teeter impacts and teeter impacts typically on the lower blade when the blades are vertical.
6) I did not model the generator, high speed shaft, rotor brake, or transmission in the analysis. However, I did apply the loads that they create. The peak LSS shaft torque Mx is 3,801 ft-lb.

The corresponding HSS shaft torque is 151 ft-lb (the transmission ratio is 25.13:1). The difference between the LSS and HSS torque is resisted by a force couple between the LSS and the transmission mount (1.2 ft). The magnitude of this couple is (3,801 – 151 ft-lb) / 1.2 ft = 3,042 lb. I applied this force couple to the LSS main bearing and the transmission mount.

7) I constrained the yaw bearing to zero displacement.

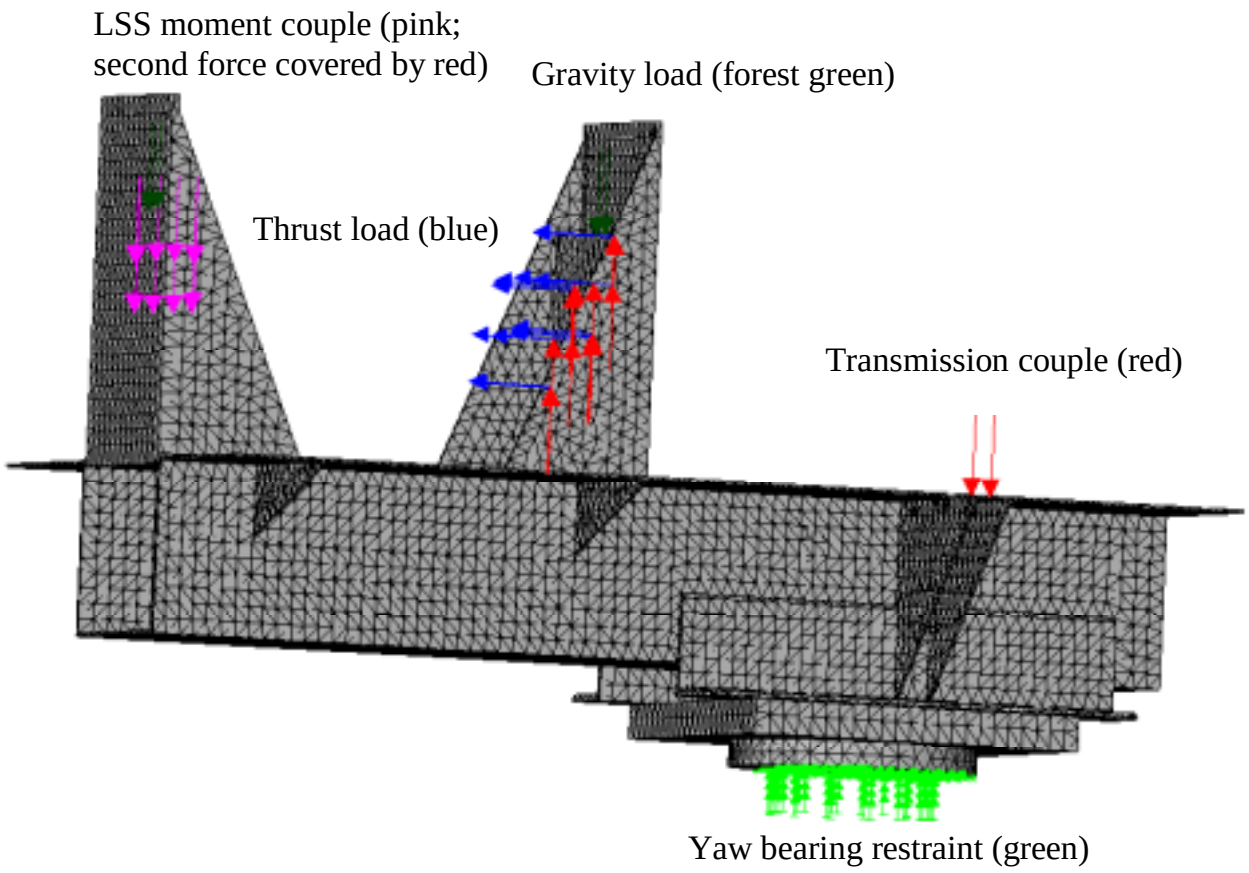

Figure 3.32: Loads applied for the nacelle analysis.

3.7.1.1.2. FEA results

The von Mises stress plot of the LSS is presented in Figure 3.33. The peak stress (18 kpsi) is a localized stress near the junction between the box beam and the nacelle mount. The safety factors against the yield strength and ultimate strength for the mainframe are

$$F.S._{yield} = S_{yield} / \sigma' = 36{,}000 / 12{,}000 = 3.0$$

$$F.S._{ultimate} = S_{ultimate} / \sigma' = 54{,}000 / 12{,}000 = 4.5$$

Thus the safety factors for this structure are adequate.

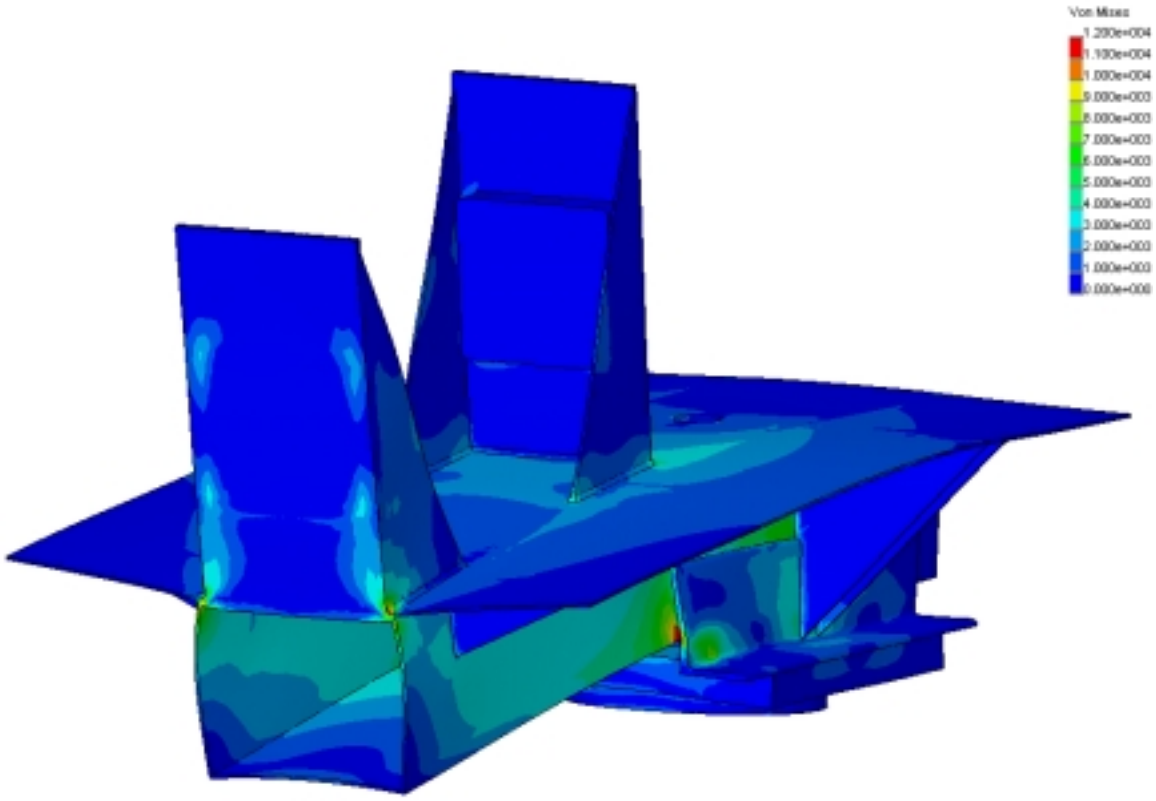

Figure 3.33: Von Mises stress plot of the nacelle assembly (deflection x25).

3.7.1.1.3. FEA validation

To check the FEA results, I computed the von Mises stress in the box beam between the two main bearings (see Figure 3.34). The box beam is subject to shear stress and bending stress at this section. The shear stress at this section is due to the forces used to simulate M_y and M_z (3,995 and 2708 lb) and the load Fz / 2 = 1,578 lb. Thus the downwards force on the main bearing mount is $((3,995 + 1,578)^2 + 2,708^2)^{.5}$ = 6,196 lb.

$$\tau = \frac{Fz}{A} = \frac{6{,}196\,lb}{13.73\,in^2} = 451\,psi$$

The bending stress at this section due is due to the couple used to simulate M_y and Mz and the load Fz / 2 = 1,578 lb. These forces are 1 foot from the section of interest. Thus the bending force on the main bearing mount is $(3,995^2 + 1,578^2)^{.5}$ ft-lb + 2,708 ft-lb = 7003 ft-lb = 84,040 lb-in

The bending stress at the section is

$$\sigma_{bending} = M_{bending}\, Z_{max} / \ I_{yy} \ = (84{,}040 * 7.14 \text{ in}) / 222 \text{ in}^4 = 2{,}703 \text{ psi}$$

A simplified formula for the von Mises stress for combined shear and bending is given by Mischke [70] as

$$\sigma' = (\sigma_x{}^2 + 3\tau_{xy}{}^2)^{\frac{1}{2}}$$

where σ_x is the tensile stress due to bending and τ_{xy} is the shear stress thus

$$\sigma' = (2{,}703^2 + 3 \times 451^2)^{\frac{1}{2}} = 2{,}813 psi$$

This value compares reasonably well with the von Mises stress determined in the FEA results of This value agrees well with the FEA von Mises stress result of 2000 to 3000 psi. Thus, I conclude the FEA analysis is sufficiently accurate.

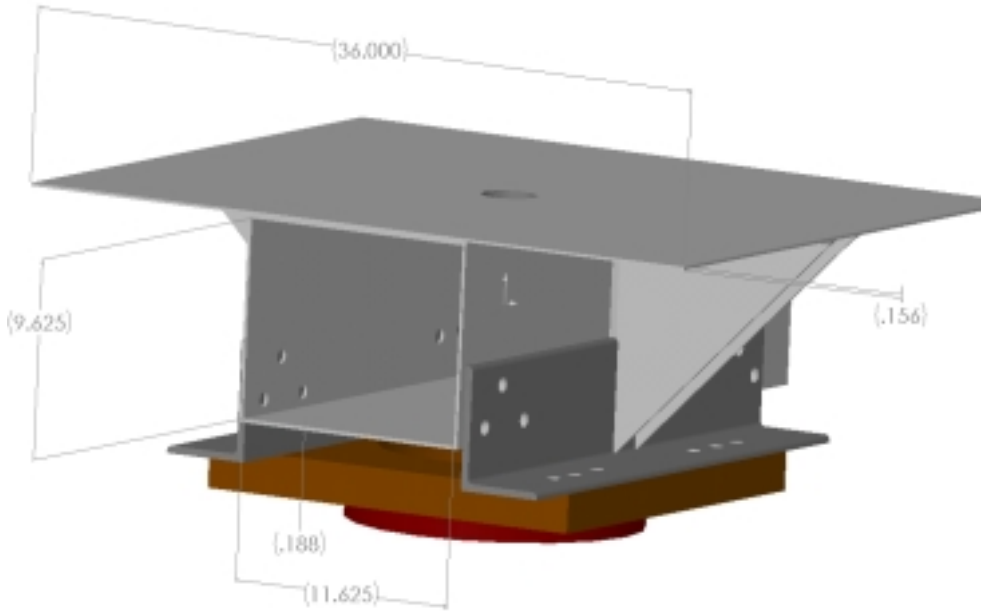

Figure 3.34: Section used to validate the mainframe FEA results.

3.7.1.1.4. Fatigue analysis

I analyzed the main beam for fatigue. I used the technique presented by Shigley and Mischke [71] for these analyses. The typical fatigue strength of low carbon steel under repeated axial tension is 32 kpsi [72]. The formula for the corrected endurance limit for a field specimen (S_e) is

$$S_e = k_a\, k_b\, k_c\, k_d\, k_e\, S_e'$$

where

k_a = surface factor

k_b = size factor

k_c = load factor

k_d = temperature factor

k_e = miscellaneous affects factor

The calculation of S_e for the hardlink mount components is presented in Table 3.34.

Table 3.34: Calculation of S_e for mainframe beam.

Component	Parameter	Deffinition	Value	Comments	Se' kpsi	Se kpsi	Von Mises stress kpsi
Hardlink pin	ka	surface factor	0.82	Rolled finish			
	kb	size factor	1.00	-			
	kc	load factor	1.00	Von Mises stress			
	kd	temp. factor	1.00	Room temp			
	ke	misc. affects factor	1.00	-			
	Effective k		0.82		32.0	**26.3**	12

The predicted von Mises stresses in the mainframe beam (12 kpsi) is less than the component endurance limits (23.6 kpsi). Thus, fatigue is unlikely to cause a failure in the mainframe.

3.7.2. Non-critical components

3.7.2.1. Transmission

The transmission transfers the torque from the LSS to the HSS. All other loads in the LSS are reacted by the main bearings. The only failure mode for the transmission is the gearing breaking. This failure could cause an rotor overspeed. However, in the NFAC, a rotor overspeed can be stopped by feathering the blades or stopping the NFAC fans. Thus, a transmission failure is not critical.

3.7.2.2. High speed shaft

The high speed shaft (HSS) transfers the torque from the transmission to the generator. The failure mode for the HSS is torsional failure. Such a failure may result in an overspeed. However, in the NFAC, a rotor overspeed can be stopped by feathering the blades or stopping the NFAC fans. Thus, a HSS failure is not critical.

3.7.2.3. Rotor brake

The rotor brake is a disk brake located inside the nacelle. The brake is rated at 3000 ft-lb. Failure of the rotor brake may result in an overspeed. However, in the NFAC, a rotor overspeed can be stopped by feathering the blades or stopping the NFAC fans. Thus, the rotor brake is not critical.

3.7.2.4. Generator

The generator is mounted to the mainframe inside the nacelle. Failures of the generator are have historically been electrical in nature. We have no structural concerns for the generator.

3.8. Tower assembly

We built a new tower for the wind tunnel testing (see Figure 3.35). The tower is 37.8 ft high (distance between the NFAC turn table and the yaw bearing). The tower will be anchored to the 80’ x 120’ semi-span mount with 12 ASTM A490 hex head bolts. No guy wires will be used because of the aerodynamic interference and the difficulty of mounting them to the NFAC turntable.

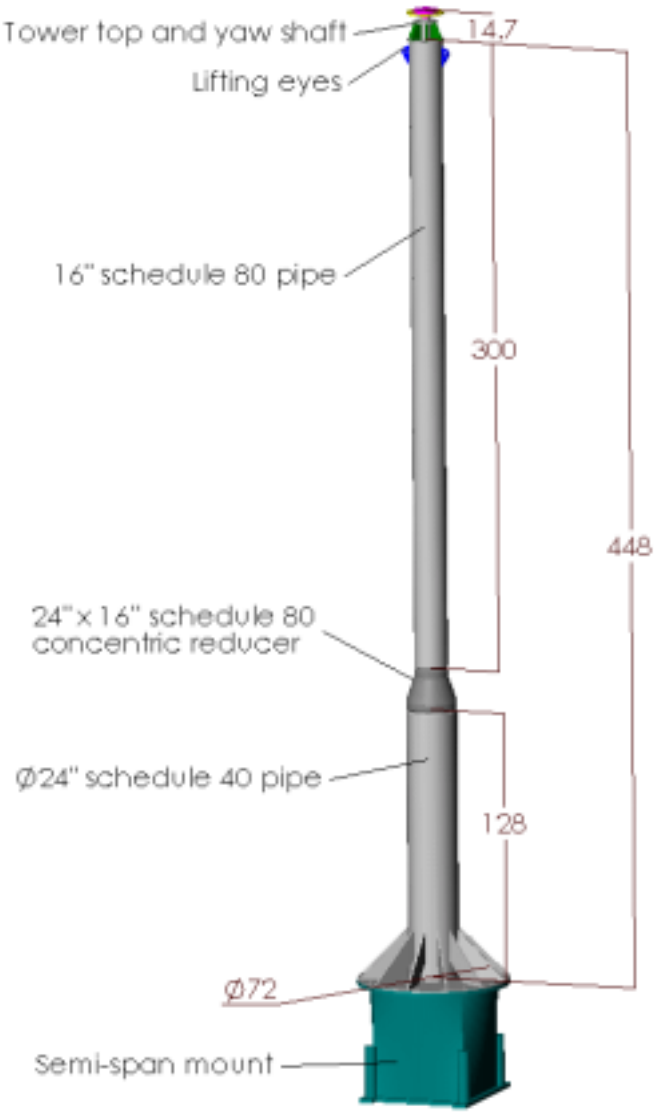

Figure 3.35: Tower assembly components.

We built a new tower for the wind tunnel testing (see Figure 3.35). The tower is 37.8 ft high (distance between the NFAC turn table and the yaw bearing). The tower will be anchored to the 80’ x 120’

semi-span mount with 12 ASTM A490 hex head bolts. No guy wires will be used because of the aerodynamic interference and the difficulty of mounting them to the NFAC turntable.

3.8.1. NFAC Semi-span mount

The semi-span mount is made from 1" plate roll-formed from a round top to a square base. It has twelve ¾" plate stiffeners (not shown in Figure 3.35) equally spaced between the round flange bolt holes.

The semi-span mount is a very robust structure compared to the tower. Such a stout structure probably does not require analysis. However, to be thorough, I have provided a rough analysis of the stresses in the mount.

According to the accompanying loads document, the peak tower base reactions (including the tower drag) are 71,173 ft-lbs bending and 1,776 lb shear. The semi-span mount has the smallest cross sectional area and moment of inertia at the T-Frame interface, 501" from the top of the yaw shaft. At this location, it is 37.25" square with a 1" thick wall (145 in^2 cross sectional area). The minimum moment of inertia at this location is roughly $(37.25^4 – 35.25^4)/ 12 = 31{,}781\ in^4$.

3.8.1.1. Bending stress

Using the formula for beam bending, the bending stress at the T-frame interface is

$$\sigma_{bending} = (M)\,(y) / (I) = (71{,}173\ \text{ft-lb} * 12\ \text{in/ft}) * (37.25\ \text{in} / 2) / 31{,}781\ in^4 = 500\ \text{psi}$$

The safety factors against bending the semi-span mount assuming A36 steel is

$$F.S._{yield} = S_y / T_1 = 36{,}000/ 500 = 72$$

$$F.S._{yield} = S_y / T_1 = 58{,}000/ 500 = 116$$

3.8.1.2. Shear stress

$$\sigma_{shear} = V/A = 1{,}776\ \text{lb} / 145\ in^2 = 12\ \text{psi}$$

This shear stress is negligible.

3.8.2. NFAC turn table

The turntable mechanism and limits for the 80' x 120' test section are described in the NFAC planning guide [73]. Four lift posts support the turntable. The shortest distance between each lift post is 36.771 ft. The limits on each lift are –50,000 to 100,000 lbs. The limit on the drag force is ±50,000 lb.

According to the accompanying loads document, the peak tower base reactions (including the tower drag) are 71,173 ft-lbs bending and 1,776 lb shear.

The safety factor against exceeding the force on the drag link is

$$F.S._{tension} = S_y / T_1 = 50{,}000 / 1{,}776 = 28.1$$

The peak post load is calculated by adding the gravity load to the moment reaction to the peak bending force. The weight of the nacelle is 3733 lb; the NASA tower weight is 7105 lbs; and the semi-span mount is 5016 lbs for a total weight of 15,854 lb.

Peak post load = 71,173 ft-lb / 37.771ft + 15,854 lb/ 4 = 5,847 lb.

The safety factor against exceeding the lift post limits is

$$F.S._{tension} = S_y / T_1 = 50{,}000 / 5{,}847 = 8.6$$

3.8.3. Tower base bolts

The tower is bolted to the semi-span mount using twelve ASTM A490 hex head bolts.

3.8.3.1. Tensile strength check

The peak bending load in the tower base (including the tower drag) is 71,173 ft-lbs. This bending load is resisted by tension in the bolts. In the tensile strength analysis I assume that tension in the bolts is a linear load distribution (similar to that shown in Figure 3.27).

The stress in the i^{th} bolt due to bending can be found using the flexure formula for beams:

$$\sigma_i = (M)\,(y_i) / (I) = (M)\,(y_i) / \Sigma(y_i^2)\,dA$$

Thus the bolt tension in the i^{th} bolt is

$$\text{Bolt tension}_i = (\sigma_i)\,(A_{bolt}) = (M)\,(y_i)\,(A_{bolt}) / A_{bolt}\,\Sigma(y_i^2)$$

$$\mathbf{Tension_i = (M)\,(y_i) / \Sigma(y_i^2)}$$

(see Table 3.35 for y_i and $\mathbf{\Sigma y_i^2}$ values)

Therefore

$$\text{Tension} = (M)(y_1) / \Sigma(y_i^2)$$

$$\text{Tension} = (71{,}173*12)(33) / 6{,}534 = 4313 \text{ lb}$$

$$\mathbf{F.S._{tension} = S_{ultimate} / T_1 = 210{,}600 / 4313 = 49}$$

Table 3.35: Component distances from the adapter center.

Bolt	yi	yi^2
1	33.0	1089.0
2	28.6	816.8
3	16.5	272.3
4	0.0	0.0
5	-16.5	272.3
6	-28.6	816.8
7	-33.0	1089.0
8	-28.6	816.8
9	-16.5	272.3
10	0.0	0.0
11	16.5	272.3
12	28.6	816.8
		6534.000

3.8.3.2. Shear strength check:

The peak shear force on the tower base bolts is 1,776 lb. Assuming the bolts are loaded equally, each bolt is subject to 148 lbs of shear which is negligible.

3.8.3.3. Joint preload check

According to the NFAC Test-Planning Guide, "A sufficient number of bolts shall be provided with preloads so that the net joint preload for all loading is at least two times the operating loads. [74]"

For the preload analysis, I assumed that the bolts were torqued to 50% of their proof load (.5 * 210,600 = 105,300 lb). This is a conservative assumption since we preloaded the bolts using a torque wrench to 75% ± 25% of their proof load.

The tensile strength check results indicate that the peak tension in the adapter bolts is 4,313 lb. The safety factor against exceeding the preload in this bolt is

$$F.S._{\text{Tension preload}} = 105{,}300 / 4{,}313 = 24$$

This high factor of safety exceeds the NFAC preload recommendation of 2 times the operating load; thus the joint is adequately pre-loaded.

3.8.4. Tower base and body

The tower base plate, webs, and tower top plates are made from A36 ¾" plate. The tower body is made from ASTM A106 schedule 40 (.688" wall thickness) and schedule 80 Type B pipe (.844" wall thickness). The two pipes are joined with a schedule 80 concentric reducer. The reducer has been welded

to the two pipes with welding procedure is AWS D1.1-98, joint B-U2a. All other welds are ½" fillet welds which meet AWS D1.1-98.

3.8.4.1. Stress analysis

3.8.4.1.1. FEA methodology

I performed a finite element analysis on the tower. I modeled the tower as I did in the vibration analysis. I assumed that the bolt preload and welds sufficiently joined the main frame mount to the main frame so that I could model both components as one unit and I modeled the nacelle as a steel cylindrical mass.

FEA loads:

1) I calculated the peak bending load in the loads document. I represented the peak bending load (71,173 ft-lbs) as a 1,795 lb force distributed on the cylindrical mass representing the nacelle.
2) I restrained the tower to zero displacement at twelve washer sized areas on the base of the tower (see Figure 3.36).
3) I applied a gravity load throughout the structure.
4) I applied a torsional load of 8,260 ft-lb on the cylindrical mass representing the nacelle.

Figure 3.36: Loads and restraints for the FEA analyses.

3.8.4.1.2. FEA results

The von Mises stress plot of the tower is presented in Figure 3.37. The von Mises stresses are all less than 6,000 psi. The peak stresses occur at the adapter transition. The weld a few inches above this transition is also highly stressed. According to AWS D1.1-98, the allowable stress in this weld is the same as the base material [75]. The safety factor against yielding the parent material or the weld is

$$F.S._{yield} = S_{yield} / \sigma' = 35{,}000 / 6{,}000 = 5.8$$

and the safety factor against exceeding the ultimate strength of the parent material is

$$F.S._{ultimate} = S_{ultimate} / \sigma' = 60{,}000 / 6{,}000 = 10$$

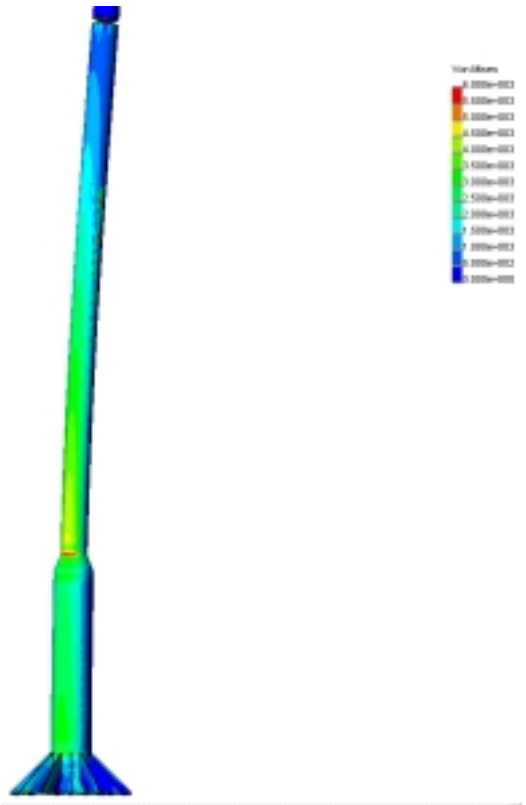

Figure 3.37: Von Mises stress plot of the tower.

3.8.4.1.3. FEA validation

To check the FEA results, I computed the peak von Mises stress at the top of the reducer. In this model, the top of the reducer is roughly 5" above the top of the taper. At this distance, the stresses should be relatively unaffected by the stress concentrations of the taper. The stresses at the top of the reducer are due to the bending, gravity, and torsional loads on the tower.

At this location, the moment of inertia about the tower 'X' axis is $\pi (16^4\text{-}14.312^4) / 64 = 1157$ in^4. The bending moment at the base of the ∅16" pipe from the load applied in the FEA analysis is

$$M = (1795 \text{ lb})(345 \text{ in}) = 618{,}467 \text{ lb-in} = 51{,}539 \text{ ft-lb}$$

Using the formula for beam bending, the bending stress at this section is

$$\sigma_{bending} = (M)\,(y) / (I_x) = (618{,}647 \text{ in-lb})(8 \text{ in}) / 1157 \text{ in}^4 = 4277 \text{ psi}$$

The compressive stress due to gravity is due the weight of the nacelle, yaw shaft, and ∅16" pipe. These weights are 2820 lb, 80 lb, and 3412 lb. The total weight on the section is 6,312 lb.

$$\sigma_{gravity} = (6{,}312 \text{ lb} / 40.2 \text{ in}^2) = 157 \text{ psi}.$$

Thus, the gravity load is negligible compared to the bending stress.

The torsional stress at the tower base is

$$\tau_{xy} = (Mz)\,(d_o / 2) / J$$

where $J = 2 * I_x = 2 * 1{,}157 = 2{,}314$ in^4

$$\tau_{xy} = (8{,}260 \text{ ft-lb} * 12 \text{ in/ft})(16"/ 2) / 2314 \text{ in}^4 = 343 \text{ psi}$$

A simplified formula for the von Mises stress for combined torsion and bending is given by Mischke [76] as

$$\sigma' = (\sigma_x^{\,2} + 3\tau_{xy}^{\,2})^{\frac{1}{2}}$$

where σ_x is the tensile stress due to bending and τ_{xy} is the shear stress thus

$$\sigma' = (4{,}277^2 + 3 \times 343^2)^{\frac{1}{2}} = 4{,}318\, psi$$

This stress calculation result (4,318 psi) compares reasonably well with the predicted range of stresses in the FEA results (4,500 psi to 5000) psi. One possible reason that the analytical solution does not fall within the range of the numerical results is that I did not account for the shear stress causing a tri-axial stress state. Thus, I conclude that the FEA results are accurate.

3.8.4.2. Fatigue analysis

I analyzed the tower root for fatigue. I used the technique presented by Shigley and Mischke [77] for these analyses. The typical fatigue strength of low carbon steel under repeated axial tension is 32 kpsi [78]. The formula for the corrected endurance limit for a field specimen (S_e) is

$$S_e = k_a\, k_b\, k_c\, k_d\, k_e\, S_e'$$

where

k_a = surface factor

k_b = size factor

k_c = load factor

k_d = temperature factor

k_e = miscellaneous affects factor

The calculation of S_e for the redesigned yaw shaft and the adapter plates is presented in Table 3.36.

Table 3.36: Calculation of S_e for the redesigned yaw shaft and the adapter plates.

Component	Parameter	Deffinition	Value	Comments	Se' kpsi	Se kpsi	Von Mises stress kpsi
Tower root	ka	surface factor	0.76	Hot rolled finish			
	kb	size factor	0.60	Large diameter			
	kc	load factor	1.00	Von Mises stress			
	kd	temp. factor	1.00	Room temp			
	ke	misc. affects factor	1.00	-			
	Effective k		0.46		32.0	**14.6**	6.0

The predicted von Mises stress at the tower root (6 kpsi) is significantly less than the component endurance limit (14.6 kpsi). Thus, fatigue is unlikely to cause a failure in tower.

3.8.5. Tower lifting eye analysis

The tower lifting eyes are made from 1" thick A36 steel (Sy= 36 kpsi, Sut= 58 kpsi). They were welded using a .75" symmetric fillet weld along the 10" dimension (see Figure 3.38).

The lifting force F causes shear (Fy) and tensile (Fx) forces in the welds. The geometry of the eyes is designed to withstand a 45 degree lift without inducing any bending in the eye welds. That is, when the lifting cable is angled 45 degrees from vertical, the force vector is coincident with the centroid of the weld area. Although a small amount of bending occurs at shallower angles, the bending is offset by the significantly reduced tension in the cable causing. Thus, a 45° cable angle is the worst case scenario.

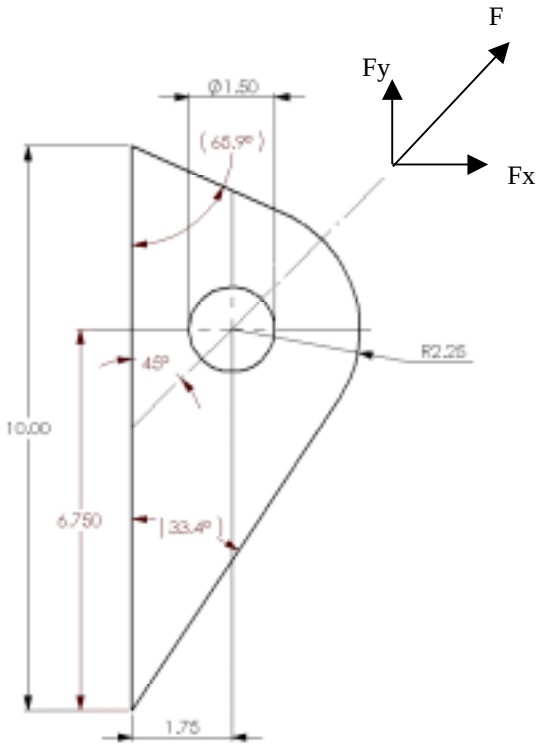

Figure 3.38: Tower lifting eye geometry.

The total weight of the tower, nacelle, and rotor is roughly 13,520 lbs. I multiplied this weight by a load factor of 1.5 to account for any dynamic affects which occur during lifting. I also assumed that the weight is evenly distributed among both of the lifting eyes. Therefore, the force components are

$$F = 13{,}520 * 1.5 / 2 * .707 = 14{,}342 \text{ lbs}$$

$$Fx = Fy = .707 * F = 10{,}140 \text{ lb}$$

The total weld effective area is

$$A = 1.414 * .75" * (1" + 10") = 11.665 \text{ in}^2$$

The shear stresses on the weld effective area are

$$\tau_x = \tau_y = Fx/A = 869 \text{ psi}$$

The stresses τ_x and τ_y are perpendicular to each other so there resultant is

$$\tau_{xy} = (\tau_x^2 + \tau_y^2)^{.5} = 1229 \text{ psi}$$

According to AWS D1.1-98, the allowable connection stress is .3 * the nominal strength of the filler material (70,000 psi). Thus the safety factor against exceeding the AWS allowable stress is

$$\boxed{F.S. = S/\sigma' = .3 * 70{,}000 / 1{,}229 = 17}$$

3.8.6. Tower top

Figure 3.39 displays the components at the top of the tower. The loads are transferred from the main frame mount to the tower-top via the bedplate, yaw bearing, and yaw shaft. The yaw shaft is fixed in the tower top with a pin. The bending loads applied to the yaw shaft are reacted at the upper and lower reaction points (see Figure 3.40). The weight of the nacelle is transferred through the small flange on the yaw shaft to the yaw shaft tube.

The tower top is constructed by welding six ¾" thick webs and two ¾" thick end plates to the yaw shaft tube and tower. The tower top webs and end plates are made from A572 grade 50 steel (minimum yield strength = 50 Kpsi; minimum tensile strength = 65 Kpsi). All seams were welded using F70XX SMAW electrodes to AWS D1.1-98 specifications.

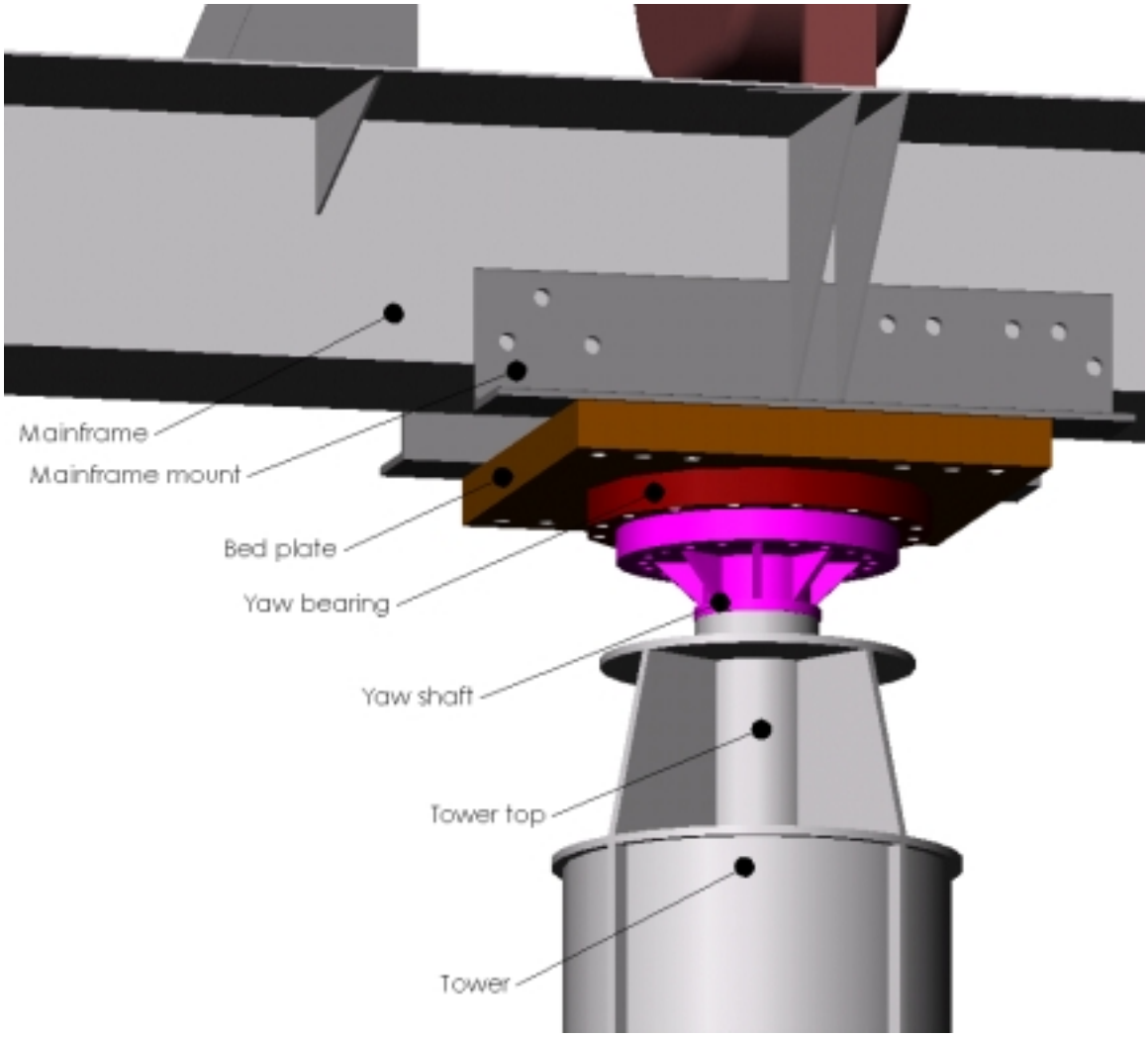

Figure 3.39: Nacelle and tower-top structure.

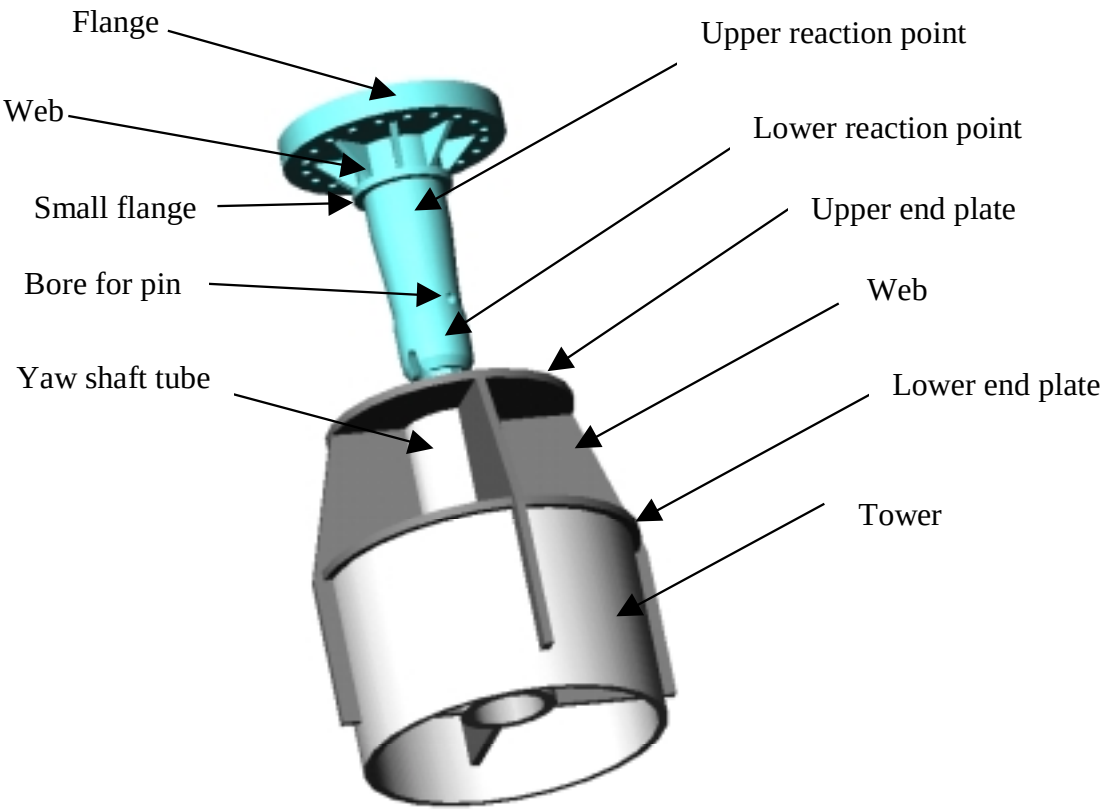

Figure 3.40: Yaw shaft and tower top structure.

3.8.6.1. FEA methodology

I performed a finite element analysis of the tower top. I used ADAMS to predict the forces and moments at the yaw shaft / tower-top interface. The FEA assumptions and loads are described below.

FEA assumptions:

1) I assumed the plates forming the tower top assembly were not welded but solidly joined. This assumption was necessary to obtain a meshable structure.
2) I applied the load in the direction in which resulted in highest stresses in the tower top. That is, I applied the bending moment in the same plane as one of the tower top webs.

FEA loads:

1) The peak loads in each direction predicted by ADAMS are listed in Table 3.38. I assumed each of these peak values occurred simultaneously.
2) I applied the resultant moment for Mx and My (Mxy = 16,736 ft-lb) to the tower top upper and lower reaction locations. The distance between the centers of the upper and lower

reaction points is 6.875". Thus, the couple I applied is 16,736 * 12 lb-in / 6.875 in =29,212 lb (blue arrows).

3) I split the resultant force for Fx and Fy (Fxy = 1,357 lb) on the tower top upper and lower reaction locations (orange arrows).
4) I applied the gravity force (5,376 lb) to the top of the yaw tube (red arrows).
5) The simulated yaw moment exceeds the capacity of the yaw brake. I assumed a yaw moment equal to the yaw brakes capacity (6000 ft-lb). I neglected the friction at the top of the yaw tube which acts to reduce the force on the yaw pins. I applied the entire yaw moment as a couple to each side of the yaw pin holes (pink arrows). The magnitude of the applied force couple is 6000 ft-lb * 12 in/ft / 5 in = 14,400 lb
6) I restrained the bottom of the tower top to zero displacement (green arrows).

Table 3.37: Predicted peak NFAC testing loads.

Component	Description	Maximum value (lb or ft-lb)
Fx	Thrust	1,181
Fy	Edgewise	669
$F_{x\&y}$	Resultant	1,357
Fz	Gravity	5,376
Mx	In-rotor-plane moment	4,805
My	Out-of-rotor-plane moment	16,031
$M_{x\&y}$	Resultant	16,736
Mz	yaw moment	8,260

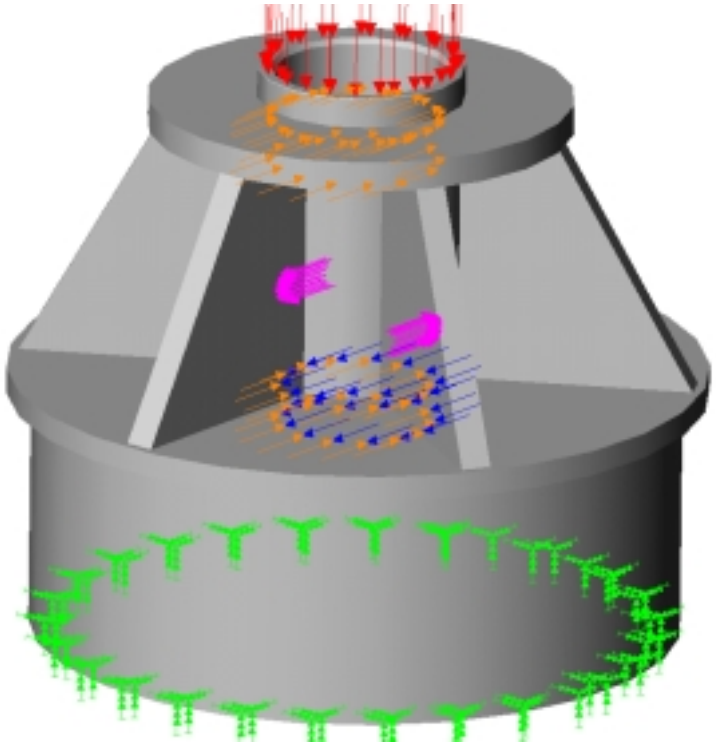

Figure 3.41: FEA loading of the tower top.

3.8.6.2. FEA results

Figure 3.42 presents the FEA results for the tower top. The peak stress in the yaw tube occurs near the yaw shaft pin. A comprehensive analysis of the yaw pin stresses is presented in Section 3.8.8.

The peak stress in the tower top plates and welds is 16,000 psi. Using this stress, the factors of safety for the plates and welds are

$$F.S._{yield} = S_{yield} / \sigma' = 50{,}000 / 16{,}000 = 3.1$$

$$F.S._{ult} = S_{ult} / \sigma' = 55{,}000 / 16{,}000 = 3.4$$

The welds are made to AWS D1.1-98. According to this standard, the allowable stress in a fillet weld is .3 * the nominal tensile strength of the filler metal (.3 * 70 = 21 kpsi). The safety factor to meet this standard is

$$F.S._{yield} = S_{yield} / \sigma' = 21{,}000 / 16{,}000 = 1.3$$

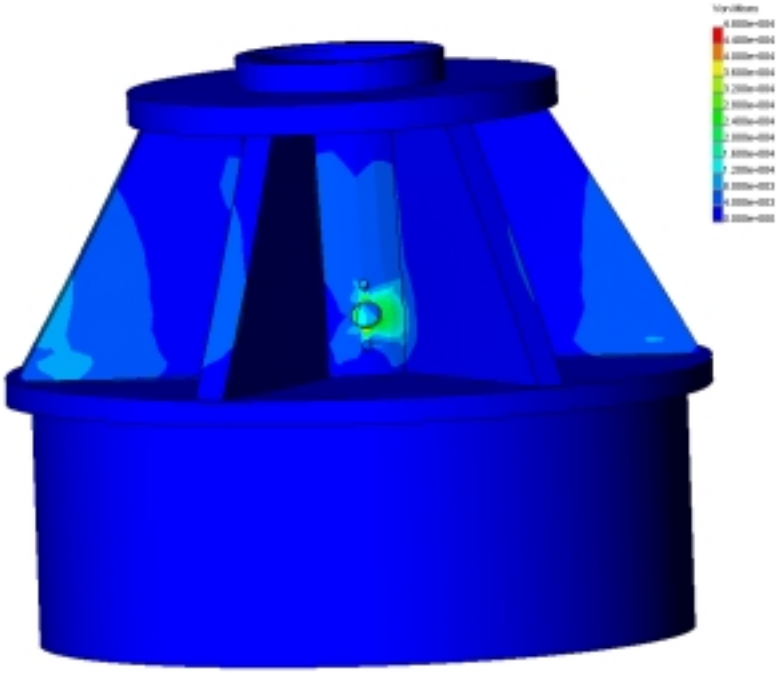

Figure 3.42: Von Mises stress plot of the tower top .

3.8.6.3. FEA validation

In addition to performing a mesh refinement study, I checked the finite element results analytically. The bearing stress from the yaw pin provides a good means of checking the FEA results analytically. The bearing stress can be calculated as

$$\sigma_{bearing} = F / A_{bearing} = 14{,}400 \text{ lb} / (.7 \text{ in} * .675 \text{ in}) = 30{,}476 \text{ psi}$$

This result compares well with the FEA results (28,000 to 32,000 psi). Thus I conclude that the FEA results are accurate.

3.8.7. Yaw shaft

The yaw shaft transfers the loads from the nacelle to the tower top. It also mounts the brake disk. Grumman aerospace designed the yaw shaft. The Grumman design documentation for the yaw shaft is not available. Therefore we sacrificed a spare yaw shaft to reverse engineer the part.

The yaw shaft is a weldment made of four types of components: the large flange, the webs, the ring, and the shaft. All of the components were made from annealed 4340 steel. All of the components except the ring were welded to the shaft using 308 stainless steel welding wire. The ring was welded to the shaft using 410 stainless steel welding wire. The typical tensile and yield strength of 4340 bar in the quenched and tempered condition is 140 Kpsi and 110 Kpsi [79]. The minimum tensile and yield strengths

for 308 filler metal are 81 Kpsi and 55 Kpsi [80]. The typical tensile and yield strengths for 410 stainless steel 135,000 psi and 105,000 psi [81].

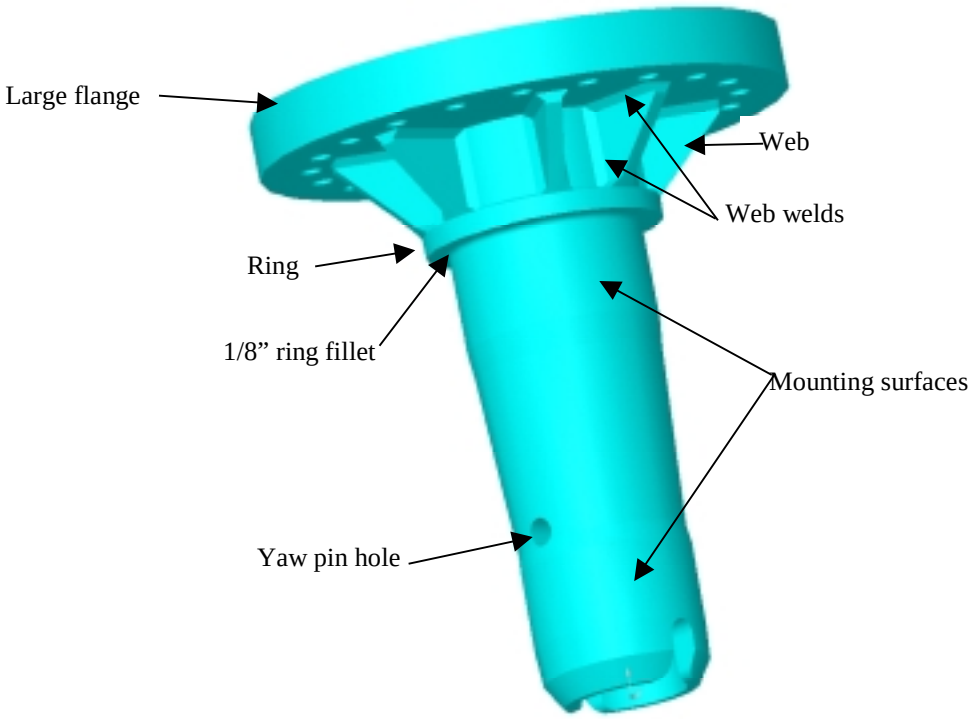

Figure 3.43: Yaw shaft construction.

3.8.7.1. FEA methodology

The bending load (My) is the primary contributor to the yaw shaft stress. The bending on the yaw shaft results from the nacelle “nodding” (oscillating about the nacelle Y-axis.) This motion also results in bending of the low speed shaft which is monitored. Thus, there is a strong correlation between LSS bending and the yaw shaft bending (see Figure 3.44). We will use the LSS bending stain gages to monitor the yaw shaft during operation. We will use a conservative line fit to predict the loads on the yaw shaft.

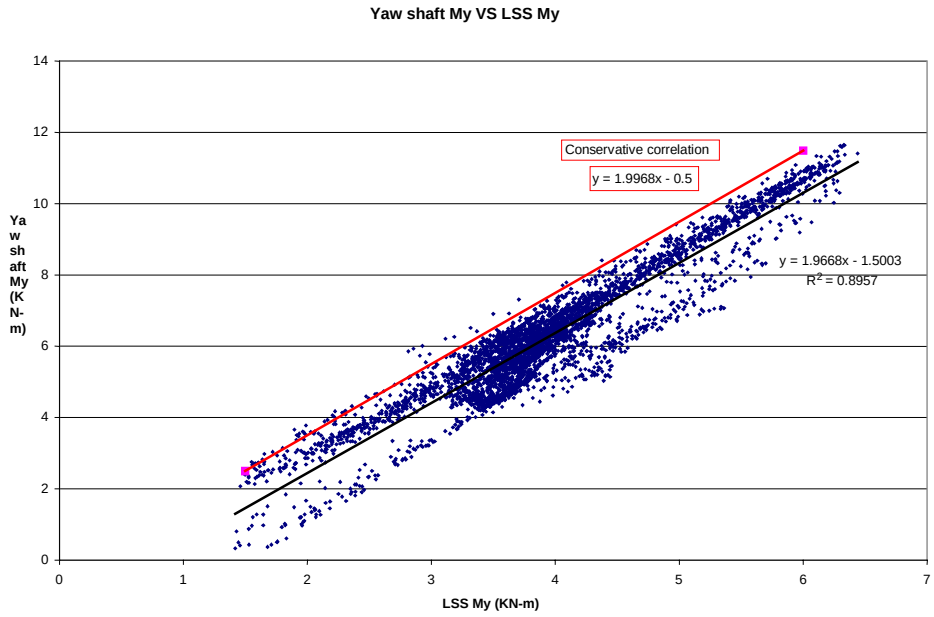

Figure 3.44: Correlation between yaw shaft moment My and LSS moment My.

Preliminary stress analyses of the LSS indicate that in the downwind teetered configuration, the yaw shaft stresses exceed the NASA recommendations during the 25 m/s wind speeds between 30° and 75° yaw angles. In order to meet the NASA recommended safety factor of 2.5 on tensile for a class 2 load, we will restrict the turbine to 15 m/s when running between the 30° and 75° yaw angles range. I performed the stress analysis of the yaw shaft using the peak loads from the 0° to 180° load case using 15 m/s wind. These loads are presented in Table 3.38.

I performed an finite element analysis on the yaw shaft. I describe the FEA assumptions and loads below.

FEA assumptions:

1) I shortened the distance between the yaw shaft mounting surfaces to reduce the size of the model. This assumption is justified because the region between the mounting surfaces is not a highly stressed region.
2) I assumed the yaw shaft webs, flange, yaw bearing, and the tower top assembly were solidly joined. This unconservative assumption was necessary to perform the finite element analysis.
3) The yaw flange is actually 1.25” thick. I modeled the flange as 3.25” thick (see Figure 3.45). I increased the thickness of the flange so that I could apply a force couple to the flange without causing unrealistic distortion in the yaw shaft.
4) I applied the bending moment in the direction in which resulted in highest stresses in the yaw shaft webs. That is, I applied the bending moment in the same plane as one of the webs.

FEA loads:

1) The peak loads as by ADAMS for 15 m/s wind are listed in Table 3.38. I assumed each of these peak values occurred simultaneously.
2) I applied the resultant moment for Mx and My (Mxy = 8891 ft-lb) to two flats on the large flange (orange arrows) as a couple.
3) I neglected the forces Fx and Fy because they are small compared to the gravity load and the bending moments.
4) I applied the gravity load to the top of the large flange and it's reaction to the ring. The ring sits atop the tower and takes all of the gravity load.
5) I restrained the mounting surfaces of the yaw shaft to zero displacement (green arrows).

Table 3.38: Predicted peak NFAC testing loads.

Component	Description	Maximum value (lb or ft-lb)
Fx	Thrust	593
Fy	Edgewise	137
Fz	Gravity	4358
Mx	In-rotor-plane moment	2294
My	Out-of-rotor-plane moment	8590
$M_{x\&y}$	Resultant	8891
Mz	yaw moment	6000

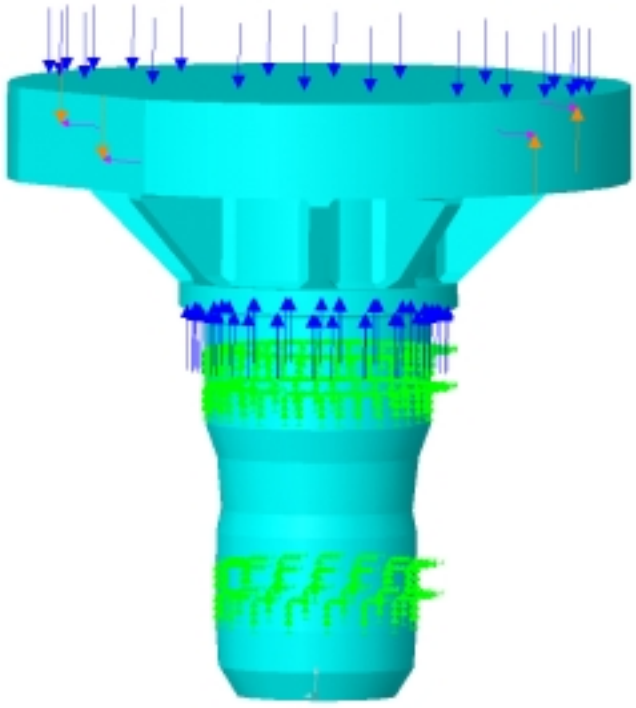

Figure 3.45: FEA loading and mesh of the yawshaft and tower top assembly.

3.8.7.2. FEA results

Figure 3.46 presents the FEA results for the tower top and yaw shaft. The two critical regions in the yaw shaft are at the .125" fillet beneath the ring and the welds at the base of the webs. The peak load in the yaw shaft webs is 27,000 psi. The web welds were made using 308 stainless steel rod. [82]. The minimum tensile and yield strengths for 308 filler metal is 81 Kpsi and 55 Kpsi [83]. The factors of safety for the yaw shaft web welds are

$$F.S._{yield} = S_{yield} / \sigma' = 55{,}000 / 27{,}000 = 2.0$$

$$F.S._{ult} = S_{ult} / \sigma' = 81{,}000 / 27{,}000 = 3.0$$

The peak load in the .125" fillet beneath the ring is 48,000 psi. The weld beneath the ring was made using 410 SS rod. After welding the ring to the shaft, the welds were tempered and the fillet was machined. The typical tensile strength of 410 stainless in the heat treated condition is 135,000 psi [84]. The typical tensile and yield strength of the 4340 parent material in the quenched and tempered condition is 140,000 psi. The factor of safety for the yaw shaft ring weld is

$$F.S._{yield} = S_{yield} / \sigma' = 105{,}000 / 45{,}000 = 2.3$$

$$F.S._{ult} = S_{ult} / \sigma' = 135{,}000 / 45{,}000 = 3.0$$

Although these safety factors do not meet the standard NFAC safety factor requirements ($F.S._{ultimate}$ is below 4.0), they meet the requirements for a class 2 load. ($F.S._{yield}$ = 2.0 and $F.S._{ultimate}$ = 3.0 * FB). FB for 4340 Q&T steel in this condition is at most 1 [85].

We have LSS field loads during the phase IV experiment of LSS bending loads up to 10,671 ft-lb (14,471 N-m). Using the correlation derived in Figure 3.44, this correlates to a yaw shaft load of 20,939 ft-lb. In order to qualify for a class 2 load, the yaw shaft must be proof tested up to 150% of the peak load. The peak value of $M_{x\&y}$ used in this analysis was 8,891 ft-lb. 150% of this value is 13,336 ft-lb. Thus, the yaw shaft has been successfully proof tested for a class 2 load. The LSS meets the requirements for a class 3 load case.

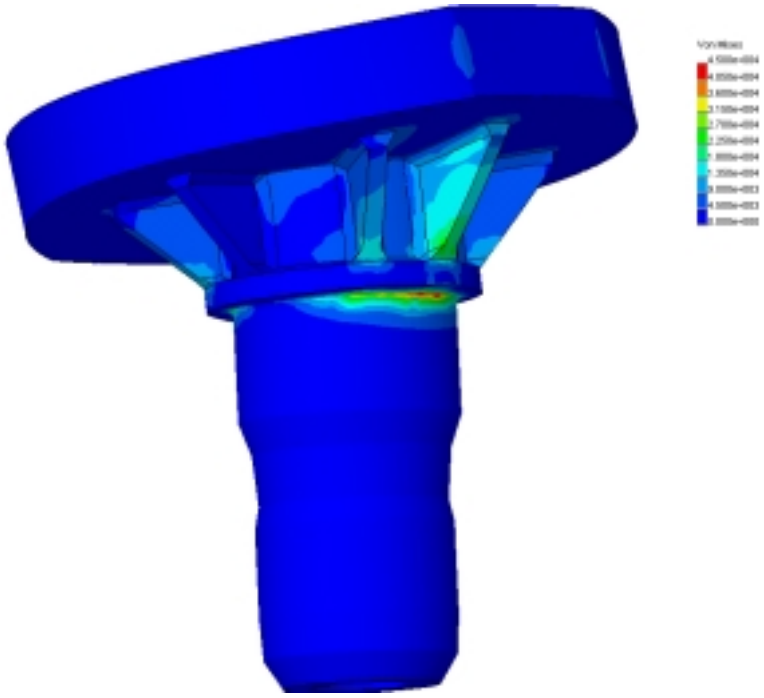

Figure 3.46: Yaw shaft FEA results.

3.8.7.3. FEA validation

In addition to performing a mesh refinement study, I computed the bending stresses in the yaw shaft at the section shown in Figure 3.47 to validate the FEA results. The moment of inertia about the 'X' axis is 26.08 in^4. The bending moment at the section is due primarily to $M_{x\&y.}$ Using the formula for beam bending, the bending stress at this section is

$$\sigma = (M)\,(y) / (I) = 8820 * 12 * 3.6 / 26.08 = 14{,}610 \text{ psi}$$

The gravity load adds to the peak compressive stress. The compressive stress due to gravity is 4,011 lb / 16.8 in^2 = 239 psi. Thus, the peak compressive stress at this section is 14,610 + 239 psi = 14,849 psi. This stress calculation compares favorably with the predicted range of stresses in the FEA results (12,000 psi to 16,000) psi. Thus, I conclude that this these are valid FEA results.

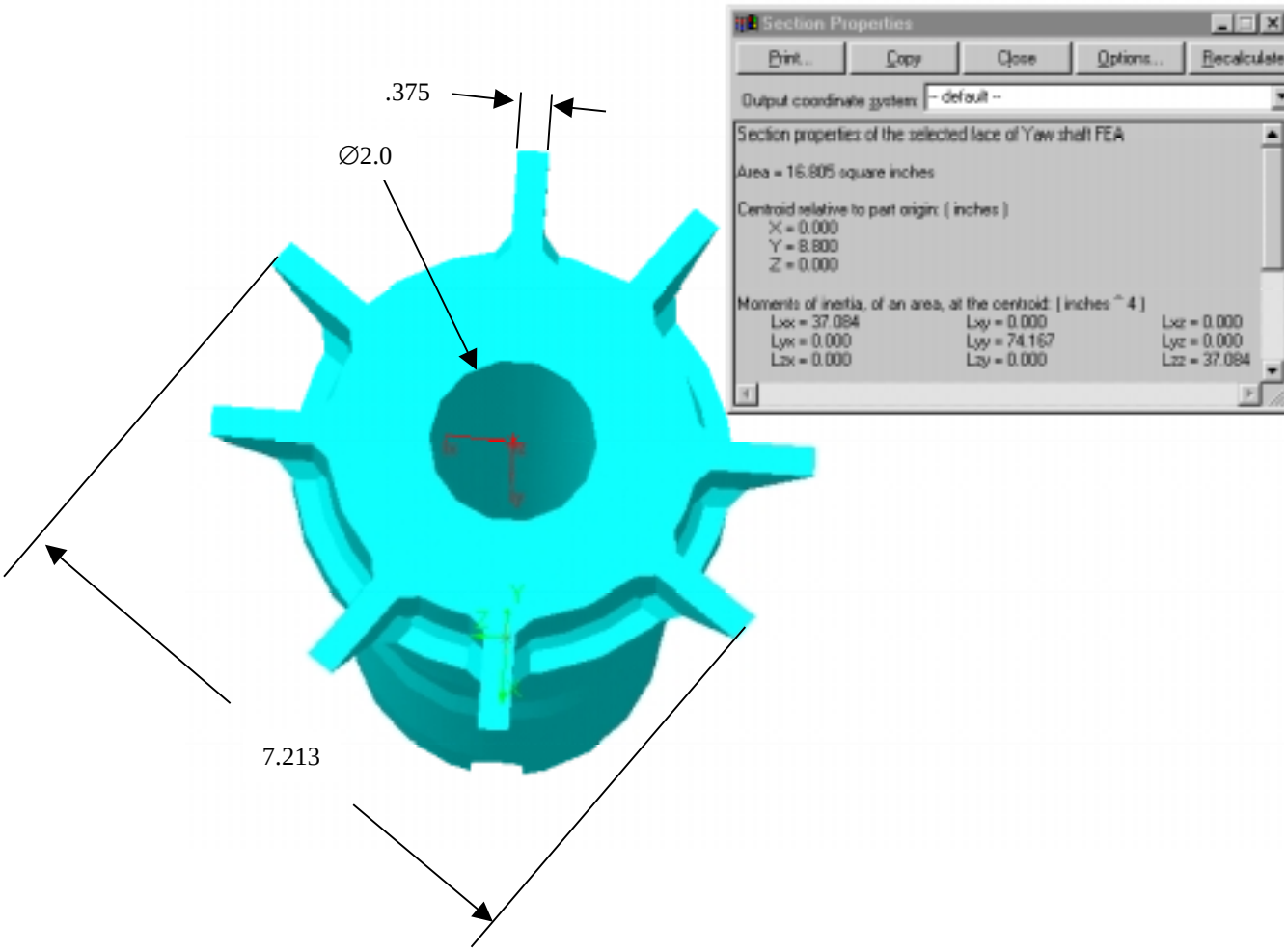

Figure 3.47: Section geometry for FEA validation.

3.8.7.4. Fatigue analysis

I analyzed the yaw shaft for fatigue. The primary stress driver of the yaw shaft is the bending load My. My is an oscillating load. The worst oscillations occur during 15 m/s testing of the 0° to 180° Yaw angle at about 45° of yaw angle. For the fatigue analysis, I assumed that this load cycle occurs throughout the life of the yaw shaft. The mean bending load during this cycle is 5,229 ft-lb with an oscillating component of ± 3,023 ft-lb.

The Soderberg criteria is the a conservative predictor of failure for alternating stresses with a mean load [86] and is given by

$$\frac{\sigma_a}{S_e} + \frac{\sigma_m}{S_{yt}} = \frac{1}{n}$$

where

σ_m is the mean stress component

σ_a is the alternating stress component

S_e is the component endurance limit

S_{yt} is the material yield strength

n is the factor of safety for fatigue (assuming an infinite life)

Because the FEA results are linear, the mean and alternating stress components are

$$\sigma_m = 48 \text{ kpsi} * 5{,}229 \text{ ft-lb} / 8{,}590 \text{ ft-lb} = 29.2 \text{ kpsi}$$

$$\sigma_a = 48 \text{ kpsi} * 3{,}023 \text{ ft-lb} / 8{,}590 \text{ ft-lb} = 16.9 \text{ kpsi.}$$

The formula for the corrected endurance limit for a field specimen (S_e) is

$$S_e = k_a k_b k_c k_d k_e S_e'$$

where

k_a = surface factor

k_b = size factor

k_c = load factor

k_d = temperature factor

k_e = miscellaneous affects factor

The calculation of S_e for the yaw shaft is presented in Table 3.39.

Table 3.39: Calculation of S_e for the yaw shaft ring weld.

Component	Parameter	Deffinition	Value	Comments	Se' kpsi	Se kpsi	Von Mises stress kpsi
Redesigned yaw shaft	ka	surface factor	1.00	Machined finish			
	kb	size factor	1.00	Non rotating bending load; de = .37*5.2 =1.92"			
	kc	load factor	1.00	Von Mises stress			
	kd	temp. factor	1.00	Room temp			
	ke	misc. affects factor	0.50	Welds			
	Effective k		0.50		88.0	**44.0**	48

Thus the factor of safety against fatigue is

$$n = \frac{1}{\frac{\sigma_a}{S_e} + \frac{\sigma_m}{S_{yt}}} = \frac{1}{\frac{16.9}{44} + \frac{29.2}{135}} = 1.7$$

Thus the Soderberg formula predicts an infinite life with a safety factor of 1.7. Therefore the component is unlikely to fail in fatigue.

3.8.8. Yaw shaft pins

The yaw shaft is pinned to the tower top using two ∅5/8" pins on either side of the yaw shaft. These pins resist the torque from the yaw brake. The yaw brake can generate up to 6,000 ft-lb before it slips. The yaw shaft ring sits on top of the yaw tube. This friction resists the yaw brake torque.

This frictional torque can be estimated using

Friction = μ * Weight * $D_{\text{yaw tube}}$ = .25 * 4,011 lb * 5 in = 5,014 lb-in = 418 ft-lb

The torque transferred to the yaw pin is then 6,000 ft-lb – 418 ft-lb = 5,582 ft-lb. This torque is applied to the yaw pins as a shear load. The magnitude of the shear load on each pin can be calculated using

F_{shear}= Torque / Yaw tube ID = 5,582 ft/lb * 12 lb/in / 4.2 in = 15,949 lb.

Bearing stress: The yaw tube has a wall thickness of .9" at the yaw shaft pins. The bearing area on the yaw tube is .9" * .625" = .5625 in^2. The bearing stress of the yaw pin on the yaw shaft is

σ_{bearing} = 15,949 / .5625 in^2 = 28,353 psi

The yaw tube is made from A572 grade 50 steel (minimum yield strength = 50 Kpsi; minimum tensile strength = 65 Kpsi). The factor of safety against deforming the yaw tube is

$F.S._{\text{Yaw tube bearing}}$= 50 kpsi /28.3 kpsi = 1.8

The yaw shaft must also be checked for it's bearing strength. The yaw pin extends .9" into the yaw shaft. The bearing area on the yaw tube is .625 in * .9 in = .5625 in^2. The bearing stress on the yaw pin and yaw shaft is roughly

σ_{bearing} = 15,949 / .5625 in^2 = 28,354 psi

The yaw shaft is made from annealed 4340 steel (minimum yield strength = 69 Kpsi; minimum tensile strength = 101 Kpsi). The factor of safety against deforming the yaw shaft is

$F.S._{\text{Yaw shaft bearing}}$= 69 kpsi / 28.3 kpsi = 2.4

Shear stress:

The shear stress in the pin is

$$\sigma_{shear} = 15{,}949 / (\pi * d^2 / 4) = 15{,}949 / (\pi * .625^2 / 4) = 52.0 \text{ kpsi}$$

According to the distortion energy theory, the allowable shear strength can be estimated as .577 * S_y. The pins are made from 15-5 stainless steel aged to the H 925 condition. The yield strength for this material is 155 kpsi. Thus, the allowable shear strength of the material is .577 * 155 kpsi = 89.4 kpsi. The factor of safety against shearing the pin is

$$F.S._{Yaw\ pin\ shear} = 89.4 \text{ kpsi} / 52.0 \text{ kpsi} = 1.7$$

This safety factor is acceptable since a shear pin failure is not critical. The consequence of this failure would simply allow the nacelle to yaw freely. Furthermore the torque on the yaw shaft is a value which is monitored using the force sensor integrated into the yaw brake.

3.9. Boom assembly

The boom assembly was recently redesigned and rebuilt and is shown in Figure 3.48. The complete boom assembly now weighs approximately 325 lb and the center of gravity is 42.5" from the teeterpin axis. The boom is rigidly mounted to the boom mount using 5/16" UNC grade 8 bolts. The boom mount is clamped to the boom adapter using eight ¾" UNC grade 8 bolts. The boom adapter is bolted to the boom spacer and teeterpin cap using the eight ½" UNF L9 teeter pin cap bolts.

The boom adapter plate, boom mount, boom bars, boom bar gussets, boom bar flanges, 5/16" flange bolts, ¾" adapter bolts, and ½" teeter pin cap bolts are critical because they suspend the entire boom mass. The mounting of the three large boxes is also critical because each box weighs approximately 53 lb each. These items are analyzed in the following sections.

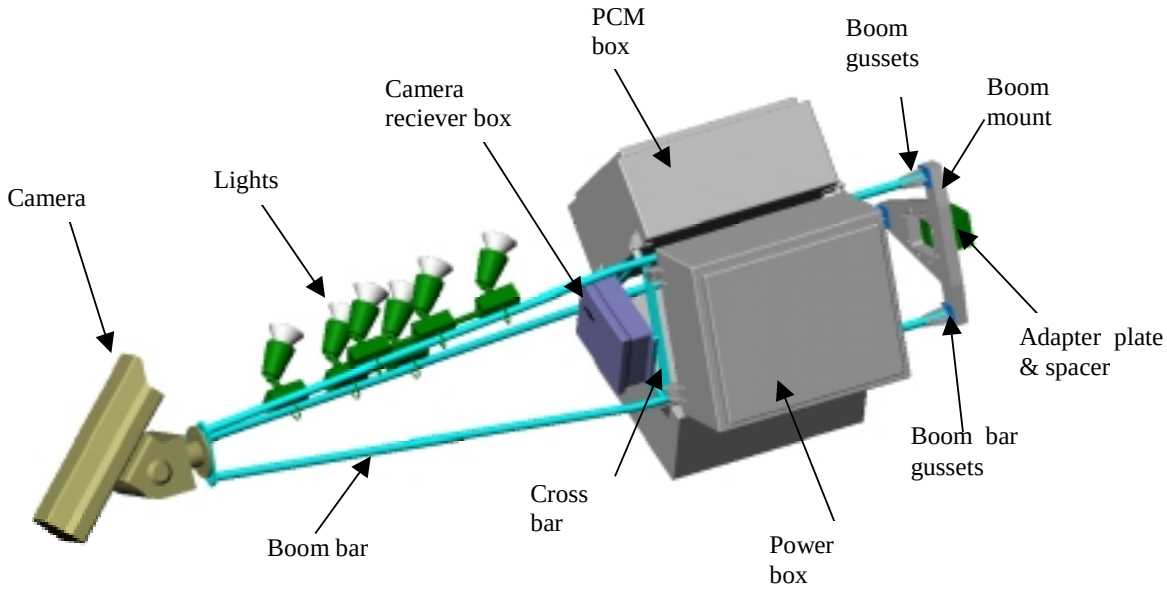

Figure 3.48: New boom assembly.

3.9.1. Boom arm loading

The boom is subjected to gravitational and inertial loads. The boom bars transfer these loads to the boom mount. The boom mount transfers the loads to the spacer and hub shaft. We used the ADAMS simulations to determine the six force and moment reactions at the boom gusset / boom mount interface (see Table 3.40). The shear forces (Fy and Fz) and bending forces (My and Mz) dominate at this location. Although I did not assume the peak values of My and Mz occur simultaneously, I added these two vector components for each time step using a spread sheet and used the largest resultant as the peak load.

The bending forces and thrust forces on the boom assembly are transmitted through the boom arms in tension and compression. The following section discusses how these loads were resolved into tension and compression loads.

Table 3.40: Boom loads at the gusset / boom mount interface.

Component	Maximum value (lb or ft-lb)
Fx	248
Fy	676
Fz	1071
Mx	442
My	3414
Mz	1919
$(My^2 + My^2)^{.5}_{max}$	3,589

3.9.1.1. Boom arm tension

The boom tubes form an equilateral triangle with the vertices on a circle centered on the rotor axis. (see Figure 3.49). The loads which create tension in the boom tubes are Mx, My, and Fx. I assumed that Fx is spread evenly among the three boom tubes. The resulting load in each tube due to Fx is 248 lb / 3 = 83 lb which is negligible compared to the tension due to Mx and My.

I assumed that the bending moments Mx and My are resisted by forces which vary linearly across the horizontal axis as shown in Figure 3.51. For this force distribution, the tension in each rod end due to bending can be found using

$$\mathbf{Tension_i = (M)\ (y_i) \ / \ \Sigma(y_i^2)}$$

where M = 3,589 ft-lb = 43,068 in-lb

Using this formula, I plotted the tension in each rod end as a function of θ (where θ is the angle from the vertical). The results of this calculation are presented in and plotted in Figure 3.51.

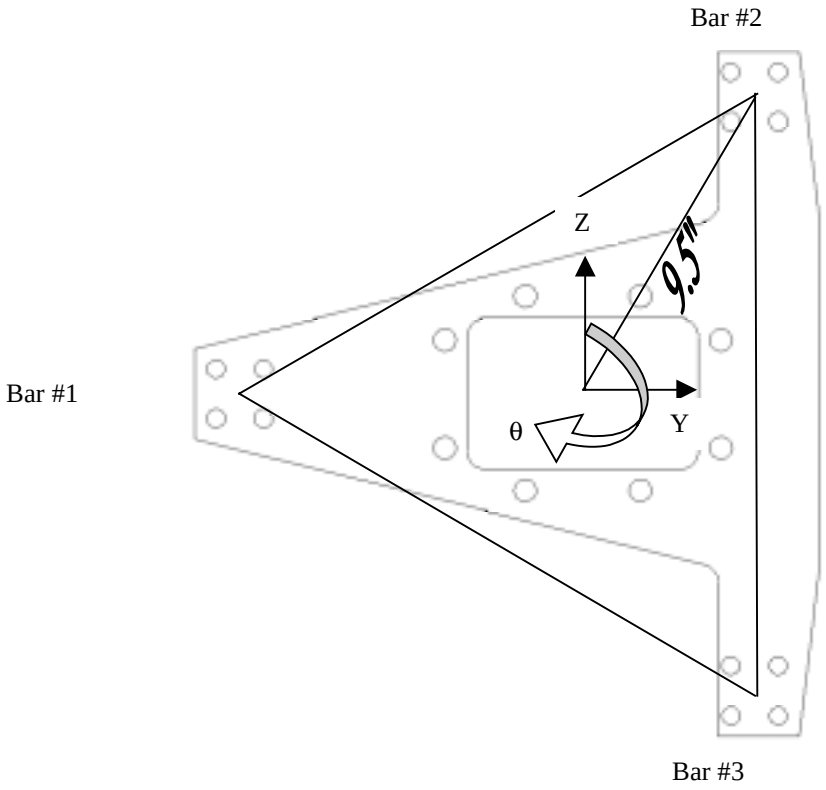

Figure 3.49: Boom mount geometry.

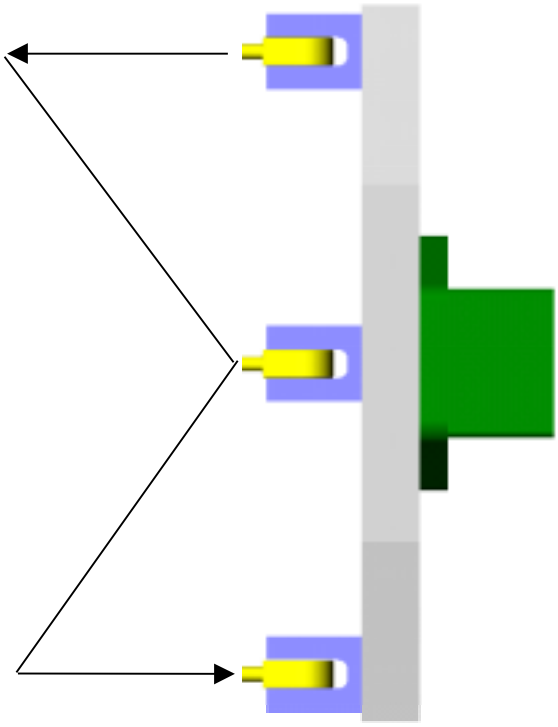

Figure 3.50: Bar load distribution.

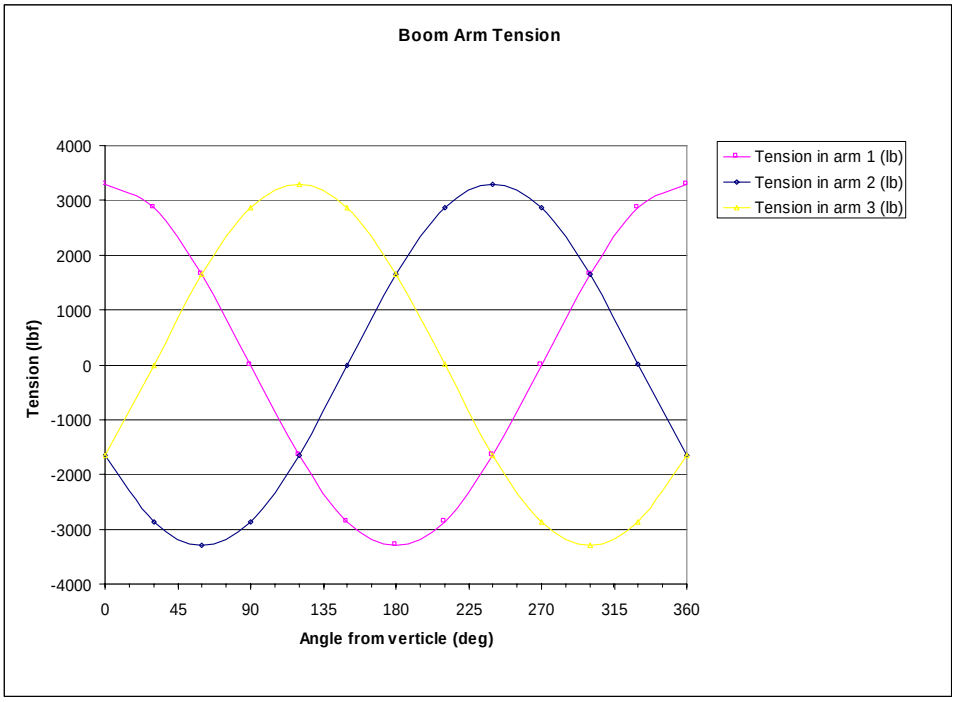

Figure 3.51: Tension values in boom arms as a function of angle (0° is vertical).

Table 3.41: Tension in boom arms due to bending as a function of boom angle.

Theta (deg)	Distance y1 (in)	Distance y2 (in)	Distance y3 (in)	Tension in arm 1 (lb)	Tension in arm 2 (lb)	Tension in arm 3 (lb)
0	9.50	-4.75	-4.75	3,022	-1,511	-1,511
30	8.23	-8.23	0.00	2,617	-2,617	0
60	4.75	-9.50	4.75	1,511	-3,022	1,511
90	0.00	-8.23	8.23	0	-2,617	2,617
120	-4.75	-4.75	9.50	-1,511	-1,511	3,022
150	-8.23	0.00	8.23	-2,617	0	2,617
180	-9.50	4.75	4.75	-3,022	1,511	1,511
210	-8.23	8.23	0.00	-2,617	2,617	0
240	-4.75	9.50	-4.75	-1,511	3,022	-1,511
270	0.00	8.23	-8.23	0	2,617	-2,617
300	4.75	4.75	-9.50	1,511	1,511	-3,022
330	8.23	0.00	-8.23	2,617	0	-2,617
360	9.50	-4.75	-4.75	3,022	-1,511	-1,511

3.9.1.2. Boom arm shear

The shear load is also carried through the boom arms. The shear load is calculated by adding the force vectors Fy and Fz. If I assume that the peak loads occur simultaneously, the result of the two loads is $(676^2+1{,}071^2)^{.5}$ = 1,266 lb. Assuming that this loads is distributed evenly among all three boom bars results in a shear force in bar of 1,266 / 3 = 422 lb

3.9.2. Boom mount and adapter plate

The boom mount is made from 1.5" thick 2024-T351 aluminum plate. According to the certificate of test provided by the manufacturer, the minimum tensile strengths for this material are S_{yield} = 45.9 kpsi, $S_{ultimate}$ = 66.3 kpsi.

The boom mount bolts to the adapter plate which is bolted to the teeterpin cap (see Figure 3.53). The adapter plate is made from quenched and tempered 4150 steel. This steel has typical tensile strengths of S_{yield} = 115 kpsi, $S_{ultimate}$ = 145 kpsi [87].

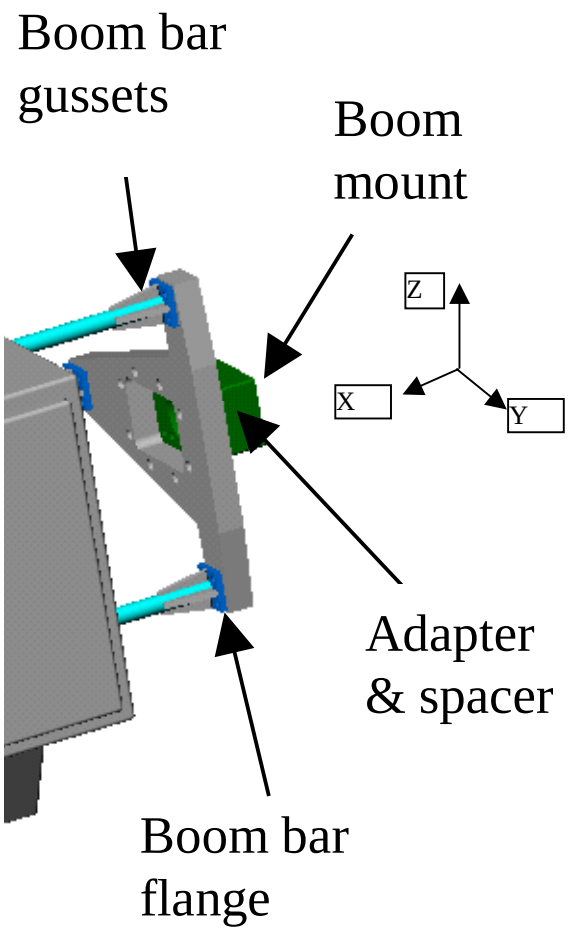

Figure 3.52: Boom mount assembly.

3.9.2.1. FEA methodology

I performed an finite element analysis on the boom mount and adapter plate. In the analysis, I used the loads derived in section *3.9.1.1 Boom arm tension.* In that section, the peak axial load on each rod end was predicted to be 3,589 lbs. In the finite element analysis of the boom mount I assumed the following

1) The loads on the boom mount change as the rotor rotates (see Figure 3.51). I investigated two significantly different load combinations. These load configurations are shown in Figure 3.53; they correspond to the azimuth angles $\theta = 60°$ and $90°$ (θ is the angle of boom arm #1 from vertical).
2) I did not model the shear loads as they are negligible compared to the bending moment on the boom.
3) I restrained the upwind face of the spacer to zero displacement.

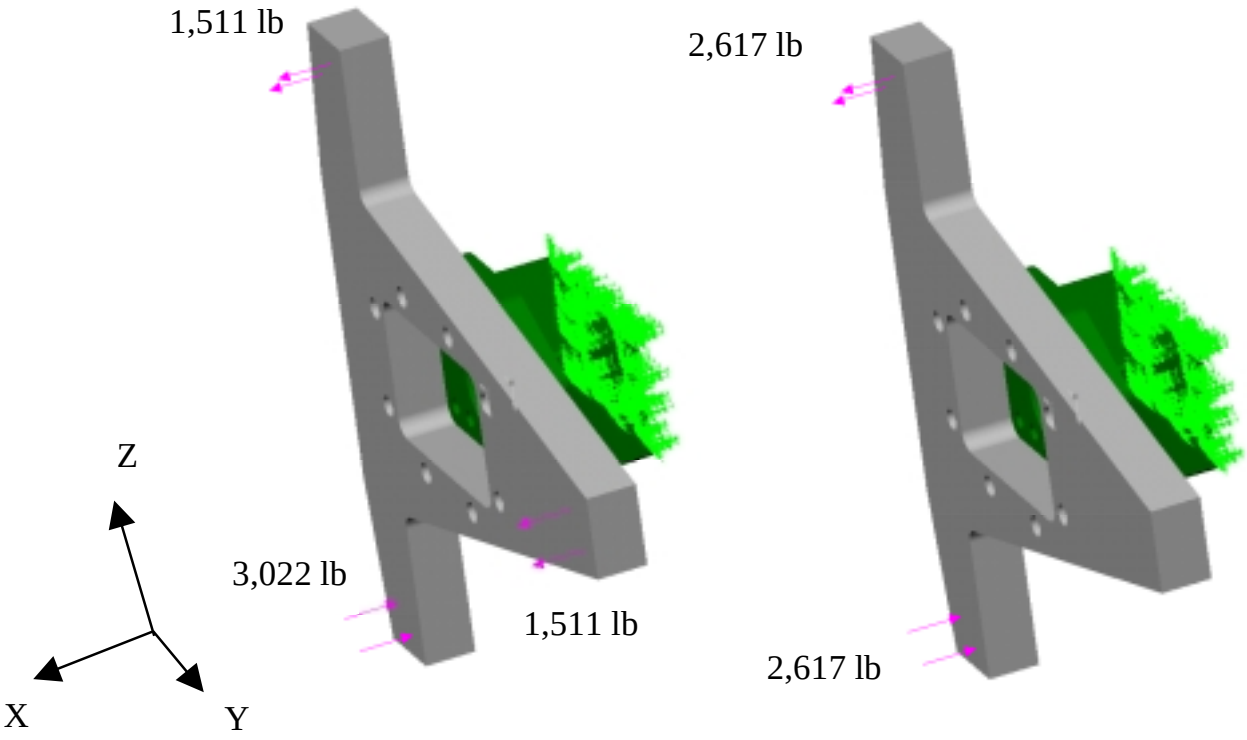

Figure 3.53: Load cases investigated for the boom mount finite element analysis (θ = 60° and 90°).

3.9.2.2. FEA results

The von Mises stress plots of the boom mount is presented in Figure 3.54 for the θ = 60° and 90° load cases. The stresses in the two load case are very similar. The peak von Mises stress in the boom mount in either case is less than 16,000 psi. The safety factor against yielding the boom mount is

$$F.S._{yield} = S_{yield} / \sigma' = 45{,}900 / 15{,}000 = 3.1$$

and the safety factor against exceeding the ultimate strength is

$$F.S._{ultimate} = S_{ultimate} / \sigma' = 66{,}300 / 15{,}000 = 4.4$$

The peak von Mises stresses in the adapter plate in either case is also less than 16,000 psi. The safety factor against yielding the adapter plate is

$$F.S._{yield} = S_{yield} / \sigma' = 115{,}000 / 15{,}000 = 7.7$$

and the safety factor against exceeding the ultimate strength is

$$F.S._{ultimate} = S_{ultimate} / \sigma' = 145{,}000 / 15{,}000 = 9.7$$

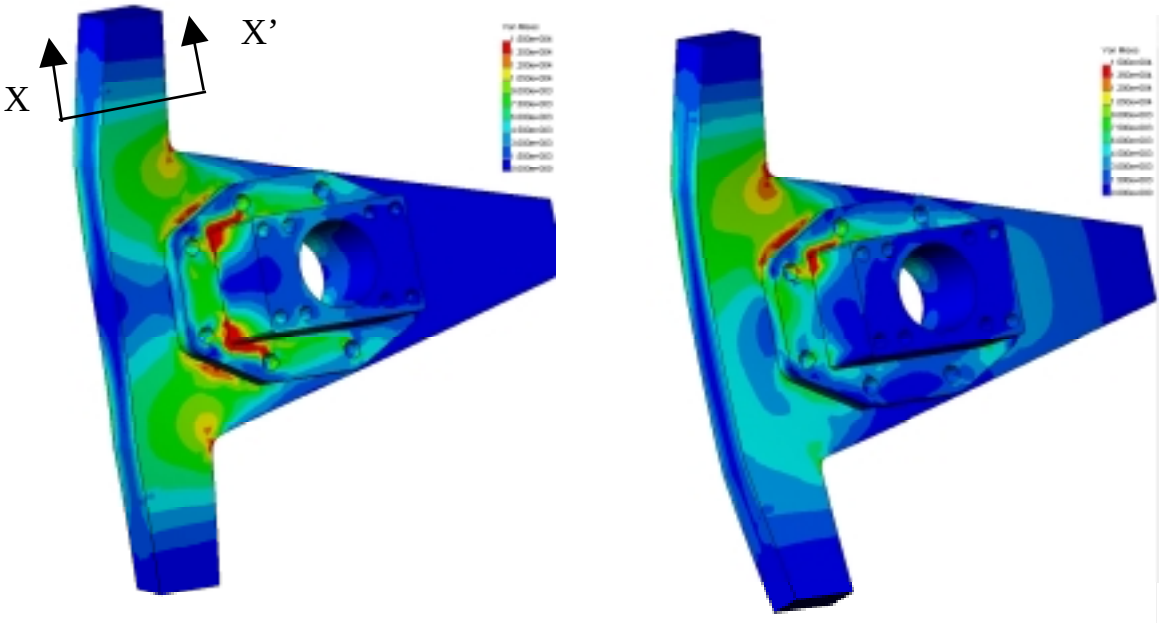

Figure 3.54: Von Mises stress plots of the boom mount for θ = 60° and 90°.

3.9.2.3. FEA validation

To check the FEA results, I computed the bending and shear stresses in arm #1 at section X-X' in Figure 3.54. I chose this section because it is just above the stress concentration of the fillet in the arm. The cross section at X-X' is a 2.0" x 3.2" rectangle. The bending and shear stress calculations are given in Table 3.42.

Table 3.42: Boom arm #1 section properties.

Property	Formula	Value
Width of base	b	3.2"
Height	h	2.0"
Cross sectional area (A)	bh	6.4 in^2
Moment of inertia	$I = b\ h^3 / 12$	2.133 in^4
Moment at section X-X'	My = (Force)(Distance) = (3,022 lb) (3.0 in)	9066 lb-in

Table 3.43: Stress calculations for the hub shaft.

Stress	Formula	Calculation	Value (psi)
Bending	$\sigma_x = (M)(h / 2) / I$	(9,066)(2.0 / 2) / 2.133	4,250
Shear	$\tau_{xy} = Fx / A$	3,022 / 6.4	515

The shear stress is (515 psi) is small compared to the Bending stress (4,250 psi) thus the von Mises stress is slightly greater than 4,250 psi. This value compares reasonably well with the von Mises stress determined in the FEA results at section X-X' which ranges from 4,500 to 6000 psi. Thus, I conclude the FEA analysis is accurate.

3.9.2.4. Fatigue analysis

In this section, I present the fatigue analysis for the boom mount. The formula for the corrected endurance limit for a field specimen (S_e) is

$$S_e = k_a\, k_b\, k_c\, k_d\, k_e\, S_e'$$

The typical fatigue limit for a specimen (S_e') of 2024-T351 Aluminum is 20 kpsi [88]. This fatigue limit is based on 500,000,000 cycles of completely reversed stress for a smooth specimen tested as a rotated beam. The calculation of the effective fatigue limit Se for the boom mount is presented in Table 3.44.

Table 3.44: Calculation of S_e for the boom mount.

Parameter	Deffinition	Value	Comments	Se' kpsi	Se kpsi	Von Mises stress kpsi
ka	surface factor	0.98	Machined finish			
kb	size factor	1.00	-			
kc	load factor	1.00	Von Mises stress			
kd	temp. factor	1.00	Room temp			
ke	misc. affects factor	1.00	-			
Effective k		0.98		20.0	**19.7**	15

The peak von Mises stress in the boom mount (15 kpsi) is less than the component fatigue limit. This fatigue limit is based on 500,000,000 cycles at the peak load. This equates to over 115,000 run hours. We anticipate that the turbine will have been run no more than 50 hours before beginning the NFAC testing and at most another 150 hours in the NFAC for a total runtime of at most 200 hours. In light of these conditions, it is extremely unlikely that fatigue will cause a failure in boom mount.

3.9.3. Boom bars

The boom bars are made from ∅1" 15-5 stainless steel bars. I performed an analytical check on the boom bar strength. The bar is subjected to tensile and shear loads. The peak tensile load in the boom bars was derived in derived in section *3.9.1.1 Boom arm tension.* In that section, the peak axial load on each rod end was predicted to be 3,298 lbs. Similarly, the peak shear load in each bar was calculated to be 422 lbs.

I used the von Mises stresses to determine the factor of safety for a fastener in combined tension and shear. The boom gussets are welded to the boom bars at this location. I used a stress concentration factor of Kt = 2.0 for the tensile and shear loads due to these welds. This stress concentration factor was computed by comparing FEA results with analytical results calculated without a stress concentration factor. A simplified formula for the von Mises stress for combined shear and tension is given by Shigley and Mischke [89] as

$$\sigma' = (\sigma_x{}^2 + 3\tau_{xy}{}^2)^{\frac{1}{2}}$$

where σ_x is the tensile stress and is equal to

$$Kt^* \text{ Tension} / \text{Area}_{bar} = 2.0 * 3{,}022 \text{ lb} / (\pi\ 1^2 \text{ in}^2 / 4) = 7{,}695 \text{ psi.}$$

τ_{xy} is the shear stress and is equal to

Kt^* Shear / Area_{bar} = Kt * 422 lb / .78625 in^2 = 1,073 psi. The von Mises stress is

$$\sigma' = (7{,}695^2 + 3 \times 1{,}073^2)^{\frac{1}{2}} = 7{,}916\, psi$$

The boom bars are made from ∅1" 15-5 stainless steel bars heat treated after welding to the H1025 condition. The minimum yield and tensile strengths for the material in this condition are 145 Kpsi and 155 Kpsi [90]. Thus the safety factors are

$$\boxed{F.S._{\sigma' \text{ yield}} = 145{,}000 / 7{,}916 = 18.3}$$

$$\boxed{F.S._{\sigma' \text{ ultimate}} = 155{,}000 / 7{,}916 = 19.5}$$

These safety factors are more than adequate to meet NASA requirements.

3.9.4. Boom bar gusset and flange welds

The boom bar gusset and flange welds are shown in Figure 3.55. I analyzed these welds analytically. I used the weld analysis methodology presented in AWS D1.1-98 Structural Welding Code for Steel.

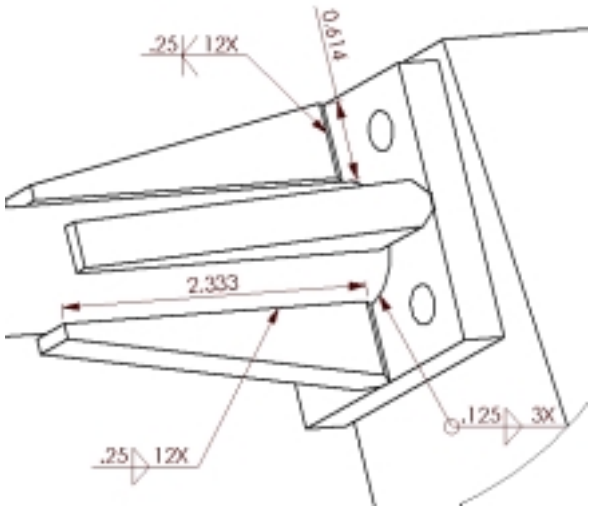

Figure 3.55: Boom gusset and flange welds.

3.9.4.1. Gusset / flange weld

The gusset / flange weld is a .614" long, symmetric fillet weld with a .25" leg length (see Figure 3.55). It qualifies as an AWS prequalified complete joint penetration groove weld (AWS joint designation TC-U5-GF) [91].

This weld joins the gussets to the flange. The peak tensile load in the boom bars was derived in section *3.9.1.1 Boom arm tension.* In that section, the peak axial load on each rod end was predicted to be 3,022 lbs. Similarly, the peak shear load in each bar was calculated to be 422 lbs.

Weld analysis assumptions:

1) The .125" fillet weld around the perimeter of the bar joins the bar to the flange thereby reducing the load on the gusset/flange weld. I neglected this weld because I could not determine how much load sharing this weld carries. This is a conservative assumption.
2) I assumed that the bending moments in the boom assembly are reacted solely by tension and compression in the boom bars. That is, there are no bending forces in the welding joint.

The stress for a complete joint penetration groove weld is calculated by dividing the tensile force (3022 lb / 4 beads = 755 lb) by the effective area. The effective area of a complete penetration groove weld is the weld length (.614") multiplied by the weld size. The weld size is the thickness of the part (.375") [92]. Thus the effective area is .614" * .375" =.230 in^2. Thus the tensile stress is

$$755 \text{ lb} / .230 \text{ in}^2 = 3{,}284 \text{ psi}$$

The allowable stress for this weld is the same as the base material [93]. The gussets and bars are made of 15-5 stainless steel. The welds were TIG welded using 17-4 stainless steel electrode. These two

steels are have essentially the same strength properties. After welding, the boom assembly was aged to H 1025 specifications. 17-4 and 15-5 stainless steel in this condition have S_{ut} = 155 kpsi. Thus the safety factor against exceeding the allowable stress is

$$F.S._{allowable} = 155{,}000 / 3284 = 47.2$$

The AWS standard D1.1-98 also specifies that for an unground groove welded connection, the alternating component of the stress can not exceed 13 Kpsi for an infinite life [94]. Assuming that the loads are completely reversing, the factor of safety against exceeding this requirement is

$$F.S._{fatigue} = 13000 / 3284 = 4.0$$

This exceeds NFAC requirement of $F.S._{fatigue}$ = 2.0.

3.9.4.2. Gusset / bar weld

The gusset / bar weld is a 2.333" long, symmetric fillet weld with a .25" leg length (see Figure 3.55). This weld joins the gussets to the bar. The peak tensile load in the boom bars was derived in section *3.9.1.1 Boom arm tension.* In that section, the peak axial load on each rod end was predicted to be 3,022 lbs. Similarly, the peak shear load in each bar was calculated to be 422 lbs.

Weld analysis assumptions:

1) The shear load on each weld bead (422 lbs / 8 = 53 lbs) is negligible compared to the tensile load on each weld bead (3022 / 8 = 377 lbs).
2) I assumed that the bending moments in the boom assembly are reacted solely by tension and compression in the boom bars. That is, there are no bending forces in the welding joint.

The shear stress in a fillet welds is given by [95]

$$\tau = P / (.707\ h\ l)$$

where

P = the load on the weld bead = 3022 lb / 8 = 377 lb

h = the leg length = .25

l = the length of the weld = 2.333"

thus

$$\tau = 377 / (.707 * .25 * 2.333) = 916 \text{ psi}$$

The AWS standard D1.1-98 specifies that the allowable connection stress for a fillet weld is .3 * nominal tensile strength of the filler metal [96]. The gussets and bars are made of 15-5 stainless steel. The welds were TIG welded using 17-4 stainless steel electrode. These two steels are have essentially the same strength properties. After welding, the boom assembly was aged to H 1025 specifications. 17-4 and 15-5

stainless steel have the same tensile strength in this condition (155 kpsi). Thus the allowable shear stress is .3 * 155 kpsi = 46.5 kpsi. The safety factor against exceeding the allowable stress is

$$F.S._{allowable} = 46{,}500 / 916 = 50.8$$

The AWS standard D1.1-98 also specifies that for a fillet welded connection loaded parallel to the line of stress, the endurance limit occurs at an alternating load of 7 kpsi [97]. Thus, the factor of safety against the endurance limit is

$$F.S._{fatigue} = 7{,}000 / 916 = 7.6$$

These safety factors exceed NASA's weld requirements in section C.5.5.

3.9.5. 5/16" boom flange bolts

Each cleavis mount is bolted to the boom mount using four 5/16-18 UNC grade 8 bolts, nuts, and washers (not shown in figures). In the following analyses, I use the loads derived in section 3.9.2 for the boom rod ends. In that section, the peak axial load on each rod end is was predicted to be 3,022 lbs. I also consider the affect of the shear load on the bolts.

3.9.5.1. Tensile strength check

In the tensile strength analysis I assume

1) The load applied by the rod end is purely a tensile load. There is no bending across the cleavis mount.
2) The tensile loads is applied evenly to all four bolts.

Tension in each bolt:

$$\text{Tension}_{\text{in each bolt}} = 3{,}022 / 4 = 755 \text{ lb}$$

The tensile strength of each bolt is 7,860 lb. Thus the safety factor against exceeding the ultimate strength a bolt is

$$F.S._{tension} = S_{ultimate} / \text{Tension} = 7{,}860\text{lb} / 755 = 10.4$$

3.9.5.2. Shear strength check

The shear loads on the boom mount bolts are due to the resultant of Fy and Fz. The resultant load on each boom bar at the boom plate interface is 422 lb (see section 3.9.1.2). I made the following assumptions while calculating the shear on the boom mount bolts.

Assumptions:

1) Assume there is no friction between the boom plate and boom spacer. This is a conservative assumption since the approximate preload clamping force of 162,000 lb in the joint creates roughly 16,000 lb of friction between faces.
2) Assume the shear load is equally distributed among the four bolts.

The shear force on each bolt is

$$\text{Shear force} = 422 / 4 = 105 \text{ lb}$$

The allowable shear strength for a bolt in single shear is roughly 2/3 of the bolt's ultimate strength [98]. Thus the allowable shear for the adapter bolts is .667 * 33,900 lb = 22,713 lb

$$F.S._{shear} = V_{allow} / V_1 = 22{,}713 / 105 = 215$$

This high safety factor indicates the shear load on the bolts is negligible.

3.9.5.3. Joint preload check

According to the NFAC Test-Planning Guide, "A sufficient number of bolts shall be provided with preloads so that the net joint preload for all loading is at least two times the operating loads. [99]"

The cleavis mount bolts were torqued by measuring the elongation of the bolts. For the preload analysis, I assumed that the bolts were torqued to 75% of their proof load (.75 * 6,300 = 4,725 lb). This is a conservative assumption since we preloaded the bolts to 90 ± 5% of their proof load.

The tensile strength check results indicate that the peak tension in each cleavis mount bolt is 755 lb. The safety factor against exceeding the preload in this bolt is

$$F.S._{Tension\ preload} = 4{,}725 / 755 = 6.3$$

3.9.6. 5/8" boom mount bolts

The boom mount is bolted to the boom mount spacer using eight 5/8-11 UNC grade 8 bolts (not shown in figures). In the following analyses, I perform a tensile strength check and shear strength check on the bolts.

3.9.6.1. Tensile strength check

The loads on the adapter which create tension in the bolts are My, Mz, and Fx (see Figure 3.57). The loads which stress the bolts in shear are Fy and Fz. The magnitudes of these loads are listed in Table 3.40.

In the tensile strength analysis I assume

1) Tension loads are applied evenly to all eight bolts.
2) Moments applied to the teeterpin cap create a linear load distribution on the bolts as shown in Figure 3.57.

3) The resultant of My and Mz act across the axis with the smallest moment of inertia (the Y-axis). The resultant Myz = $(3{,}414^2 + 1{,}919^2)^{.5}$ = 3,916 lb.

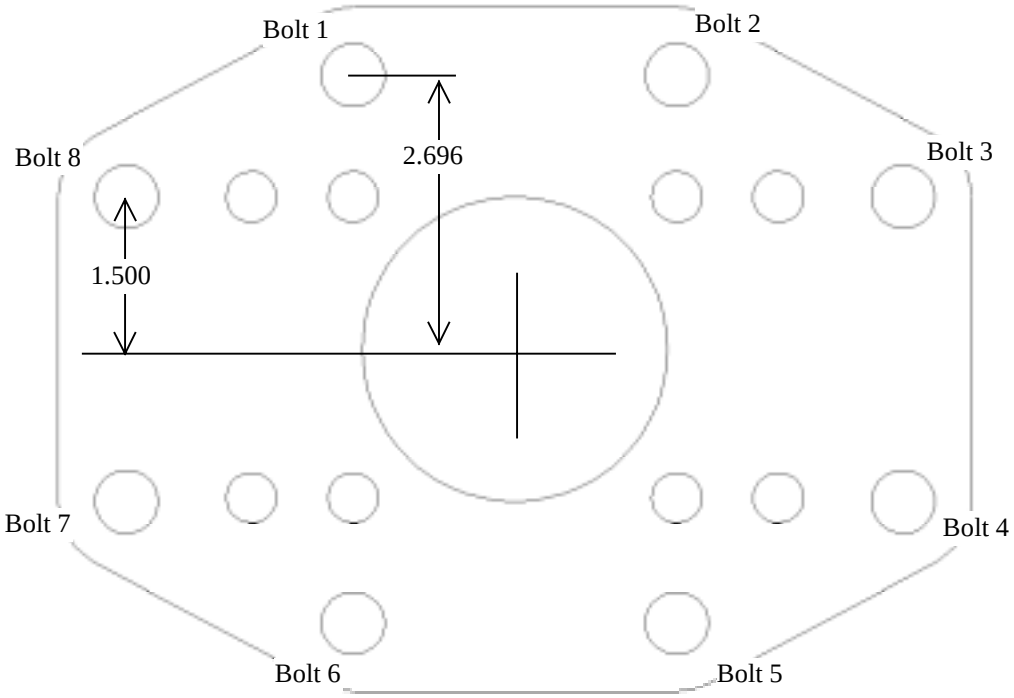

Figure 3.56: Bolt tension distribution in the adapter.

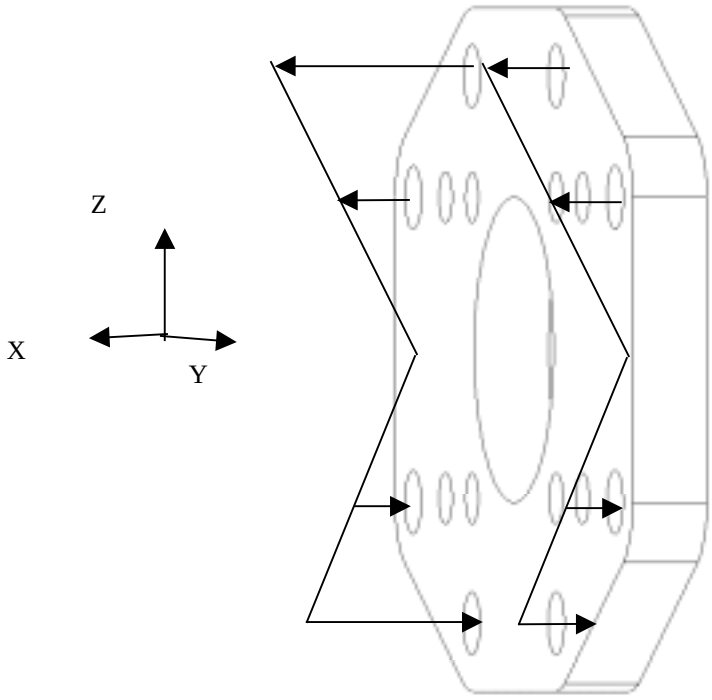

Figure 3.57: Moment load distribution on the boom mount and boom mount spacer bolts.

Tension on bolt 1 due to Rx:

$$Tension_{Rx} = Fx / 8 = 248 / 8 = 31 \text{ lb}$$

Tension on bolt 1 due to My :

The stress in the i^{th} bolt can be found using the flexure formula for beams:

$$\sigma_i = (Myz)\,(z_i) / (I) = (My)\,(z_i) / \sum(z_i^2)\,dA$$

Thus the bolt tension in the i^{th} bolt is

$$\text{Bolt tension}_i = (\sigma_i)\,(A_{bolt}) = (Myz)\,(z_i)\,(A_{bolt}) / A_{bolt} \sum(z_i^2)$$

$$\mathbf{Tension_i = (Myz)\,(z_i) / \sum(z_i^2)}$$

(see Table 3.45 for z_i and $\mathbf{\sum z_i^2}$ values)

Therefore

$$Tension_{MRy} = (Myz)(z_1) / \Sigma(z_i^2)$$

$$Tension_{MRy} = (3{,}916)(2.696) / 38.074 = 277 \text{ lb}$$

Table 3.45: Component distances from the rotor axis.

Bolt	zi	zi^2
1	2.696	7.268
2	2.696	7.268
3	1.500	2.250
4	1.500	2.250
5	2.696	7.268
6	2.696	7.268
7	1.500	2.250
8	1.500	2.250
Sum		38.074

Total tension in bolt 1 = T_1 = $Tension_{Rx}$ + $Tension_{Myz}$ = 31 + 242 = 308 lb

$$F.S._{tension} = S_{ultimate} / T_1 = 33{,}900 / 308 = 109$$

This high safety factor indicates that the tension on the bolts is insignificant.

3.9.6.2. Shear strength check:

The shear loads on the boom mount bolts are due to the resultant of Fy and Fz. The resultant load is Fyz = $= (676^2 + 1{,}071^2)^{.5}$ = 1,266 lb. I made the following assumptions while calculating the shear on the boom mount bolts.

Assumptions:

1) Assume there is no friction between the boom plate and boom spacer. This is a conservative assumption since the bolt pre-load creates a significant amount of friction between the two faces.
2) Assume the shear load is equally distributed among the eight bolts.

The shear force on each bolt is

$$\text{Shear force} = 1266 / 8 = 158 \text{ lb}$$

The allowable shear strength for a bolt in single shear is roughly 2/3 of the bolt's ultimate strength [100]. Thus the allowable shear for the adapter bolts is .667 * 33,900 lb = 22,713 lb. The safety factor against exceeding the shear load capacity of the adapter bolts is

$$\boxed{F.S._{shear} = V_{allow} / V_1 = 22{,}713 / 158 = 144}$$

This high safety factor indicates the shear load on the bolts is insignificant. In addition, since the tension in the bolts is insignificant, a pre-load check of the bolts is unnecessary.

3.9.7. Power box, PCM box, and PSC box mounts

The forces on the large boom boxes are primarily gravitational and inertial. Each of the three large boom boxes are fastened to the boom using four bolts. The bolts are inserted through tabs welded on the boxes and through the beams which span the boom tubes. In this section I analyze the boom cross bars, the boom box bolts, and the boom box tabs.

The heaviest box weighs 56 lbs (25.4 kg). We used ADAMS to simulate the accelerations on the boom boxes. The peak acceleration components (including gravity) were 35 m/s^2 radially and 19 m/s^2 tangentially. The corresponding radial and tangential forces on the boxes are

$$\text{Force}_{radial} = \text{mass} * \text{acceleration}_{radial} = 25.4 \text{ kg} * 35 \text{ m/s}^2 = 889 \text{ N} = 200 \text{ lb}$$

$$\text{Force}_{tangential} = \text{mass} * \text{acceleration}_{tangential} = 25.4 \text{ kg} * 19 \text{ m/s}^2 = 483 \text{ N} = 108 \text{ lb}$$

3.9.7.1. Boom cross bars

The boom cross-bars are made from .4" thick, 1.0" wide 15-5 stainless steel bars (see Figure 3.58). Each end of the cross bars has a circumferential fillet weld. I analyzed these welds according to AWS specifications. The AWS code treats any stress on a fillet weld as a shear stress. The effective area of a fillet weld is defined as the effective throat multiplied by the effective length. The effective throat of the cross bar weld is the minimum distance from the root of the joint to its face. For the boom cross bars this distance is roughly .125". The effective length of each weld is equal to the perimeter of each bar or

$$2 * 1" + 2 * .4" = 2.8"$$

Thus the effective area is

$$2.8" * .125" = .35 \text{ in}^2$$

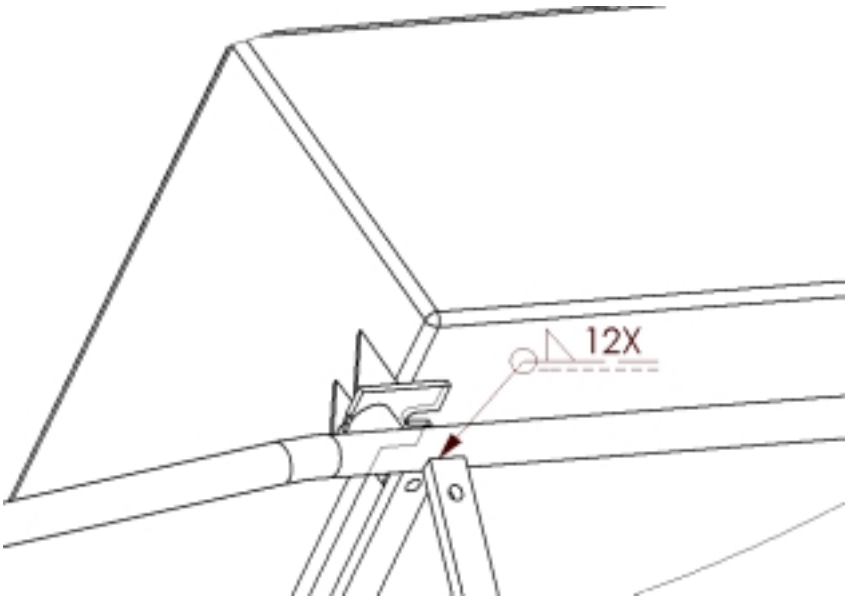

Figure 3.58: Boom cross bar welds.

Each weld is subjected to shear and bending loads. The radial force on each box is 200 lbs. Assuming this load is distributed equally on each cross bar weld, the shear load on each weld is 50 lb. The mounting holes are drilled ¾" from the end of the cross bars. The bending load on each weld is then ¾" * 50 lb = 37.5 lb-in or 3.1 ft-lb.

The primary shear stress in a fillet welds (due to the shear load) is given by the AWS as

$$\tau_{primary} = P / A_{effective}$$

where

P = the load on the weld bead = 50 lb

$A_{effective}$ = the effective area = .35

thus

$$\tau_{primary} = 50 / .35 = 142 \text{ psi}$$

The bending moment on the weld causes a secondary shear stress. The secondary shear stress in a fillet welds (due to the bending load) is given by the Shigley and Mischke as [101]

$$\tau_{secondary} = M * c / (\text{effective throat} * I_u)$$

Where

c = the distance to the furthest point on the weld across the bending axis = .4" / 2 = .2"

I_u = is the unit second moment of area = $d^2 *(3b + d) / 6$

d = .4

b = 1

thus

$$Iu = .091$$

$$\tau_{secondary} = 37.5 * .2 / (.125 * .091) = 659 \text{ psi}$$

Adding $\tau_{primary}$ and $\tau_{secondary}$ results in a total shear stress of 802 psi.

The AWS standard D1.1-98 specifies that the allowable connection stress for a fillet weld is .3 * nominal tensile strength of the filler metal [102]. The bars are made of 15-5 stainless steel. The welds were TIG welded using 17-4 stainless steel electrode. These two steels are have essentially the same strength properties. After welding, the boom assembly was aged to H 1025 specifications. 17-4 and 15-5 stainless steel have the same tensile strength in this condition (155 kpsi). Thus the allowable shear stress is .3 * 155 kpsi = 46.5 kpsi. The safety factor against exceeding the allowable stress is

$$F.S._{allowable} = 46{,}500 / 802 = 58$$

The AWS standard D1.1-98 also specifies that for a fillet weld loaded parallel to the line of stress, the endurance limit occurs at 5 kpsi [103]. Thus, the factor of safety against the endurance limit is

$$F.S._{fatigue} = 5{,}000 / 802 = 6.2$$

These safety factors exceed NASA's requirements.

3.9.7.2. Boom box bolts

Each boom box is bolted to the boom cross bars using four SAE grade 5 3/8-16 bolt.
As described in the previous section, the force on each of the four bolts is subjected to a peak tensile load of 50 lb. This load is negligible compared to the proof strength of the bolt—6,600 lb. Similarly, the shear load on each bolt is 27 lbs. This load is also negligible.

3.9.7.3. Boom box welds

Figure 3.59 and Figure 3.60 displays the boom box gusset welds and geometry. The boxes are made from 5052 AL. The horizontal tabs were welded to the base of the boxes by the manufacturer. We fabricated the triangular gussets from 5052 AL and TIG welded them to the boxes for additional strength.

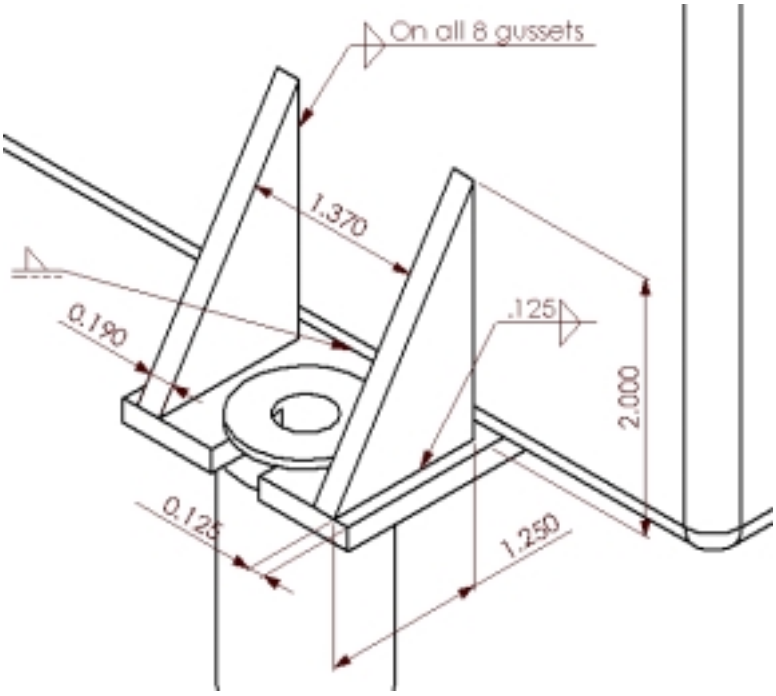

Figure 3.59: Gusset / box and gusset / tab welds.

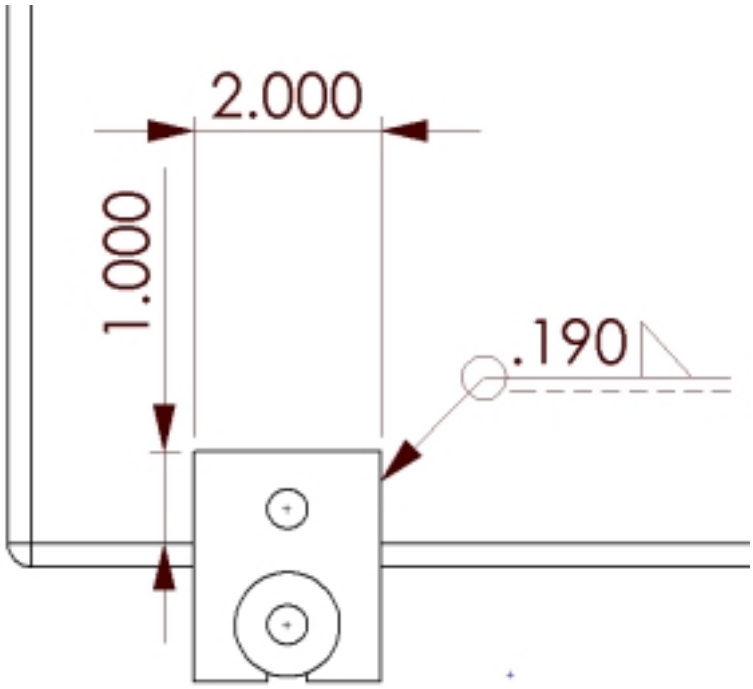

Figure 3.60: Box / tab weld.

3.9.7.3.1. Gusset / box weld

The load applied to the gusset / tab weld is applied by the boom box bolt reaction. In the previous section, this load was calculated to be 50 lb. In this analysis, I assume the tension in the gusset can be represented as a concentrated force which acts through the centriod of the gusset tab weld. Thus, there is no bending across the gusset / tab weld.

The peak force on each bolt is 50 lbs. Assuming this load is applied even to each gusset, the peak force in each gusset weld is 50 lb / 2 = 25 lb.

The shear stress in a fillet welds (due to the tensile load) is given by the AWS as

$$\tau = P / A_{effective}$$

where

P = the load on the weld bead = 25 lb

$A_{effective}$ = the effective area = effective throat * effective length = (.707*.190")*(2*2")=.537 in^2

thus

$$\tau = 25 / .537 = 47 \text{ psi}$$

The AWS standard D1.1-98 specifies that the allowable connection stress for a fillet weld is .3 * nominal tensile strength of the filler metal [104]. The welds were TIG welded using 5356 aluminum electrode (tensile strength = kpsi). Assuming the electrode has tensile properties similar to 5052 AL, the un-heat-treated tensile strength is 28 kpsi. Thus the allowable shear stress is .3 * 28 kpsi = 8.4 kpsi. The safety factor against exceeding the allowable stress is

$$\boxed{F.S._{allowable} = 8{,}400 / 47 = 180}$$

The fatigue strength of 5052 at 5 x 10^8 cycles is 16 kpsi. Assuming the allowable fatigue strength in shear is also .3 * the fatigue strength, the allowable fatigue strength is .3*16kpsi = 4.8 kpsi. Thus, the factor of safety against exceeding the fatigue strength is

$$\boxed{F.S._{fatigue} = 4{,}800 / 47 = 102}$$

These safety factors exceed NASA's requirements.

3.9.7.3.2. Gusset / box weld tearout

The box is made from 5052 thin-walled aluminum (.08" wall) thus the box must be analyzed for tearout. The tearout path would likely be a rectangle encompassing both gussets, 2" tall by 1.75" wide. Assuming the base of the rectangle does not contribute to the tear out, the length of the tear out path is 5.75". Thus, the tear area is .08" * 5.75" = .46 in^2. The shear force on this area resulting from the radial acceleration is 50 lb. Thus the shear stress in the box is 50 lb / .46 in^2 =108 psi.

The yield stress for 5052 AL is 28 kpsi. According to the maximum shear stress theory, the allowable shear stress is **.557** * 28 kpsi = 15.6 kpsi. The safety factor against exceeding the allowable stress is

$$\boxed{F.S._{allowable} = 15{,}600 / 108 = 144}$$

The fatigue strength of 5052 at 5 x 10^8 cycles is 16 kpsi. . According to the maximum shear stress theory, the allowable shear stress is **.557** * 16 kpsi = 8.9 kpsi. Thus, the factor of safety against exceeding the fatigue strength is

$$\boxed{F.S._{fatigue} = 8{,}900 / 108 = 82.4}$$

These safety factors exceed NASA's requirements.

3.9.7.3.3. Gusset / tab weld

Assuming the load path for the bolt centripetal and dynamic loads is through the gusset, then the load applied to the gusset / tab weld are identical to the loads applied to the gusset / box weld in the previous section. Thus, the only difference between this analysis and the analysis of the gusset / box weld in the previous section is that the gusset / tab weld has a shorter effective length. Therefore

$A_{effective}$ = the effective area = effective throat * effective length = (.707*.190")*(2* 1.25") = .336in^2 thus

$$\tau = 25 / .336 = 74 \text{ psi}$$

$$\boxed{F.S._{allowable} = 8{,}400 /74 = 112}$$

$$\boxed{F.S._{fatigue} = 4800 / 74 = 65}$$

These safety factors exceed NASA's requirements

3.9.7.3.4. Tab / box weld

Torsional loads on each tab result from the tangential acceleration of the boxes. The tangential acceleration is caused by torque fluctuations, gravity, and the dynamic effect of the nacelle "nodding". These torsional loads are resisted by the tab / box weld around the perimeter of the tab and they cause a primary and secondary shear stress in the weld.

The peak tangential force on the boxes (108 lb) acts in the plane of the tab. Assuming this load is distributed equally among the four tabs, the load on each weld is 108 lb / 4 = 27 lb. The mounting holes are drilled 2.5" from the center of the tab weld centriod. The torsional load on each weld is then 2.5" * 27 lb = 67.5 lb-in or 5.6 ft-lb.

The primary shear stress in a fillet weld is given by the AWS as

$$\tau_{primary} = P / A_{effective}$$

where

P = the load on the weld bead = lb

$A_{effective}$ = the effective area = effective throat * effective length = (.707*.190")*(2*2" + 2*1")=.806 in^2

thus

$$\tau_{primary} = 27 / .806 = 33.5 \text{ psi}$$

The torsion on the weld causes a secondary shear stress. The secondary shear stress in a fillet weld (due to the bending load) is given by the Shigley and Mischke as [105]

$$\tau_{secondary} = T * r / (\text{effective throat} * J_u)$$

Where

Effective throat = .707 * weld length = .707 * .190" = .134"

T = the torsion load

r = the distance to the furthest point on the weld = 1.1"

J_u = is the unit second polar moment of area = $(b + d)^3 / 6$

d = 2

b = 1

thus

$$Ju = 4.5$$

$$\tau_{secondary} = 67.5 * 1.1 / (.134 * 4.5) = 123 \text{ psi}$$

Adding $\tau_{primary}$ and $\tau_{secondary}$ results in a total shear stress of 157 psi.

The AWS standard D1.1-98 specifies that the allowable connection stress for a fillet weld is .3 * nominal tensile strength of the filler metal [106]. The welds were TIG welded using 5356 aluminum electrode (tensile strength = kpsi). Assuming the electrode has tensile properties similar to 5052 AL, the un-heat treated tensile strength is 28 kpsi. Thus the allowable shear stress is .3 * 28 kpsi = 8.4 kpsi. The safety factor against exceeding the allowable stress is

$$\boxed{F.S._{allowable} = 8{,}400 / 157 = 53.6}$$

The fatigue strength of 5052 at 5×10^8 cycles is 16 kpsi. Assuming the allowable fatigue strength in shear is also .3 * the fatigue strength, the allowable fatigue strength is .3*16kpsi = 4.8 kpsi. Thus, the factor of safety against exceeding the fatigue strength is

$$\boxed{F.S._{fatigue} = 4{,}800 / 157 = 30.6}$$

These safety factors exceed NASA's requirements.

4. References

1 Mechanical Dynamics, Inc., 2301 Commonwealth Blvd., Ann Arbor, Michigan 48105, USA, http://www.adams.com

2 Structural Research & Analysis Corporation, 12121 Wilshire Blvd., 7th Floor, Los Angeles, CA 90025, USA, http://www.cosmosm.com

3 "National Full Scale Aerodynamics Complex Test Planning Guide", Part III, Revised Summer 1993, Appendix C, p C-1.

4 Daniel Roque, Applications Engineer, Telephone Conversation, 7/8/98 (909) 676-3965, Transducer Techniques, 43178-T Business Park Dr., B101, Temecula, CA 92590 USA.

5 "NFAC Test Planning Guide", Appendix C, p. C-67.

6 Shigley and Mischke, eq 3-55, p. 123.

7 "NFAC Test Planning Guide", Appendix C, p.C-29.

8 Shigley and Mischke, eq. 6-16, p. 250.

9 ASTM standard A 193, Table 1, p. 20.

10 Aerospace Structural Metals Handbook, Table 3.052, Code 1203, p. 30.—Section revised March 1987

11 Virgil Moring Faires, Design of Machine Elements, Fourth Ed.

12 Shigley and Mischke, eq. 7-14, 7-15, 7-24, p. 283-288.

13 "NFAC Test Planning Guide", Appendix C, p. C-67.

14 Shigley and Mischke Eq. 6-18, p. 251.

15 Structural Welding Code—Steel, ANSI/AWS D1.1-98, Table 2.4 & Figure 2.10, pp.15,17.

16 Shigley and Mischke eq. 6-18, p. 362.

17 Shigley and Mischke pp. 277-287.

18 Aerospace Structural Metals Handbook, Table 3.514, Code 1501, p. 38.—Section revised October 1995

19 Aerospace Structural Metals Handbook, Table 3.052, Code 1203, p. 30.—Section revised March 1987

20 Boyer, Howard E., Atlas of Fatigue Curves, ASM publications, p.62, 1997.

21 Shigley and Mischke p. 299.

22 Aerospace Structural Metals Handbook, Table 3.1.1, Code 1501, p. 19.—Revised October 1995.

23 Joseph T. Ryerson & Son Stock List, p. 395.

24 Shigley and Mischke pp. 277-287.

25 Aerospace Structural Metals Handbook, Table 3.514, Code 1501, p. 38.—Section revised October 1995

26 Shigley and Mischke p. 740.

27 Shigley and Mischke, eq. 8-43, p. 362.

28 "Machinery's Hand Book", 25th edition, Industrial Press Inc., New York, p. 1577, 1996.

29 *Final Design and Analysis Report, NREL/CEB Project, Phase Three,* Barker, MA: Composite Engineering, 1994, p 8-11.

30 “NFAC Test Planning Guide”, Appendix C, p. C-25.

31 Ibid.

32 “Fastener Facts”, manufacture catalog, Bowman Distribution 850East 72nd Street, Cleveland, OH 44103, USA., p. 29.

33 Shigley and Mischke, Eq. 6-18, p. 362.

34 “NFAC Test Planning Guide”, Appendix C, C-27.

35 Aerospace Structural Metals Handbook, Table 3.2.1.11, Code 1208, p. 12.—Section revised June 1992

36 Aerospace Structural Metals Handbook, Table 3.2.1.11, Code 1208, p. 12.—Section revised June 1992

37 Aerospace Structural Metals Handbook, Fig 3.5.3, Code 1208, p. 20.—Section revised June 1992

38 Shigley and Mischke, eq. 7-14, 7-15, 7-24, p. 283-288.

39 “Machinery’s Hand Book”, p. 2188.

40 Ibid., p. 1416.

41 “NFAC Test Planning Guide”, Appendix C, p. C-27.

42 “Metals Handbook”, vol. 1, 10th edition, ASM International Handbook Committee, USA, p. 432.

43 “NFAC Test Planning Guide”, Appendix C, p. C-67.

44 Aerospace Structural Metals Handbook, Table 3.514, Code 1501, p. 38.—Section revised October 1995

45 Shigley and Mischke, eq. 7-14, 7-15, 7-24, p. 283-288.

46 Shigley and Mischke Eq. 6-18, p. 251.

47 Aerospace Structural Metals Handbook, Table 3.514, Code 1501, p. 38.—Section revised October 1995

48 Shigley and Mischke, eq. 7-14, 7-15, 7-24, p. 283-288.

49 “Machinery’s Hand Book”, p. 1404, Table 2. Accuracy of bolt preload application methods.

50 “NFAC Test Planning Guide”, Appendix C, p. C-25.

51 “NFAC Test Planning Guide”, Appendix C, p. C-25.

52 Shigley and Mischke, p. 362.

53 “Fastener Facts”, manufacture catalog, Bowman Distribution 850East 72nd Street, Cleveland, OH 44103, USA., p. 29.

54 Shigley and Mischke, eq. 6-18, p. 362.

55 “NFAC Test Planning Guide”, Appendix C, p. C-27.

56 “Metals Handbook”, vol. 1, 10th edition, ASM International Handbook Committee, USA, p. 432.

57 “Machinery’s Hand Book”, p. 1404, Table 2. Accuracy of bolt preload application methods.

58 “Fastener Facts”, manufacture catalog, Bowman Distribution 850East 72nd Street, Cleveland, OH 44103, USA., p. 29.

59 Shigley and Mischke, eq. 6-18, p. 362.

60 “NFAC Test Planning Guide”, Appendix C, p. C-27.

61 “NFAC Test Planning Guide”, Appendix C, p. C-67.

62 Aerospace Structural Metals Handbook, Table 3.514, Code 1501, p. 38.—Section revised October 1995

63 Shigley and Mischke, eq. 7-14, 7-15, 7-24, p. 283-288.

64 “Machinery’s Hand Book”, p. 2188.

65 “Machinery’s Hand Book”, p. 1416.

66 “Machinery’s Hand Book”, p. 1672 & 2188.

67 “Machinery’s Hand Book”, p. 1416.

68 “NFAC Test Planning Guide”, Appendix C, p. C-27.

69 “Machinery’s Hand Book”, p. 1399.

70 Shigley and Mischke Eq. 6-18, p. 251.

71 Shigley and Mischke pp. 277-287.

72 Boyer, Howard E., Atlas of Fatigue Curves, ASM publications, p.43, 1997.

73 “NFAC Test Planning Guide”, p. 4-16.

74 “NFAC Test Planning Guide”, Appendix C, p. C-27.

75 Structural Welding Code—Steel, ANSI/AWS D1.1-98, p.13.

76 Shigley and Mischke Eq. 6-18, p. 362.

77 Shigley and Mischke pp. 277-287.

78 Boyer, Howard E., Atlas of Fatigue Curves, ASM publications, p.43, 1997.

79 Joseph T. Ryerson & Son Stock List, p. 399.

80 http://www.selectarc.com/inox308hb.html, Selectarc manufacturer web site, Forges De Saint-Hippolyte S.A.

81 Aerospace Structural Metals Handbook, Figures 1.601 & 3.0214, Code 1401—Revised December 1982p. 9 and p. 16.

82 Joseph T. Ryerson & Son Stock List, p. 399.

83 http://www.selectarc.com/inox308hb.html, Selectarc manufacturer web site, Forges De Saint-Hippolyte S.A.

84 Aerospace Structural Metals Handbook, Figures 1.601 & 3.0214, Code 1401—Revised December 1982, p. 9 and p. 16.

85 “NFAC Test Planning Guide”, Appendix C, p. C-67.

86 Shigley and Mischke p. 299.

87 Joseph T. Ryerson & Son Stock List, p. 399.

88 Aerospace Structural Metals Handbook, Table 3.052, Code 3203—Revised December 1980, p. 13.

89 Shigley and Mischke, eq. 6-18, p. 362.

90 Aerospace Structural Metals Handbook, Table 3.1.11, Code 1513—Revised March 1997, p. 33.

91 Structural Welding Code—Steel, ANSI/AWS D1.1-98, p.73.

92 Structural Welding Code—Steel, ANSI/AWS D1.1-98, p.4.

93 Structural Welding Code—Steel, ANSI/AWS D1.1-98, p.13.

94 Structural Welding Code—Steel, ANSI/AWS D1.1-98, Table 2.4 & Figure 2.10, pp.15,17.

95 Structural Welding Code—Steel, ANSI/AWS D1.1-98, p.4.

96 Structural Welding Code—Steel, ANSI/AWS D1.1-98, p.13.

97 Structural Welding Code—Steel, ANSI/AWS D1.1-98, Table 2.4 & Figure 2.10, pp.15,17.

98 "Fastener Facts", manufacture catalog, Bowman Distribution 850East 72nd Street, Cleveland, OH 44103, USA., p. 29.

99 "NFAC Test Planning Guide", Appendix C, p. C-27.

100 "Fastener Facts", manufacture catalog, Bowman Distribution 850East 72nd Street, Cleveland, OH 44103, USA., p. 29.

101 Structural Welding Code—Steel, ANSI/AWS D1.1-98, p.4.

102 Structural Welding Code—Steel, ANSI/AWS D1.1-98, p.13.

103 Structural Welding Code—Steel, ANSI/AWS D1.1-98, pp.15,17.

104 Structural Welding Code—Steel, ANSI/AWS D1.1-98, p.13.

105 Structural Welding Code—Steel, ANSI/AWS D1.1-98, p.4.

106 Structural Welding Code—Steel, ANSI/AWS D1.1-98, p.13.